A mining research final report PCC 4679 04
NOVEMBER 1981

A FEASIBILITY STUDY FOR THE DETECTION OF WEAK ELECTROMAGNETIC SIGNAL/BURSTS WITH HARD-LIMITED ARRAYS

Contract J0318033
University of Pittsburgh

BUREAU OF MINES
UNITED STATES DEPARTMENT OF THE INTERIOR

The views and conclusions contained in this document are those of the authors and should not be interpreted as necessarily representing the official policies or recommendations of the Interior Department's Bureau of Mines or of the U.S. Government.

REPORT DOCUMENTATION PAGE

1. Report No.	2.	3. Recipient's Accession No.
PCC 4679 04		

4. Title and Subtitle
A Feasibility Study for the Detection of Weak Electromagnetic Signal Bursts with Hard-Limited arrays.

5. Report Date

6.

7. Author(s)
M. Kanefsky
A.Q.K. Rajput

8. Performing Organization Report No.

9. Performing Organization Name and Address
University of Pittsburgh
Department of Electrical Engineering
Pittsburgh, PA 15260

10. Project/Task/Work Unit No.

11. Contract or Grant No.
J0318033

12. Sponsoring Organization Name and Address

13. Type of Report
Final Report

14.

15. Supplementary Notes

16. Abstract

Two channel polarity coincidence and polarity difference statistics are analyzed. The signal, common to both channels, consists of sinusoidal bursts where the exact frequency of the signal is nearly known, but other parameters such as amplitude, phase, and pulse starting time are unknown. The noise inputs are dependent, narrow band, Markov processes.

It is shown that the performance depends not only on the signal uncertainties, but on the precise shape of the cross-correlation functions between the noise inputs. By using two polairty difference statistics in addition to the polarity coincidence statistic, it is shown that the decrease in performance, as well as the cost of hard limiting due to correlated inputs, can be made small.

17. Originator's Key Words
Array Detectors
Correlated Noise Model
Polarity Coincidence Correlation

18. Availability Statement

19. U. S. Security Classif. of the Report	20. U. S. Security Classif. of This Page	21. No. of Pages	22. Price
		136	

FOREWORD

This report was prepared by the University of Pittsburgh under USBM Contract number J0318033. This contract is administered under the Department of Electrical Engineering with Morton Kanefsky as the Principal Investigator. John Durkin is the contract admistrator for the Bureau of Mines.

This final report is a summary of the work completed for this contract, during the period October 1980 to October 1981. This report was submitted by the authors on November 9, 1981.

TABLE OF CONTENTS

Summary

A prototype detector using electromagnetic signals for finding trapped miners has previously been built and tested. The signals used are generated from transmitters carried on the miner's belt and powered by his head lamp battery and the receiver is a human listener. This system has been found to be very efficient for the detection and location of trapped miners in most existing mines. However, for very deep mines, they are not adequate. Unfortunately, the signals employed (0.1 second bursts of a 1000 H, sinusoid repeated every second) while ideally suited for a human listener, is not useable for coherent detection schemes.

This study investigates the use of a noncoherent detector based on the polarity coincidence statistic. In this study the problem of location was not considered, only the problem of detection. Since this two input statistic was always used previously for two noise inputs that are essentially uncorrelated, and since this is hardly the case with electromagnetic signals, a principle goal of this work was to analyse the proposed detector for various kinds of correlated noise inputs. Furthermore, this detector is normally used with a random signal. While the signal cannot be presumed to be known with precision it is at least partially known. Another principle goal was to determine whether other statistics using delayed versions of one of the inputs is practical. It is also necessary to determine the effect of the signal uncertainties.

A general expression was derived for the detection parameter of the polarity coincidnece correlator, the inputs of which are assumed to consist of a common signal plus correlated, stationary gaussian noises. An expression

was obtained for the expectation of the product of four hard limited (clipped) gaussian inputs with arbitrary crosscorrelation, which is needed in order to evaluate the detection parameter of the PCC. A program to evaluate this expression has been implemented on the computer, evaluated and tested. This represents the most significant contribution of this study.

A general model for the kinds of cross-correlation functions that would result when passing two heavily correlated noise processes through identical band-pass filters was developed. Based on this model, the performance of the PCC was evaluated and compared with the unclipped correlator and the sum and square detector. The sum and square detector is a near optimum detector. For large positive values of cross-correlation, the unclipped correlator outperforms the sum and square detector, and so may be optimum in this range. We observed that, for positive cross-correlations, while the performance of all three detectors fall off substantially with an increase in the correlation coefficient, the cost of clipping relative to the optimum increases only slightly, increasing from 2db to 3 db as the correlation increases form 0 to 0.5. For negative crosscorrelation, while the unclipped correlator performed as before, the performance of the PCC and the sum and square detector increased as the magnitude of the correlation coefficient increased. As before, the cost of clipping compared to the optimum increases slightly. The increase in performance of the PCC is comparable for negatively correlated noise to the decrease for positively correlated noise.

The analysis is extended to two statistics, i.e., polarity coincidence and differences for 0.1 second duration sinusoidal bursts of nearly known frequency when the noise inputs are correlated. The decrease in performance relative to uncorrelated noise inputs is quite small. Indeed, for certain cross-correlation functions the performance increases. The increase in the

cost of clipping with the correlation coefficient is also quite small. For the worst case, and perhaps the most likely case, where the cross-correlation function is proportional to the autocorrelation, i.e., $R_{n_1 n_2}(\tau) = \alpha R(\tau)$, the degradation can be kept low using the polarity difference statistic. For $\alpha = 0.5$, the degradation compared to the independent case is about 1db. The cost relative to the sum and square detector, for this case also increases by only by 1db.

The detection parameter is proportional to the input signal-to-noise ratio. If we define the gain G as the ratio of the detection parameter to the input signal-to-noise ratio, it is determined that

$$G = G_o(1-D) \quad \gamma(\Delta\omega, \varepsilon\theta) \sqrt{T} \ .$$

G_o is the gain for one pulse for either the standard PCC or the other statistics considered where precise knowledge of the signal parameters are presumed.. It is precisely this gain that has been evaluated and compared with the unclipped detectors in the bulk of this report. D is the pulse sync error, $\gamma(\Delta\omega, \varepsilon\theta)$ is the degradation due to uncertainties in the signal such as frequency ($\Delta\omega$) and phase ($\varepsilon\theta$), and T is the integration time is seconds. The values of the gain for a single pulse are undoubtedly less than the gain of the human observer; perhaps by a factor of 2 or more. However, the human observer cannot accumulate information from one pulse to the next. Thus for example, after 100 seconds (or 100 pulses) the gain of the PCC statistic is improved by a factor of 10.

The pulse sync error D is always less the $\frac{5}{M}$ where M is the number of computation intervals chosen for each 1 second period. Thus, if this period is divided into 40 overlapping 0.1 second processing times, the degradation due to lack of pulse sync is at worst 7/8 which is acceptable. For the statistics considered in this study,

$$\gamma(o\omega, \varepsilon\theta) = \frac{\cos(m\pi \frac{\Delta\omega}{\omega} - \varepsilon\theta) - \rho_H}{1 - \rho_H}$$

where delays of $m\pi$ are presumed (i.e. polarity coincidences and differences only) and ρ_H is the correlation coefficient of the noise inputs. It is shown in this report that for $m = \pm 1$, the increase in G_o can be significantly larger than the decrease in γ. However, for large values of m this is not the case. Thus, this work suggests that three statistics should be used, the standard PCC and 2 polarity difference statistics.

Overall, the analysis is quite encouraging and strongly suggests that the proposed detector be implemented and tested.

LIST OF FIGURES

Figure No.

NOMENCLATURE

Symbol	Definition
H	Hypothesis that signal is absent
K	Hypothesis that signal is present
E	Expectation
D	Detection parameter
σ_s^2	Variance of the signal
σ_n^2	Variance of the noise
$n_1 n_2$	Noise inputs
N	Number of observations
s	Signal input
ρ	Correlation coefficient
Q(k)	$E[\text{sgn } x_1(t) \text{ sgn } x_2(t) \text{ sgn } x_1(t+k\tau) \text{ sgn } x_2(t+k\tau)]$
R(k)	Autocorrelation of noise
$R_{n_1 n_2}(k)$	Cross-correlation between n_1 and n_2
P(x)	Probability density
P	Represents correlation matrix
C_{ij}	Elements of P^{-1}
α	Magnitude of cross-correlation
γ	Determines the combination of odd and even cross-correlation function
a_o	Determines the combination of narrow band and wide band autocorrelation function
R	Input signal-to-noise ratio
C	Correlator
ss	Sum and square

PCC	Polarity coincidence correlation
$N, N(\omega)$	Noise spectrum
T	Integration time
B	Bandwidth of the signal
S	Test statistics
$S(\omega)$	Signal Spectrum
τ	Delay between inputs

1.0 INTRODUCTION

1.1 General Background on the Detection of an E.M. Source Buried in the Ground

The feasibility of finding trapped miners by detecting electromagnetic signals generated from transmitters carried on the miner's belt and powered by his head lamp has been investigated for roughly 10 years. Wait[1]* determined in 1971 that the location of a horizontal loop buried in a homogeneous earth can be determined from the horizontal and vertical magnetic field components at the earth surface. The geometry of this problem is shown in Figure 1. The horizontal magnetic component achieves a null and the vertical component a maxima directly above the loop. Based on these ideas, a detector was developed and a prototype built and tested.[2] While some location errors resulted from an inhomogeneous earth and non-horizontal earth interfaces, detection was achieved in almost all cases. For mines deeper than 1000 feet, of which there are few presently, detection itself becomes a problem.

The signals employed by these systems are 0.1 second long bursts of 1000 Hz sinusoids repeated every second. This signal is ideally suited for the constraints of the problem which are (a) long life (12 hours or so) for the transmitter, (b) low background noise power levels, and (c) signals that are most easily detected in noise by human listeners. For very deep mines, the human observer is an

*Parenthetical references placed superior to the line of the text refer to the bibliography.

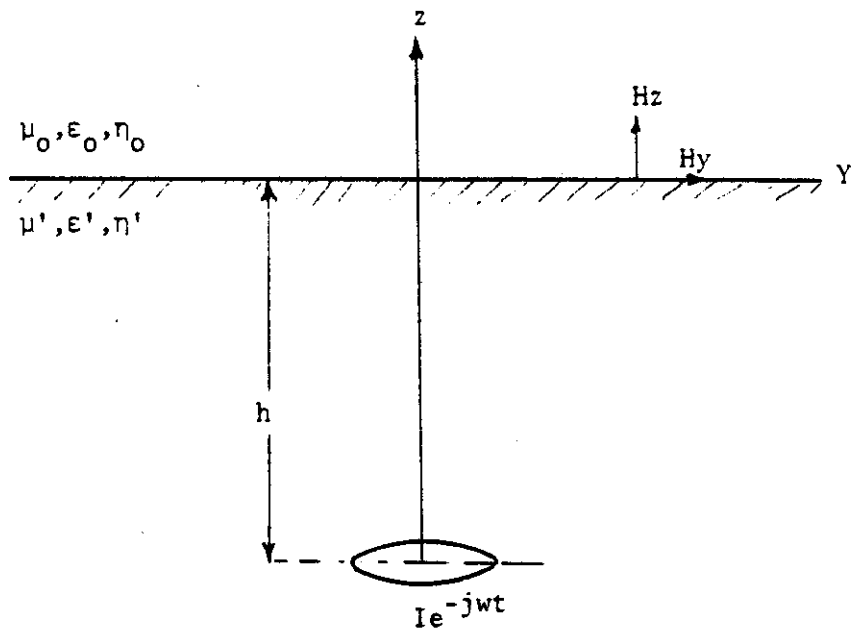

Figure 1. The geometry of horizontal loop buried at a deph of h.

inadequate detector and some kind of signal processing based on data accumulated over many seconds or minutes is required. It is not clear whether the processor should make the detection decision or merely preprocess and display the data in a form that a human observer, with his remarkably adaptive brain, can use for detection.

Coherent detection techniques, which presume accurate knowledge of the signal, are the most powerful. Unfortunately the signals used in the present system do not lend themselves to coherent reception. For one thing the frequency is much too high, relative to the skin depth of the earth, to presume accurate knowledge of the signal at the earth's surface. Also signal bursts, rather than continuous signals, complicate coherent detection. For these reasons most of the signal processing proposals and studies suggest very low frequency, less than 10 Hz, continuous signals.[3-5] While the level of the background noise is quite high, in this low frequency range, it is highly correlated in time and frequency and optimal coherent techniques could be very effective. There are a number of problems, however, with this approach. Even though most of the hardware complexity would involve the receiver, the transmitter would require precise timing references and be more expensive. Sophisticated techniques for reducing the heavy background noise and remaining phase locked with the signal rely on stationarity assumptions that may not always be valid. Perhaps most important, the signals employed cannot be heard by human listeners. This means that in the event of equipment failure, or for that matter a failure of the stationarity assumptions, a simple back-up of the human observer is not possible even for relatively shallow mines.

It is certainly important to study the feasibility of incoherent detection techniques using the same signals of the present prototypes. It should be remembered that the performance of any detector which accumulates or integrates data over some period of time (T) improves as T increases. Also the integration time of a coherent detector is limited by the uncertainty in the received signal. Beyond this limitation, integration must be incoherent in any event. Given the possibility of a sufficiently long decision time, say many minutes, a clever incoherent technique can be relatively efficient.

1.2 Analog Array Detectors

Optimum receivers for detecting the presence of a random signal common to two or more receivers with additive Gaussian noise have been discussed by Bryn and others.[6,7] Such an analysis is carried out in Appendix A where the noise inputs are presumed to have an arbitrary cross correlation function (i.e., they are not independent). It is determined in this Appendix that the optimum receiver is shown in Figure 2 where the + sign is employed when the signals are in phase and the - sign when they are 180° out of phase. Since the optimum filters depend on the signal-to-noise ratio, which is unknown, one usually implements the locally optimum detector (optimum as SNR → 0) which has the same structure with the filters replaced by

$$|H_{LOD}(jw)|^2 = \frac{S(\omega)}{N^2(\omega)} \frac{1}{[1 \pm \rho(\omega)]^2}$$

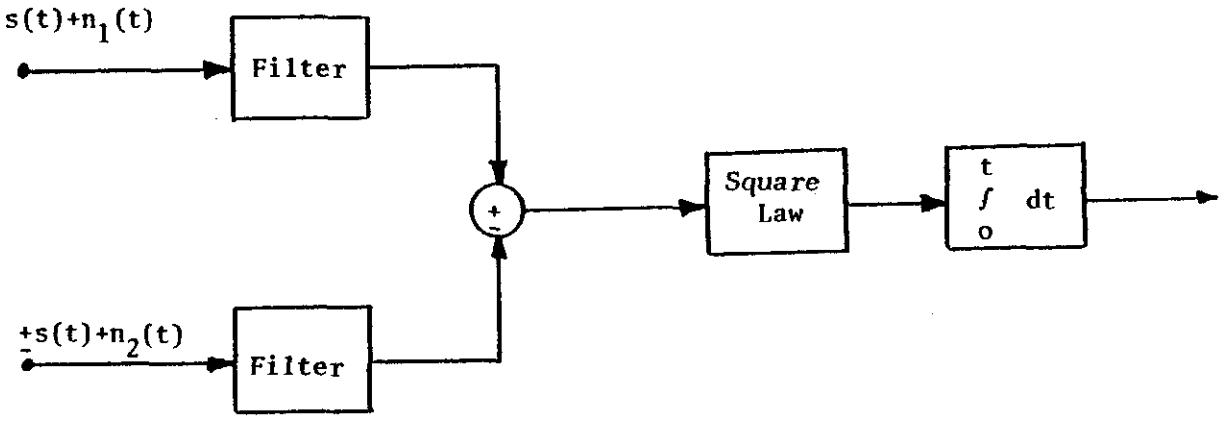

Figure 2. Block Diagram of Optimum Two-Channel Receiver.

Finally, since in our case the signal spectrum is quite narrow, the filters can be replaced with narrowband filters centered at 1,000 Hz. It is seen in Appendix A that the structure of the optimum detector, not the performance, is in fact independent of the degree of correlation between the noise inputs. In Appendix B, the output signal-to-noise ratio for this optimum detector is evaluated under the assumption of an arbitrary space/time noise correlation. It is assumed that the signals are either identical to both inputs or exactly 180° out of phase. The output signal-to-noise ratio is given by

$$SNR_{out} = SNR_{in} \sqrt{\frac{2T}{\frac{1}{2} \int_0^T (1 - \frac{k}{T})\, \psi(k,\tau)\, dk}} \qquad (1\text{-}1)$$

where T is the signal duration, τ the delay between inputs, and

$$\psi(k,\tau) = \{[\rho_{11}(k) + \rho_{22}(k)] \pm [\rho_{12}(k+\tau) + \rho_{12}(k-\tau)]\}^2 , \qquad (1\text{-}2)$$

where $\rho_{11}(\cdot)$ is the time autocorrelation function of each noise input and $\rho_{12}(\cdot)$ is the correlation function between the noise inputs.

We see that while the performance increases with signal duration, the extent of the improvement depends, in a rather complicated way, on the space/time noise correlation. It must be remembered that this receiver is said to be optimum under the assumption that the signal is random. However, for the locally optimum detector, the statistics of the signal need not be known. It is worth considering how this receiver compares with a coherent detector. In Appendix C the overly simplifying assumption that the cross-correlation between the noise

inputs is identically zero is made. This receiver is then compared with a one-channel ideal envelope detector (essentially equivalent to coherent detection) which accumulates the results of each pulse incoherently. It is found that the two-channel detector performs better particularly if the signal frequency is not known very accurately. Of course, if the inputs from two channels are summed prior to envelope detection and the signal frequency is known with precision, it will perform a little better than the non-coherent detector. This discussion is included as part of the justification for the use of a two-channel non-coherent detector. It must be shown, however, that when the noise inputs are heavily correlated, the degradation is not severe.

1.3 Polarity Coincidence Correlation (PCC)

Polarity coincidence correlation is a well documented technique for detecting a random signal imbedded in additive noise.[7-13] A detector which operates on the polarity coincidence of both channels is called a polarity coincidence correlator (PCC). The two-channel PCC, shown in Figure 3, "clips" both inputs and compares their polarities. If the polarities of two hard limited incoming signals tend to be the same, the decision that the signal is present is made.

We now make the point that for many two-channel acoustic applications the data is hard limited and the detection is made with a polarity coincidence correlator[8,10-12,15] or for signals 180° out of phase a polarity difference correlator. It is known that when the inputs are uncorrelated, the cost of this data reduction is quite

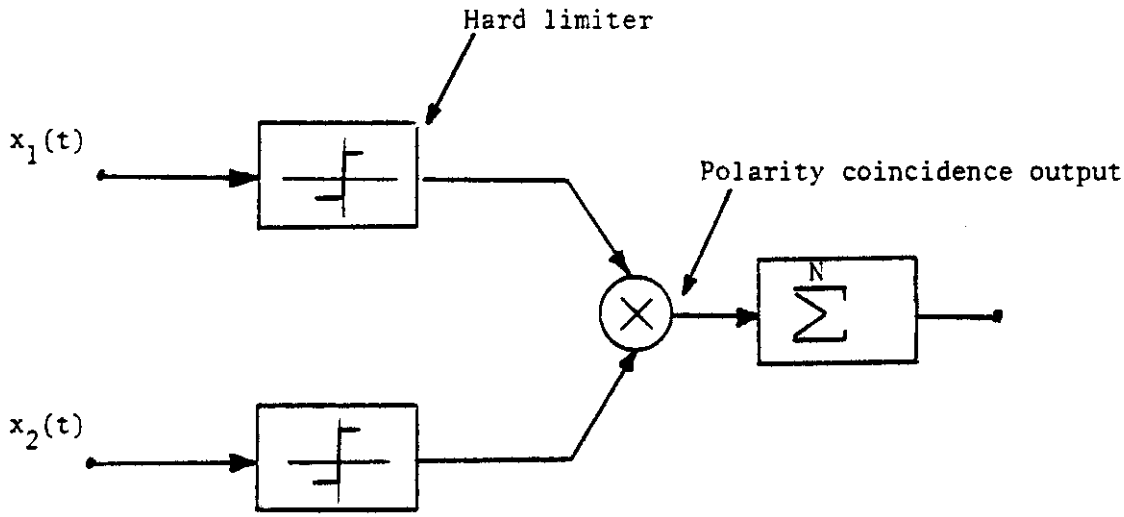

Figure 3. Block Diagram of Polarity Coincidence Correlator.

small (about 0.5 db).[16,17] There are two major advantages to compensate for this cost. The most obvious advantage is that the hardware complexity, both the data acquisition and the detector implementation, is greatly reduced. This makes the possibility of a small hand carried receiver quite feasible. A second advantage is that the hand limited receiver has certain nonparametric qualities, and indeed can outperform the so-called optimal receiver when the noise is impulsive rather than gaussian,[17-19] when the input samples are independent. Nonparametric detectors have test statistics under the hypothesis which are invariant over some class of noise process, and are therefore based on the assumption that the statistical properties of the noise are not completely known.[20] For fast sampling rate, however, the PCC is usually analyzed using the assumption of gaussian statistics. If the target, for independent noise, is not directly in line with the center of the array, the delays from the target to each receiver are sufficiently different to enable the location (bearing angle) of the target to be determined. Unfortunately, for electromagnetic signals with receivers reasonably close, the noise inputs at each receiver are heavily correlated and signal delays may be too small to measure. While the small delays mean that location by some kind of triangulation may be difficult, they have a benefit in that the signals at each receiver are nearly in phase if the horizontal coordinates of the transmitter is in the vicinity of those of the receivers.

If a delay of one half period (.5 m sec) is introduced in one channel, an equivalent detector determines polarity differences. Other statistics which compare coincidence of one pulse with those of

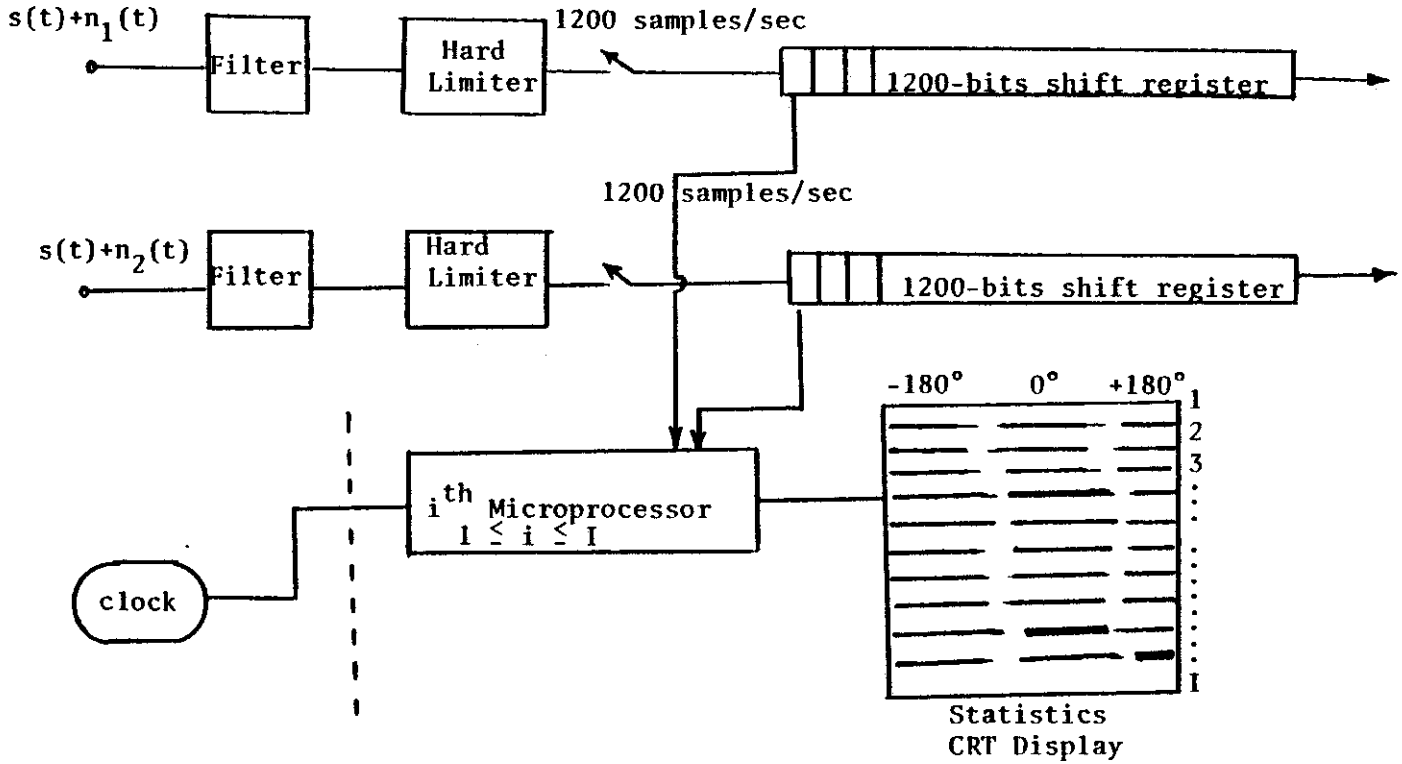

Figure 4. Architecture of Polarity Comparison Detector.

another may be more desirable. In fact a receiver that can implement many different statistics should be very useful. A receiver which has this flexibility and which overcomes the lack of pulse synchronization is shown in Figure 4. Each microprocessor, operating in parallel, assumes a particular pulse sync and accumulates data (1200 binary pulses per input) over 0.1 seconds. During much of the remaining 0.9 seconds, before the next pulse, a series of statistics are computed. These include polarity coincidences between simultaneous samples, and samples displaced by multiples of 1 m sec (or 1000 Hz cycles). Also, polarity differences between samples displaced by odd multiples of 0.5 ml sec are computed. Other statistics such as polarity coincidences with the data from a previously stored pulse can also be computed. These statistics can be accumulated and after some normalization displayed as a line on a CRT. The accumulation continues until either a target is visually observed, by a bright spot or line on the display, or the computations are stopped.

It is conceivable that, after detection, the inputs, perhaps sampled at a much faster rate, could be used for location via triangulation. In this event it should be noticed that the best statistic and pulse synchronization have been determined by the brightest spot.

1.4 Summary of Analysis

The detection parameter for weak input signals and noise is discussed in Chapter 2 and given by (D-13) in Appendix D as,

$$D_{pcc} = \frac{2/\pi \cdot \sqrt{N}\,[\mathrm{Sin}^{-1}\,\rho_K - \mathrm{Sin}^{-1}\,\rho_H]}{[1 - (2/\pi \cdot \mathrm{Sin}^{-1}\,\rho_H)^2 + 2 \cdot \sum_{k=1}^{N} (1 - \frac{k}{N})\,\{Q_H(k) - (2/\pi \cdot \mathrm{Sin}^{-1}\,\rho_H)^2\}]^{1/2}} \quad (1\text{-}3)$$

where

$$\rho_K = \frac{\sigma_s^2/\sigma_n^2 + \rho_H}{1 + \sigma_s^2/\sigma_n^2} \quad \text{and} \quad \rho_H = \frac{R_{n_1 n_2}(0)}{\sigma_n^2}$$

represent the correlation coefficient under the alternative and hypothesis respectively, $R_{n_1 n_2}(k)$ is the noise cross-correlation function, σ_s^2/σ_n^2 is the input signal-to-noise ratio, N refers to the number of sample accumulated by the test static, and

$$Q_H(k) = E_H\,\{\mathrm{Sgn}\ x_1(t)\ \mathrm{Sgn}\ x_2(t)\ \mathrm{Sgn}\ x_1(t+k\tau)\ \mathrm{Sgn}\ x_2(t+k\tau)\}\ . \quad (1\text{-}4)$$

Equation (1-3) is asymptotically valid as the input signal-to-noise ratio approaches zero. It can be extended to include finite values of σ_s^2/σ_n^2 provided the signal is gaussian as well as the noise. For non-gaussian signals, only the asymptotic evaluation is possible.

The technique for evaluating the expected value of the product of four hard limited functions (Equation 1-4) is discussed in Chapter 2 and carried out in Appendix D. This evaluation is one of the main contributions of this research, without which the only possible way of evaluating the PCC would have been extensive simulation. The solution of this problem is carried out by a computer algorithm. The memory required, computation time, and stability considerations are evaluated.

In order to test the programs, the PCC is analyzed in Chapter 3 for a first order Markov signal common to two dependent noise inputs, whose cross-correlation is proportional to the autocorrelation.

A general model of cross-correlation functions for narrow band and wide band noise process is developed in Chapter 4. Using this model, the PCC is evaluated for a wide variety of cross-correlation shapes in Chapter 5. There is shown to be a significant difference in the performance for even or odd cross-correlation functions.

The results are extended in Chapter 6 in a number of important ways. The signal is assumed to be an electromagnetic burst. Signals of this sort have been considered for the detection of trapped miners. The exact knowledge of this frequency is also not available because of variations in the transmitter. The frequency, in a two-channel receiver, can be assumed to be the same, but because of the different locations of the receivers, the amplitude and phase of the signals can be different in both channels. These uncertainties in the signal are the primary reason for considering a noncoherent PCC rather than a coherent receiver. Nevertheless, because the frequency is nearly known other statistics are possible. For example, by introducing a delay in one channel which causes a 180° phase shift and employing a polarity difference correlator, it is possible to get improved performance. The performance depends not only on the amplitudes and phase difference in the channels and more critically on the frequency uncertainty, but on the precise shape of the cross-correlation function.

In order to carry out such an analysis, the kinds of cross-correlation functions that would result when passing two heavily correlated noise processes through identical band pass filters are used. The PCC is first evaluated for identical input signals for a wide range of cross-correlation shapes, and is compared with the unclipped correlator and sum and square detectors. The sum and square detector is locally optimum when the inputs are independent. For dependent inputs, however, the unclipped correlator can, under certain conditions, outperform the sum and square detector. Next the cost due to differences in the amplitudes and phase of the signal as well as the uncertainty in both the frequency and pulse locations of the signal is analyzed. Finally, other statistics based on the fact that the frequency is nearly known are evaluated.

The main results of this analysis are:

1. The cost of clipping (i.e., the comparison between the PCC and analog devices) is quite modest even for significant amounts of cross correlation.
2. The degradation in performance due to the correlation between the inputs is not severe, particularly if one employs two polarity difference statistics in addition to polarity coincidence correlation. Statistics other than these three do not seem worthwhile.
3. The degradation in performance due to signal uncertainies can be made quite small.

These results convince the author that the use of the proposed modified PCC is quite feasible for the detection of the electromagnetic signals used by trapped miners.

2.0 EVALUATION OF THE OUTPUT SNR FOR A PCC

A detector is often evaluated by computing the output signal-to-noise ratio,

$$D = \frac{E_K(S) - E_H(S)}{\sqrt{Var_K(S)}} \tag{2-1}$$

where S is the test statistic, H refers to the hypothesis of noise only and K refers to the alternative of an additive signal common to both inputs. If one is only interested in a small input signal-to-noise ratio, this equation can be greatly simplified by replacing the variance of the test statistic under the alternative with the variance under the hypothesis. Assuming independent noise inputs, independent samples, and small signal power, the output signal-to-noise ratio becomes for gaussian statistics[8,9]

$$D_{pcc} = \frac{2}{\pi}\sqrt{N}\ \sin^{-1}\frac{\sigma_s^2}{\sigma_s^2+\sigma_n^2} \tag{2-2}$$

where σ_s^2/σ_n^2 is the input signal-to-noise ratio and N refers to the number of samples accumulated by the test statistics. For the unclipped correlator, the output signal-to-noise ration is $(\sigma_s^2/\sigma_n^2 \cdot \sqrt{N})$,[8,9] and the cost of clipping is $\pi/2$ or 2 db.

If one wishes to change some of the assumptions, particularly that of independent noise inputs and independent samples, it is necessary to examine the test statistic more closely.

$$S = \sum_{k=1}^{N} \text{sgn } x_1(t+k\tau) \text{ sgn } x_2(t+k\tau), \tag{2-3}$$

where sgn $x(t) = 1$ if $x(t) > 0$ and -1 if $x(t) < 0$, τ is the sampling interval, and where $x_1(t)$ and $x_2(t)$ refer to the two inputs. From Van Vleck[21] is is known that $E[\text{sgn } x_1(t) \text{ sgn } x_2(t)] = (2/\pi) \sin^{-1} \rho$ where ρ is the correlation coefficient between two inputs. If ρ_H and ρ_K represent the correlation coefficient under the hypothesis H and alternative K respectively, the output signal to noise ratio from (D-13) in Appendix D is

$$D_{pcc} = \frac{2/\pi \sqrt{N} \ [\sin^{-1} \rho_K - \sin^{-1} \rho_H]}{[1-\{(2/\pi)\sin^{-1} \rho_K\}^2 + 2 \sum_{k=1}^{N} [1-1/N][Q_K(k) - ((2/\pi)\sin^{-1} \rho_K)^2]]^{1/2}} \tag{2-4}$$

where

$$Q_K(k) = E_K [\text{sgn } x_1(t) \text{ sgn } x_2(t) \text{ sgn } x_1(t+k\tau) \text{ sgn } x_2(t+k\tau)] \tag{2-5}$$

Since $x_i(t)$ and $x_i(t+k\tau)$ become independent as k increases, it follows that

$$\begin{aligned} Q_K(k) &\underset{k\to\infty}{\to} E_K [\text{sgn } x_1(t) \text{ sgn } x_2(t)] \ E_K [\text{sgn } x_1(t+k\tau) \text{ sgn } x_2(t+k\tau)] \\ &= [(2/\pi) \sin^{-1} \rho_K)]^2 \end{aligned} \tag{2-6}$$

Hence the terms in the summation of equation 4 are decreasing to zero and since this summation can be truncated, the detection index ultimately depends on $\sqrt{N}$.

If the common noise inputs are assumed to be independent, $\rho_H=0$. For small signal power, the variance is evaluated under the assumption of the hypothesis and

$$D_{pcc} = \frac{2/\pi \sqrt{N} \sin^{-1} [\rho_K]}{[1+2 \sum_{k=1}^{N} (1-k/N) Q'(k)]^{1/2}} \qquad (2\text{-}7)$$

where $Q'_H(k) \simeq E_H[\text{sgn } x_1(t) \text{ sgn } s_1(t+k\tau)] E_H[\text{sgn } x_2(t) \text{ sgn } x_2(t-k\tau)]$

$$= [(\tfrac{2}{\pi}) \sin^{-1} \rho_n(k)]^2 ,$$

where $\rho_K = \dfrac{\sigma_s^2/\sigma_s^2}{1+\sigma_s^2/\sigma_n^2}$, $\rho_n(k) = \dfrac{R_n[k\tau]}{\sigma_n^2}$,

and $R_n(k\tau)$ is the autocorrelation of the noise.

For independent samples $[\rho_n(k)=0]$, equation (2-7) reduces to equation (2-2). Equation (2-7) has been evaluated for dependent samples,[7] where the cost of clipping has been found to decrease with an increase in sampling speed.

For either dependent noise inputs or large signal power, we must compute Q(k) which involves 16 integrals.

2.1 The Computation of Q(k)

The problem is to compute $E\{r(\underline{x})\}$ where

$$r(\underline{x}) = \prod_{i=1}^{4} \text{sgn } x_i(t_i)$$

and $\underline{x}$ is zero mean gaussian or

$$p(\underline{x}) = (2\pi)^{-2} [\det P]^{-1/2} \exp\{-(1/2) \sum_{i=j}^{4} \sum_{j=1}^{4} q_{ij} x_i x_j\}. \qquad (2\text{-}8)$$

The coefficients q_{ij} are the elements of P^{-1}, and both P and P^{-1} are symmetric [$q_{ij} = q_{ji}$]. Since r(x) is either +1 or -1 depending on which of the 16 "orthants" $\underline{x}$ lies in, it follows that

$$E\{r(\underline{x})\} = \sum_{\substack{8 \text{ orthants} \\ \text{where } r = +1}} \int\int\int\int p(\underline{x})dx - \sum_{\substack{8 \text{ orthants} \\ \text{where } r = -1}} \int\int\int\int p(\underline{x})d\underline{x} \; . \qquad (2\text{-}9)$$

By a simple change of variables, each of the 16 integrals can be written as

$$I \triangleq \int_{0000}^{\infty\infty\infty\infty} \int W(v)dv \quad , \qquad (2\text{-}10)$$

where W(·) is identical to p(·) with appropriate changes in the signs of the q_{ij} for $i \neq j$, and v is a dummy variable.

From (E-19) of Appendix E, equation (2-10) can be written as:

$$I = (2\pi)^{-2} [\det P]^{-1/2} \; q_{11}^{-2} \sum_{i=0}^{\infty} \sum_{j=0}^{\infty} \sum_{r=p}^{\infty} \sum_{k=0}^{i} \sum_{s=0}^{j} \sum_{m=0}^{i-k} \psi(i,j,r,k,s,m) \qquad (2\text{-}11)$$

where

$$\psi = \frac{2^{i+j+r-2} C_{12}^{k} C_{34}^{r} C_{23}^{s} C_{13}^{m} C_{24}^{j-s} C_{14}^{i-k-m} \Gamma(\frac{i+1}{2}) \Gamma(\frac{j+k+1}{2}) \Gamma(\frac{r+s+m+1}{2}) \Gamma(\frac{i+j+r-k-s-m+1}{2})}{(j-s)!\;(i-k-m)!\;k!\;s!\;m!\;r!} \qquad (2\text{-}12)$$

and $C_{ij} \triangleq \pm q_{ij}/q_{11}$, where the sign depends on which of the 16 orthants of the integral we are evaluating.

Observation reveals the Symmetry in Equation (2-9), which reduces the 16 integrals to 8. It is clear by examining equation (2-12), that the ψ (i,j,r,k,s,m) terms for each of these 8 integrals differ only in their signs. Thus we can write

$$E[r(\underline{x})] = 2[(2\pi)^{-2}[\det P]^{-1/2}C_{11}^{-2}] \sum_{i=0}^{\infty}\sum_{j=0}^{\infty}\sum_{r=0}^{\infty}\sum_{k=0}^{i}\sum_{s=0}^{j}\sum_{m=0}^{i-k}\psi'(i,j,r,k,s,m)\gamma \tag{2-13}$$

where ψ' corresponds to the ψ where all the C_{ij} are the normalized negative values of P^{-1} denoted by $\bar{C}_{ij}$ and γ can be determined to be

$$\gamma=[1-(-1)^{i-k-m+j-s+r}-(-1)^{m+s+r}+(-1)^{i-k+j}-(-1)^{k+j}+(-1)^{i-m+s+r}$$

$$+ (-1)^{k+m+j-s+r}-(-1)^{i}] . \tag{2-14}$$

Using the fact that $(-1)^{-k} = (-1)^{+k}$, this can be simplified to

$$\gamma = \begin{cases} 0 \text{ if either i, } (x + s + r), \text{ or } (k + j) \text{ is even,} \\ 8 \text{ if i, } m + s + r, \text{ and } k + j \text{ are all odd.} \end{cases} \tag{2-15}$$

Changing variables ($x \triangleq m + s + r$ and $y \triangleq k + j$) and recognizing that

$\Gamma(\frac{n+1}{2}) = (\frac{n-1}{2})!$ for n an odd integer, equation (2-13) becomes

$$E\{r(\underline{x})\} = \pi^{-2}[\det P]^{-1/2}C_{11}^{-2} \sum_{\substack{i=0\\ \text{odd}}}^{\infty}\sum_{j=0}^{\infty}\sum_{r=0}^{\infty}\sum_{\substack{y=j\\ \text{odd}}}^{i+j}\sum_{s=0}^{j}\sum_{\substack{x=r+s\\ \text{odd}}}^{r+s+i+j-y} \cdot$$

$$\cdot\alpha(i,j,r,y,s,x)\ \beta(i,j,r,y,s,x), \tag{2-16}$$

where

$$\alpha(i,j,r,y,s,x) = \frac{2^{i+j+r}\left(\frac{i-1}{2}\right)!\left(\frac{y-1}{2}\right)!\left(\frac{x-1}{2}\right)!\left(\frac{i-x-y+2j+2r-1}{2}\right)!}{(j-s)!(i+j+s+r-x-y)!(y-j)!s!(x-s-r)!r!} \quad ,$$

$$\text{and } \beta(i,j,r,y,s,x) = \bar{C}_{12}^{y-j}\ \bar{C}_{34}^{r}\ \bar{C}_{23}^{s}\ \bar{C}_{13}^{x-s-r}\ \bar{C}_{24}^{j-s}\ \bar{C}_{14}^{i+j+s+r+-x-y} \qquad (2\text{-}17)$$

Computing $E\{r(\underline{x})\}$ by equation (2-16) is computationally simpler and requires significantly less CPU time than computing each integral I via equation (2-11).

2.2 Stability Considerations and CPU Time Requirement

2.2.1 Truncation and Stability

The infinite summations of equation (2-16) have to be truncated to a finite interval T, forcing a compromise between CPU time and truncation error. The truncation error is more severe the more the inputs are correlated. For a strong, additive, Markov signal that is common to two independent, white noise inputs, the relative truncation error of equation (2-16) is plotted in Figure 5 for k=1 (the worst case) and an input signal-to-noise ration of 0.5 as a function of the truncation T. The overall error in computing the detection parameter of equation (2-4) is considerably less. Since the $\underline{i}$ summation in equation (2-16) is evaluated only for odd values, it is not surprising that significant decreases in truncation error occur for odd values of T. For T=5, the relative error for k=1 is about 1%, the overall error in the evaluation of equation (2-4) is an order of magnitude better.

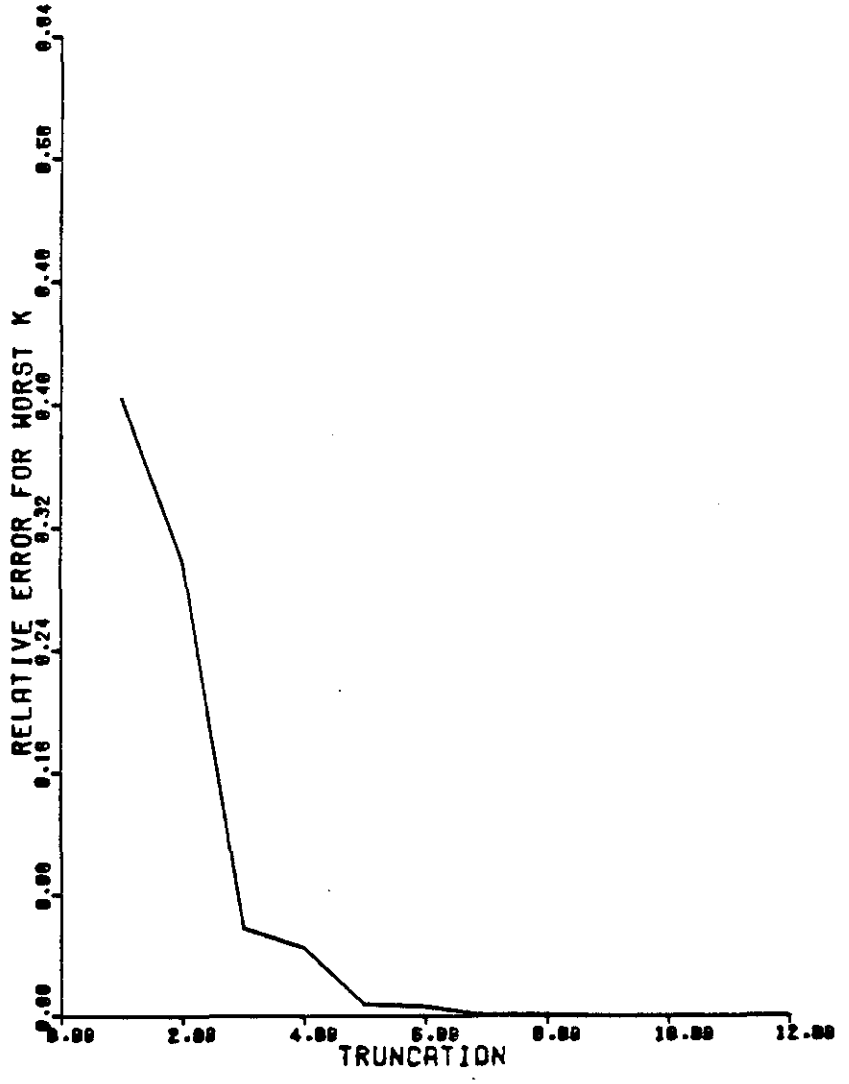

Figure 5. Dependence of relative error on truncation

There is no need to consider a truncation T greater than 9. In fact, the observations reveal that for most cases, equation (2-16) will converge very fast. However, for small signal-to-noise ratios and heavily correlated noise inputs of the order of 0.6 and more, and for small values of k ($1 \leq k \leq 3$), equation (2-16) does not converge as the truncation is increased. In this unstable region (which is evident from the eigen values of the P^{-1} matrix and hence can be isolated) computation approximations may or may not be possible.

The computations can be made stable with rapid convergence if the diagonal elements of the P matrix are all increased sufficiently. If the results of this computation are compared with the true results for those values where convergence is no problem, approximation can often be made. Such a comparison is shown in Figure 6 for $\alpha = 0.6$, where the approximations for the three points where convergence did not take place are self evident.

While there may well be problems for which our solution fails because of lack of convergence, we anticipate that for a wide class of problems convergence will take place or can be approximated.

2.2.2 CPU Time Requirement

The CPU time required to evaluate Equation (2-16) is plotted in Figure 7 for various truncation values. Since this time is essentially independent of k, this plot (appropriately scaled) also represents the overall CPU time required to compute the detection parameter D_{pcc}. We observe 15-fold an increase in CPU time when T was increased from 5 to 9.

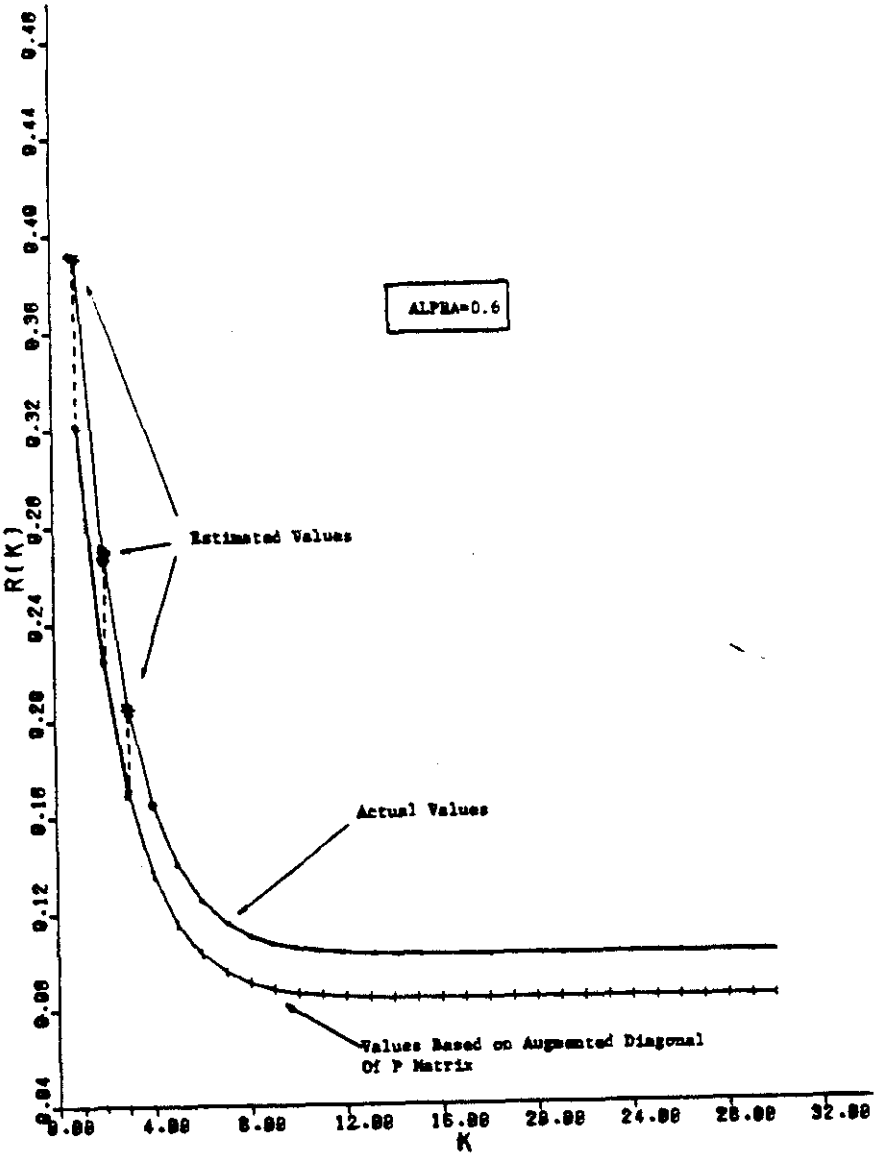

Figure 6. Approximation of R(k)

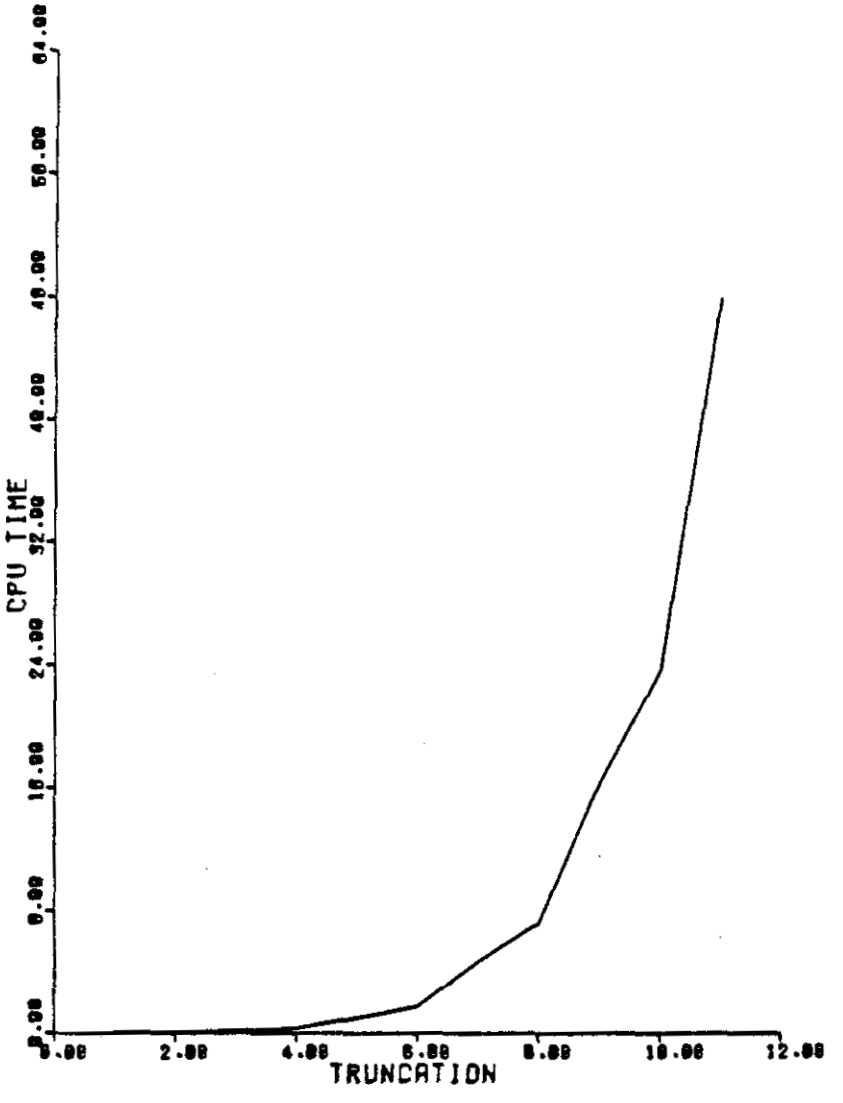

Figure 7. Dependence of CPU time on truncation

The evaluation of the detection parameter of equation (2-4) requires the computation of Q(k) N times. Therefore, if it takes n seconds to compute Q(k) via equation (2-16), the total CPU time will be nN seconds. This time can be greatly reduced, however, by using the following two procedures.

For different values of k, the only part of equation (2-16) that changes is the $\beta(i,j,r,y,s,x)$ terms. Therefore, we can calculate all of the $\alpha(i,j,r,y,s,x)$ terms and store them in a one-dimensional array. The time to compure Q(k) is greatly reduced by this time. This procedure does increase the core storage requirement as shown in Table 1.

TABLE 1

Truncation T	5	7	9	11
Core Storage Required for the α terms (words)	1098	5120	17,375	47,880

For the Markov process, and typically in general, the correlation between input samples decreases as k increases, and, for k large enough, Q(k) approaches a limit. Therefore, PCU time can be further reduced by finding k=I in equation (2-4) beyond which Q(k) remains nearly $[(2/\pi)\ \sin^{-1}\ \rho_k]$. Thus the summation of equation (2-4) is partitioned into:

$$\sum_{k=1}^{I} (1-k/N)[Q(k)-[(2/\pi)\ \sin^{-1}\rho_K]^2 + \sum_{k=I+1}^{N} (1-k/N)[(2/\pi)\ \sin^{-1}\ \rho_K)^2 - [(2/\pi)\ \sin^{-1}\ \rho_K)^2 = \sum_{k=1}^{I} (1-k/N)(Q(k)-[(2/\pi)\ \sin^{-1}\ \rho_K)^2] \quad (2\text{-}18)$$

and we need to compute Q(k) only I times.

For most cases, the value of I = 30 in equation (2-18) was found to be adequate and the total CPU time to compute the detection parameter in equation (2-4) by using T = 5 on the DEC-10 computer, in Fortran-10 language, was 30 seconds. However, if the input data in any channel is to be shifted, for more accurate results, the I in equation (2-18) should be increased by that amount.

3.0 PERFORMANCE OF PCC AND COMPARISONS WITH UNCLIPPED DETECTOR

3.1 Large Signals with Two Independent White Noise Inputs

The output signal-to-noise ratio of the PCC has been evaluated under the assumption of white independent noise and a common Markov signal. The correlation coefficients between signal samples $k\tau$ seconds apart are assumed to be $e^{-k/4}$. Since a gaussian Markov process has an autocorrelation function of the form $\sigma_s^2 e^{-2\pi B|\tau|}$, where B is the signal bandwidth, this corresponds to a sampling rate of $8\pi B$. This is sufficiently fast in that the output signal-to-noise ratio cannot be increased by faster sampling.[10] The covariance matrix P used to evaluate equation (2-16) is

$$P = \sigma_x^2 \begin{bmatrix} 1 & \rho_K & \rho_K e^{-k/4} & \rho_K e^{-k/4} \\ \rho_K & 1 & \rho_K e^{-k/4} & \rho_K e^{-k/4} \\ \rho_K e^{-k/4} & \rho_K e^{-k/4} & 1 & \rho_K \\ \rho_K e^{-k/4} & \rho_K e^{-k/4} & \rho_K & 1 \end{bmatrix} \qquad (3\text{-}1)$$

where $\sigma_x^2 = \sigma_s^2 + \sigma_n^2$ and $\rho_K = \dfrac{\sigma_s^2}{\sigma_s^2 + \sigma_n^2}$

The detection parameter D_{pcc} of equation (2-4), or output signal-to-noise ratio, is ploted in Figure 8 as a function of the input signal-to-noise ratio. Shown in the same figure is the detection

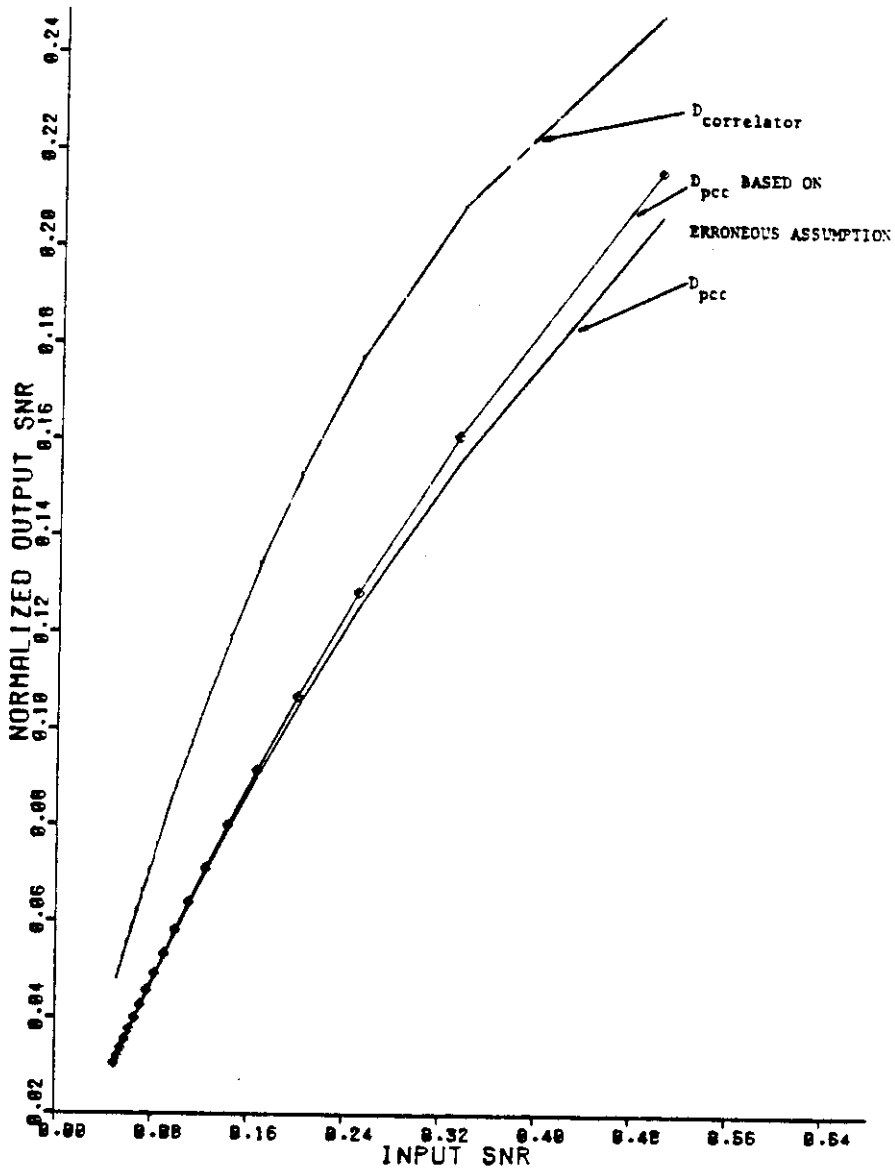

Figure 8. Performance comparison of PCC and unclipped Correlator

parameter based on the erroneous assumption of equation (2-7) or small input signal-to-noise ratios, as well as the performance for the unclipped correlator, which is

$$D_c = \frac{\sqrt{N}\, R}{\sqrt{\mathrm{Var}(S)}} \tag{3-2}$$

where $$\mathrm{Var}(S) = 1+2R^2\left[1 + 2 \sum_{k=1}^{N} \left(1 - \frac{k}{N}\right) \cdot e^{-k/2}\right] + 2R, \tag{3-3}$$

and $R = \sigma_s^2/\sigma_n^2$ input signal-to-noise ratio.

It can be seen that the assumption of small input signal-to-noise ratios appears valid over a wide range. Actually the error in the variance calculation is compensating the error in the numerator.

All three curves are continued in Figure 9 for large input signal-to-noise ratios. The difference between the PCC performance and the correlator, or the cost of clipping, is plotted in decibels in Figure 10. For large input signal-to-noise ratios the cost of clipping decreases.

3.2 Small Signals with Correlated Noise Inputs

3.2.1 Inputs Positively Correlated

In this example, the signal is assumed to be weak so that the variance of the test statistic can be evaluated under the hypothesis. Thus, equation (2-4) and (2-5) are closely approximated by

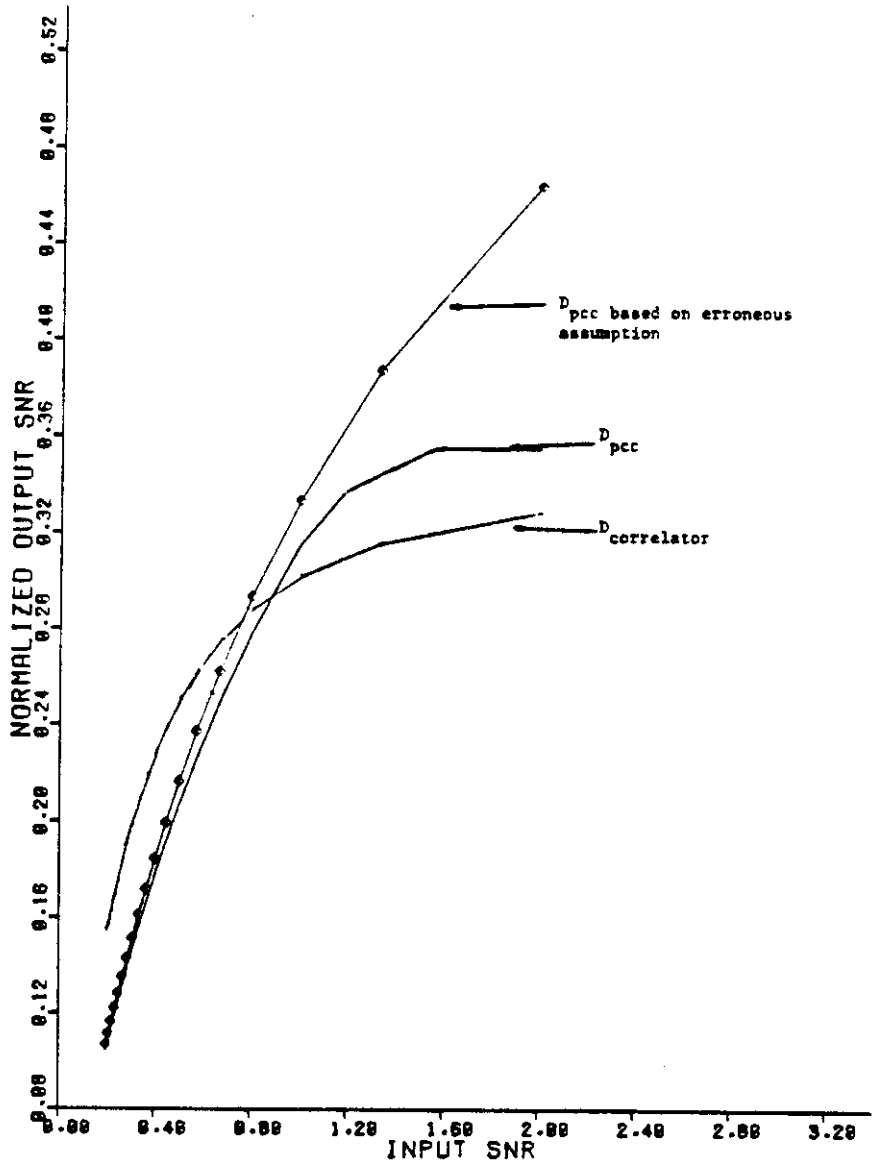

Figure 9. Performance comparison of PCC and unclipped Correlator for large input signals

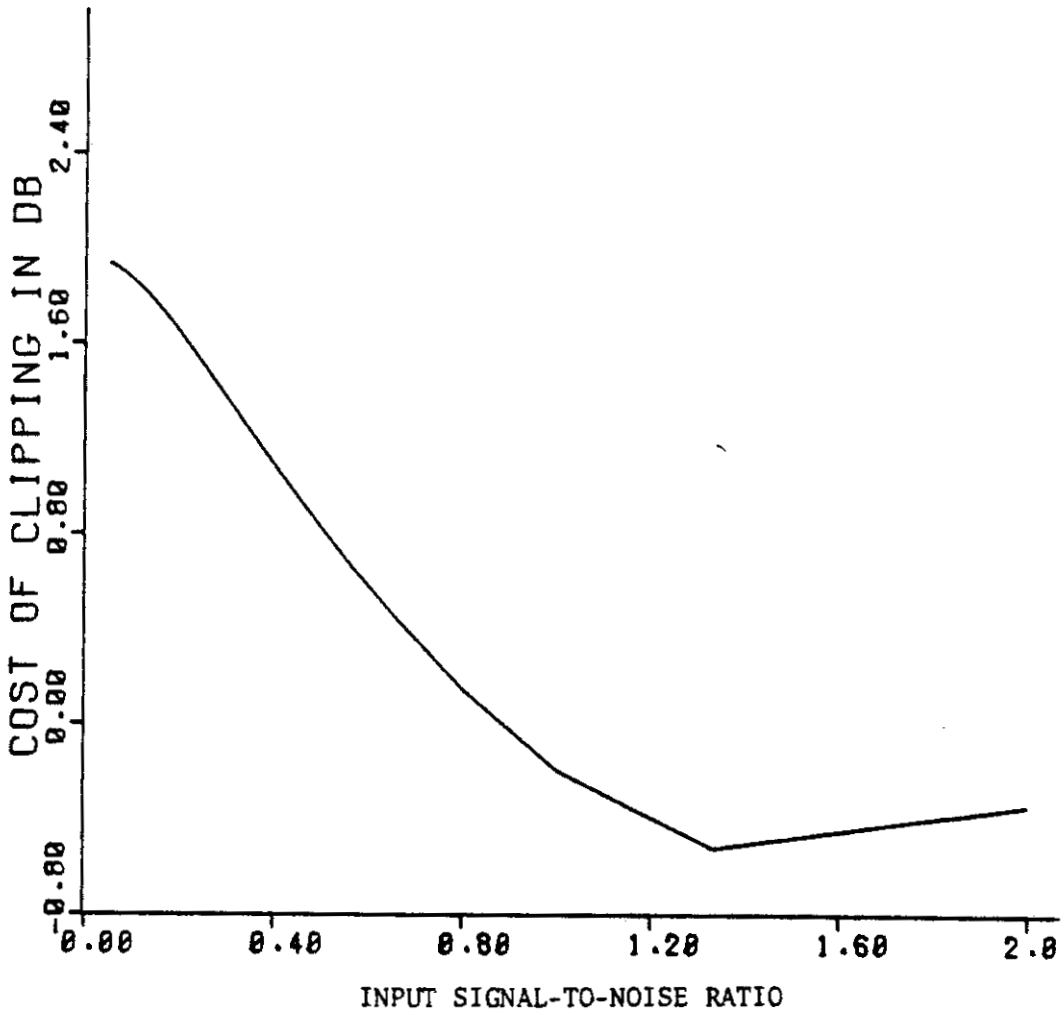

Figure 10. Cost of clipping versus input SNR

$$D_{pcc} \simeq \frac{2/\pi \sqrt{N} \left(\sin^{-1} \rho_K - \sin^{-1} \rho_H\right)}{\left[1-\{(2/\pi) \sin^{-1} \rho_H\}^2 + 2 \sum_{k=1}^{N} (1- \frac{k}{N})\{Q(k)-((2/\pi) \sin^{-1} \rho_H)^2\}\right]^{1/2}} \tag{3-4}$$

where $Q(k) = E_H \{\text{sgn } n_1(t) \text{ sgn } n_2(t) \text{ sgn } n_1(t+k\tau) \text{ sgn } n_2(t+k\tau)\}$. (3-5)

We will assume that $\rho_H = E[n_1(t)n_2(t)]/\sigma_n^2 = \alpha$ where α ranges from 0 to 1. More specifically we will assume that the noise inputs are rapidily varying Markov processes $[R_n(k\tau) = \sigma_n^2 e^{-k/4}]$ and the crosscorrelation function between them is $R_{n_1n_2}(k\tau) = \sigma_n^2 \alpha e^{-k/4}$. The analysis in no way depends on these assumptions, rather they are made as an example. ρ_K in equation (3-4) becomes $(\sigma_s^2/\sigma_n^2+\alpha)/(1 + \sigma_s^2/\sigma_n^2)$.

Using Taylor's expansion it is seen that $\sin^{-1}\rho_K \simeq \sin^{-1} \alpha + \sqrt{\frac{1-\alpha}{1+\alpha}}\, \sigma_s^2/\sigma_n^2$. Thus equation (3-4) becomes

$$D_{pcc} \simeq \frac{2/\pi \sqrt{\frac{1-\alpha}{1+\alpha}} \sqrt{N}\, \sigma_s^2/\sigma_n^2}{\left[1-(2/\pi\sin^{-1}\alpha)^2 + 2 \sum_{k=1}^{N} (1- \frac{k}{N}) \{Q(k)-(2/\pi\sin^{-1}\alpha)^2\}\right]^{1/2}} \tag{3-6}$$

The covariance matrix for this example is

$$P = \sigma_n^2 \begin{bmatrix} 1 & \alpha & e^{-k/4} & \alpha e^{-k/4} \\ \alpha & 1 & \alpha e^{-k/4} & e^{-k/4} \\ e^{-k/4} & \alpha e^{-k/4} & 1 & \alpha \\ \alpha e^{-k/4} & e^{-k/4} & \alpha & 1 \end{bmatrix} \tag{3-7}$$

The detection parameter D_{pcc}, or output signal-to-noise ratio, is plotted in Figure 11 as a function of the amount of positive cross-correlation. Shown in the same figure are the performance of the unclipped correlator and the sum and square detector, whose detection parameters can be derived from equation (D-20) and equation (D-25) of Appendix D, respectively as follows:

$$D_c = \frac{\sqrt{N}\,\sigma_s^2/\sigma_n^2}{\sqrt{(1+\alpha^2)\left[1+2\sum_{k=1}^{N}(1-k/N)\,e^{-2\alpha_0 k}\right]}} \qquad (3\text{-}8)$$

and

$$D_{ss} = \frac{\sqrt{2N}\,\sigma_s^2/\sigma_n^2}{(1+\alpha)\sqrt{1+2\sum_{k=1}^{N}(1-k/N)\,e^{-2\alpha_0 k}}}\ , \qquad (3\text{-}9)$$

where α can be positive or negative.

c = correlator

ss = sum and square

As expected, the performance of all three detectors fall off as the noise correlation increases. The cost of clipping in decibels is shown in Figure 12. It can be observed that while the performance of both the PCC and the sum and square detector fall off sharply with an increase in correlation, the cost of clipping does not change substantially, increasing from 2db to 3db for the assumed sampling rate and α=+0.5. The performance of the unclipped correlator does not fall off as sharply and, for a sufficiently high correlation coefficient, it outperforms the "sum and square" detector.

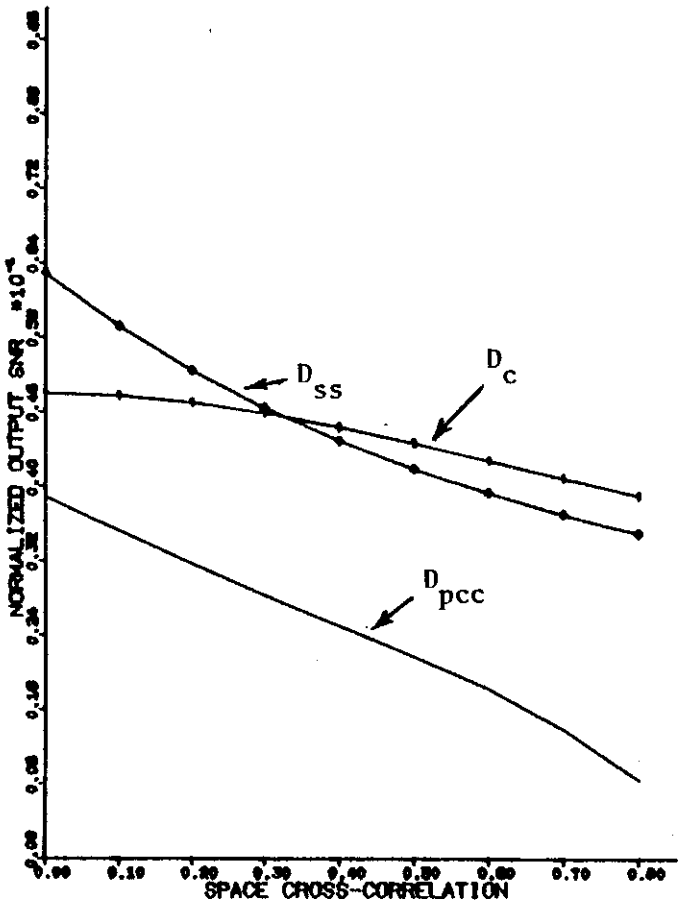

Figure 11. Performance comparison for positively correlated inputs

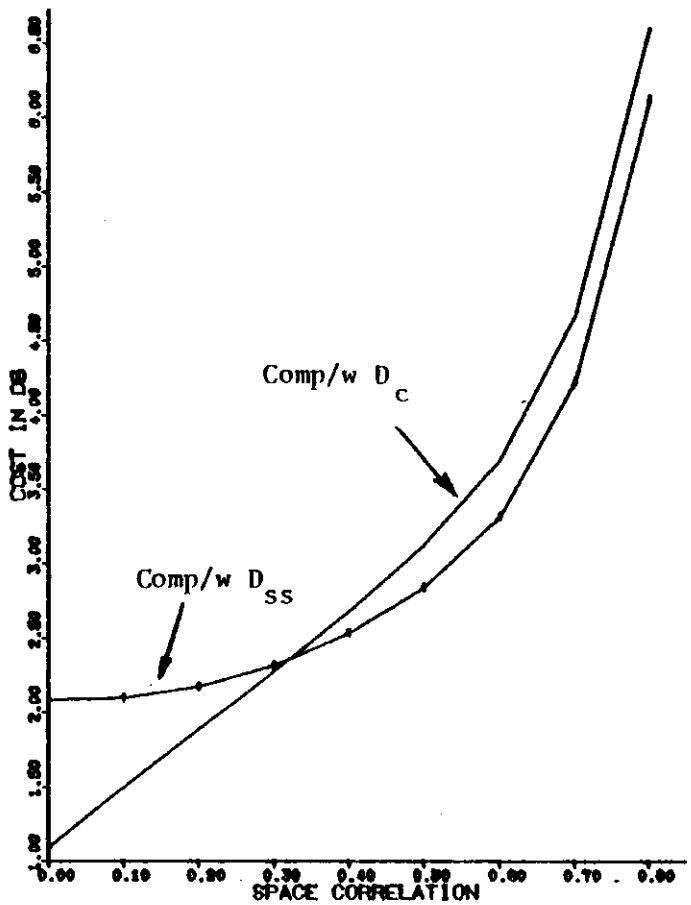

Figure 12. Cost of clipping

3.2.2 Inputs Negatively Correlated

Because the results are quite different for negative cross-correlations, the evaluations of all three detectors is discussed separately.

All three detection parameter curves are repeated in Figure 13 for negative α. The cost of clipping is shown in Figure 14. In this case the performance of the PCC and the "sum and square" detectors increase by roughly the same amount (the cost of clipping is between 2db and 3db for α=-0.5). The increase in performance is essentially the same amount for negatively correlated noise as the decrease for positively correlated noise. The unclipped correlator performs the same for negative as for positive cross correlations and is, therefore, less attractive for negatively correlated noise inputs.

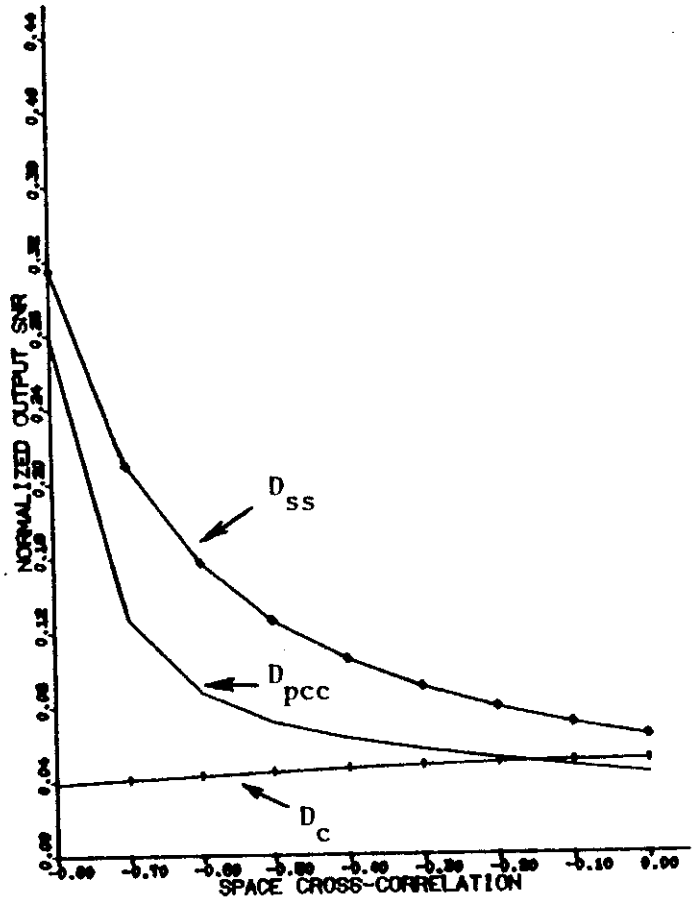

Figure 13. Performance comparison of PCC with unclipped detectors for negatively correlated inputs

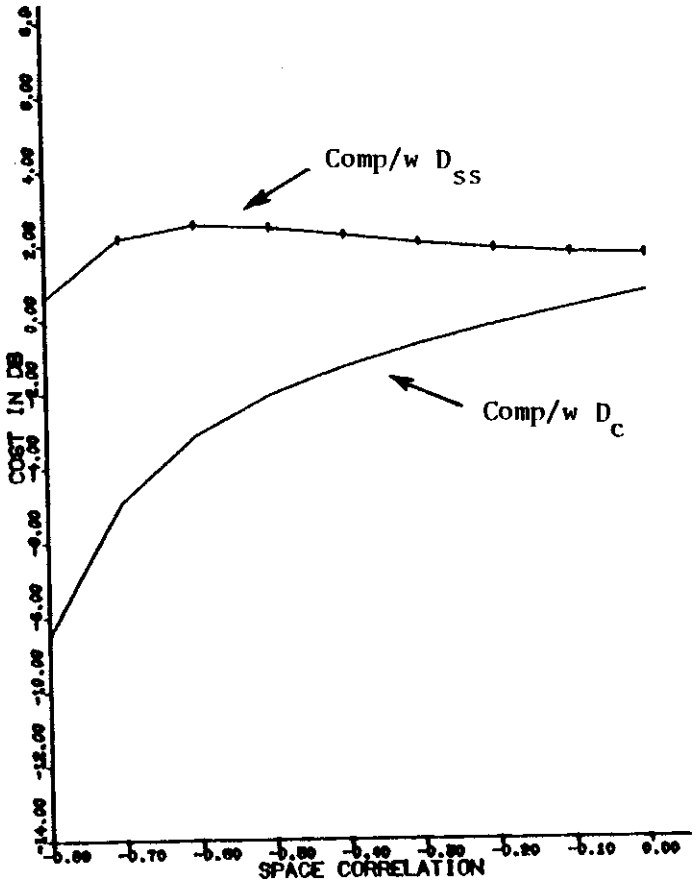

Figure 14. Cost of clipping

4.0 MODELING OF TWO CORRELATED NOISE PROCESSES

4.1 Narrow Band Noise Processes

Consider two correlated noise processes $n_i(t)$ that have been passed through identical narrow band filters whose transfer functions are both $H(f)$.

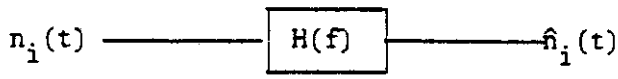

The output spectra are given by

$$S_{\hat{n}_i}(f) = S_{n_i}(f) \mid H(f)\mid^2 \quad , \qquad i=1,2$$

and

$$S_{\hat{n}_1\hat{n}_2}(f) = S_{n_1n_2}(f) \mid H(f)\mid^2 \quad , \tag{4-1}$$

where $S_{\hat{n}_1}(f)$ and $S_{\hat{n}_2}(f)$ are real and even.

If it is assumed that they are constant in the vicinity of the filter, then

$$S_{\hat{n}_1}(f) = S_{\hat{n}_2}(f) = k \mid H(f)\mid^2 \quad , \tag{4-2}$$

and

$$R(t) \cong k \int_{-\infty}^{\infty} \mid H(f)\mid^2 \cos\omega t \, df. \tag{4-3}$$

Substituting the low pass equivalent

$$H(f) = 1/2\ H_{LP}(f - f_o) + 1/2\ H_{LP}(f + f_o) \tag{4-4}$$

Equation (4-3) can be changed to

$$R(t) \cong \frac{k}{2} \int_{-\infty}^{\infty} |H_{LP}(f)|^2 \cos 2\pi f_o t \cos 2\pi f t\ df$$

$$= R_{LP}(t) \cos 2\pi f_o \quad . \tag{4-5}$$

For a first order low equivalent

$$R(t) = R(o) \cdot e^{-\lambda|t|} \cos 2\pi f_o t \quad . \tag{4-6}$$

$S_{\hat{n}_1\hat{n}_2}(f)$ does not have to be real and even but its inverse must be real. Let

$$S_{\hat{n}_1\hat{n}_2}(f) = S_{even}(f) + j\ S_{odd}(f) \quad , \tag{4-7}$$

where $S_{even}(f)$, $S_{odd}(f)$ are both real (and denoted $S_e(t)$ and $S_o(f)$ for convenience). The inverse transform of $S_e(f)$ is real and even and the inverse transform of $j\ S_o(f)$ is real and odd.

$$R_{n_1n_2}(t) = R_e(t) + R_o(t) \tag{4-8}$$

By definition

$$R_{n_1n_2}(t) = \int_{-\infty}^{\infty} |H(f)|^2\ S_{\hat{n}_1\hat{n}_2}(f)\ (\cos wt - j \sin wt)\ df, \tag{4-9}$$

Substituting (4-7) in (4-9)

$$R_{n_1n_2}(t) = \int_{-\infty}^{\infty} |H(f)|^2 S_e(f) \cos wt \, df + \int_{-\infty}^{\infty} |H(f)|^2 S_o(f) \sin wt \, df .$$

Using the low pass equivalents and assuming that $S_e(f)$ and $S_o(f)$ are nearly constant in the vicinity of f_o and $-f_o$, one obtains

$$R_{n_1n_2}(t) \cong a\int_{-\infty}^{\infty} |H_{LP}(f)|^2 \sin wt \cos 2\pi f_o t \, df + b\int_{-\infty}^{\infty} |H_{LP}(f)|^2 \sin wt \cos 2\pi f_o t \, df$$

$$\cong [aR_{LP}(t) + b\hat{R}(t)] \cos 2\pi f_o t \qquad (4\text{-}10)$$

where

$$\hat{R}(t) = \int_{-\infty}^{\infty} |H_{LP}(f)|^2 \sin wt \, df \quad . \qquad (4\text{-}11)$$

Equation (4-11) in general has no closed form solution. In order to simplify the model, we assume instead,

$$\hat{R}(t) = \text{sgn}(t) \, (1-e^{-\beta|t|}) \, R_{LP}(t) \qquad (4\text{-}12)$$

In fact the inverse of the above expression is not equavalent to an imaginary constant in the vicinity of fo. The shape is nontheless similar to a numerical computation of equation (4-11). Therefore, the simplified model becomes.

$$R_{n_1n_2}(k) = \alpha[(1-\gamma) \, \text{sgn}(k) \, (1-e^{-\beta|k|}) + \gamma] \, R(k) \quad . \qquad (4\text{-}13)$$

Thus α is related to the magnitude of the correlation and $\gamma (0 \leq \gamma \leq 1)$ determines the proportion of even and odd terms. When $\gamma = 1$, $R_{n_1n_2}(k)$ is proportional to R(k) and the proportionality constant becomes the

correlation coefficient. When $\gamma = 0$, $R_{n_1 n_2}(k)$ is an odd function whose shape has similar characteristics to R(k). The magnitude of the cross-correlation is proportional to α, but α can no longer be considered the cross-correlation coefficient. For γ between 0 and 1, a wide variety of shapes are possible, all of which have characteristics resembling R(k).

In Figure 15 the auto correlation R(k) has been plotted, which is an even function. In Figure 16 (a,b,c), α is set equal to 1 and γ is set equal to 0, 0.5, 1 respectively. The resulting curves give some idea of the possible shapes. For these curve β was set equal to 4, fo = 1000 Hz, the filter bandwidth = 500 Hz, and the sampling rate 12000 Hz. We shall see that a sampling rate of 12xfo is quite reasonable.

4.2 Wide Band Noise Processes

The autocorrelation function in equation (4-6) is extended from the low-pass Markov process to a combination of a low-pass Markov process and a band-pass process by defining

$$R(k) = a_0 e^{-\frac{|k|}{4}} + (1-a_0) e^{-\frac{|k|}{8}} \cdot \cos(\pi/6k) \ . \qquad (4\text{-}14)$$

The parameter a_0 is allowed to vary from 0 to 1 and for a_0=0 equation (4-14) is the same as equation (4-6) and the cross-correlation model in equation (4-13) is the narrow band noise process. For γ and a_0 between 0 and 1, a wide variety of shapes are possible, all of which have characistics resembling R(k).

In figures 16(d,e,f,g,h,i), α is set to 1 and a_0 is set to (0.5, 1) while γ is set to equal 0, 1/2, and 1. In general the resulting 6

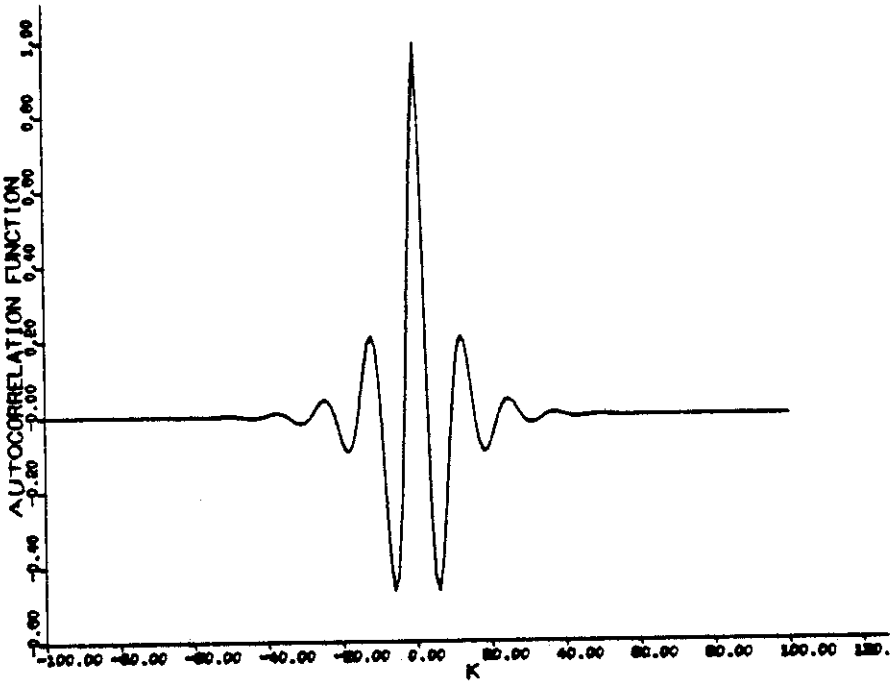

Figure 15. Autocorrelation function for A0=0

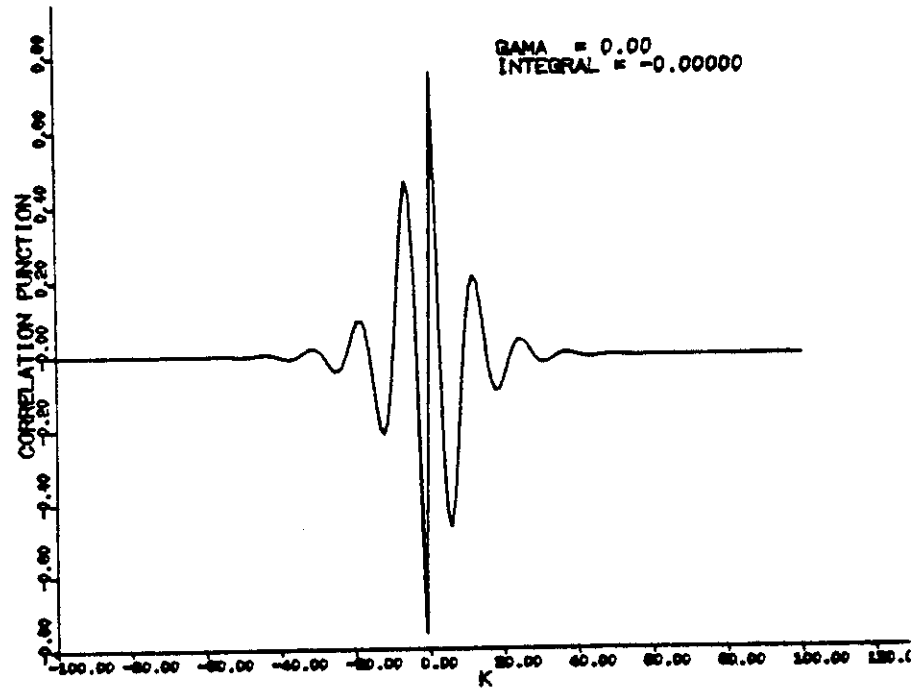

Figure 16. (a) Cross-correlation function

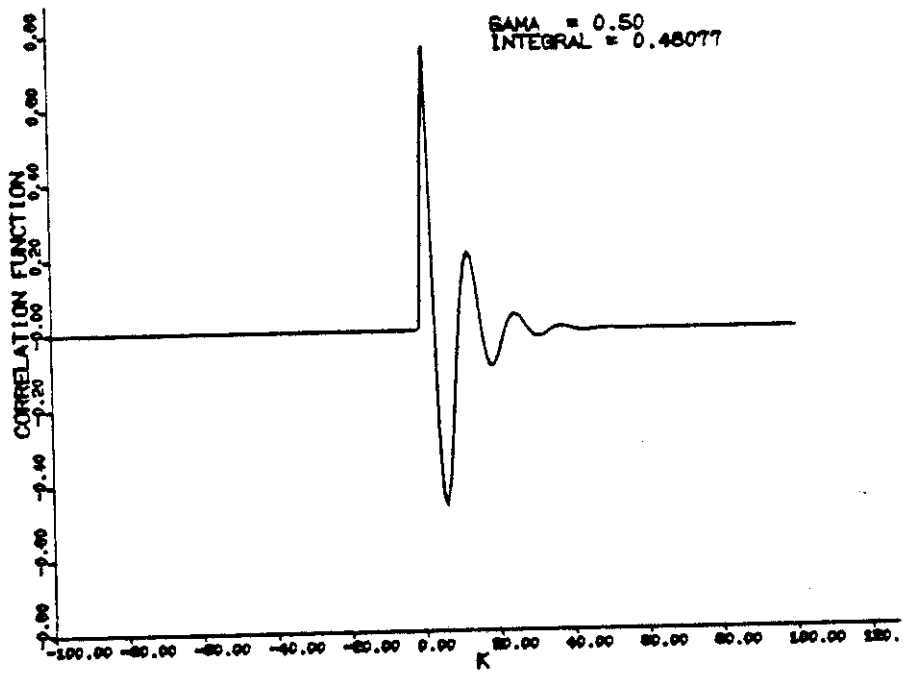

(b) Cross-correlation function

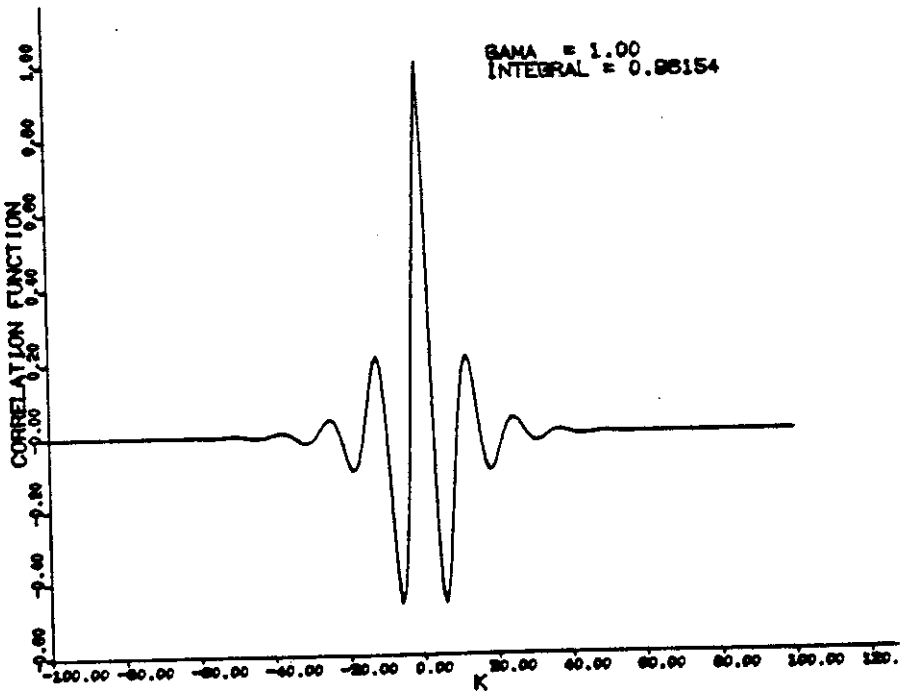

(c) Cross-correlation function

Figure 16 (cont'd.)

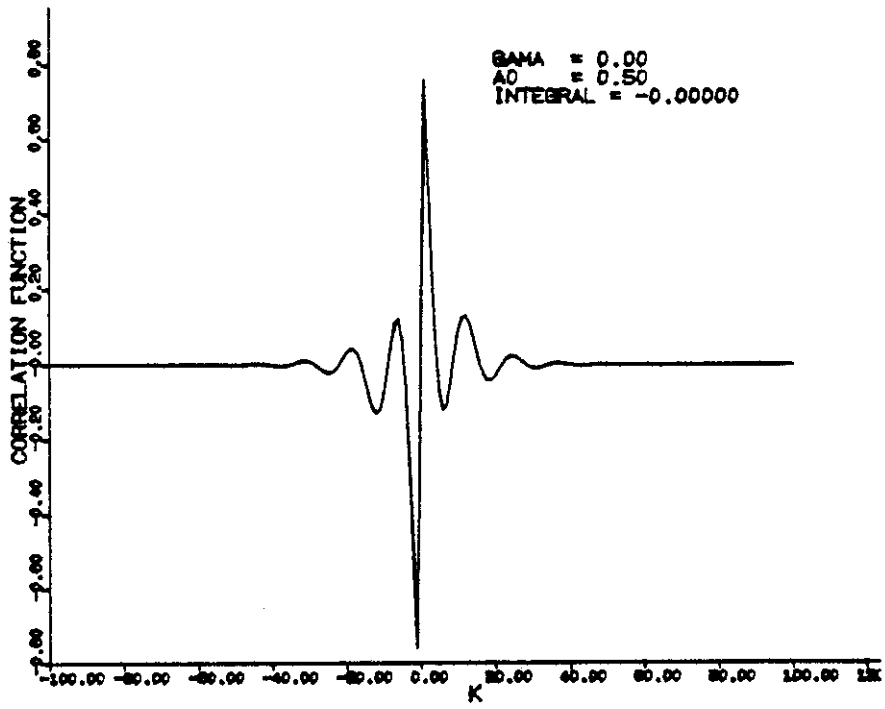

(d) Cross-correlation function

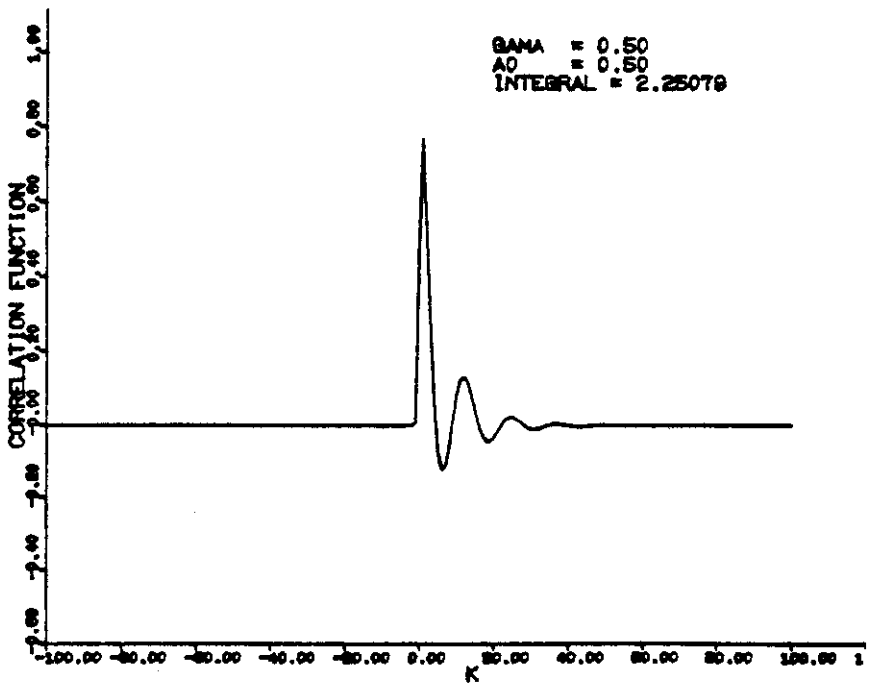

(e) Cross-correlation function

Figure 16 (cont'd.)

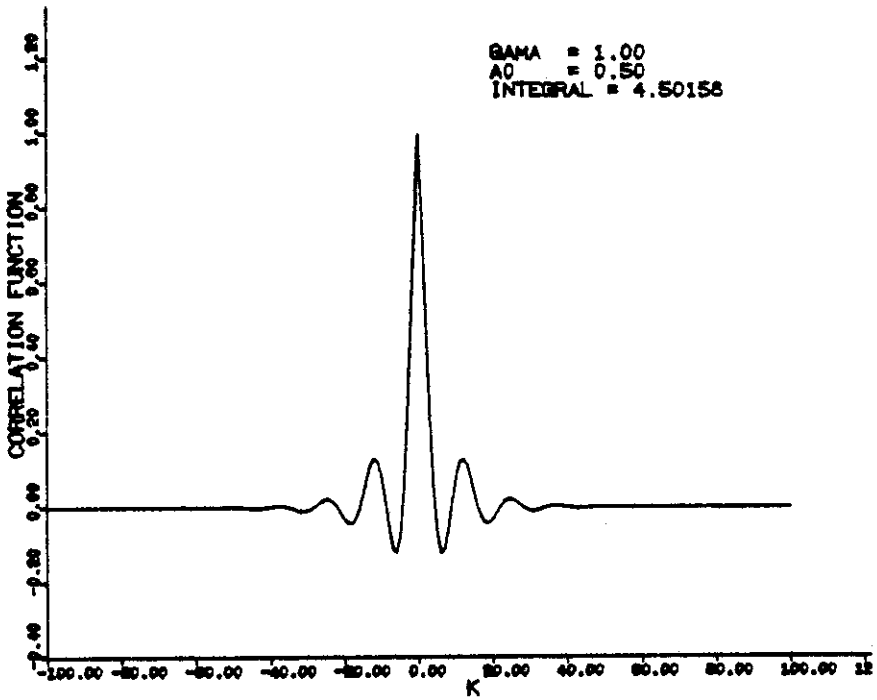

(f) Cross-correlation function

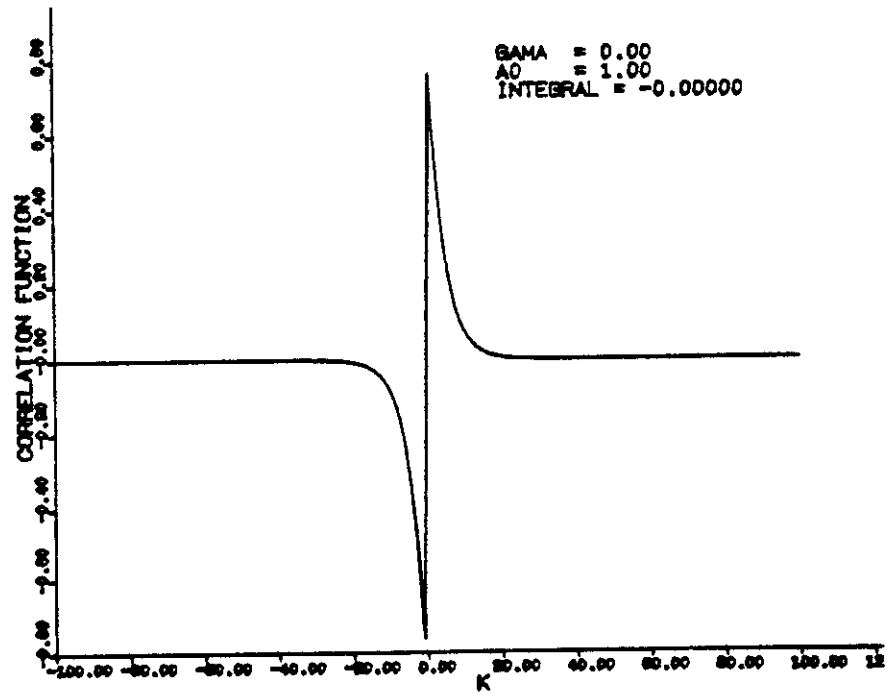

(g) Cross-correlation function

Figure 16 (cont'd.)

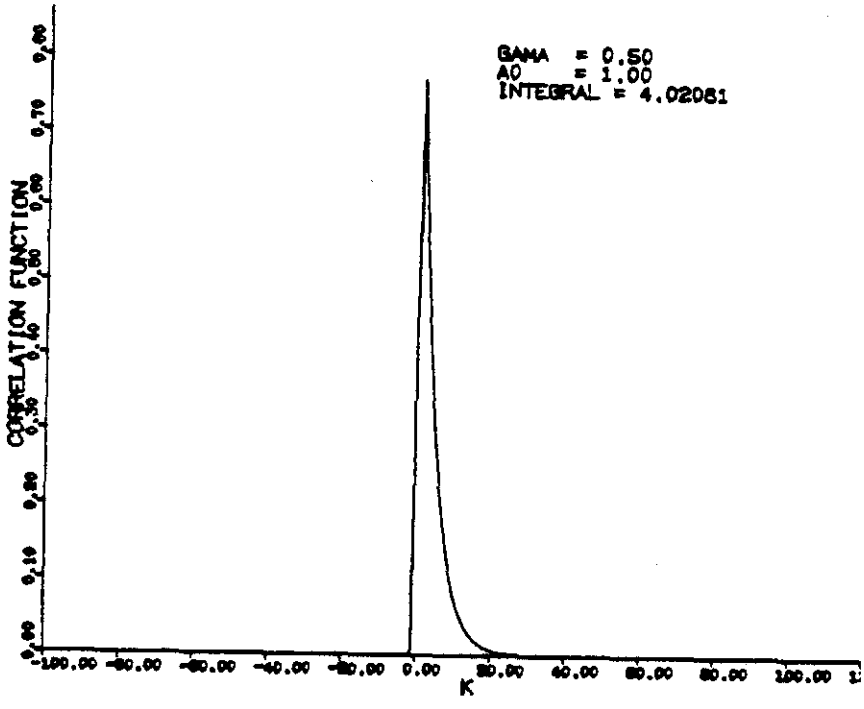

(h) Cross-correlation function

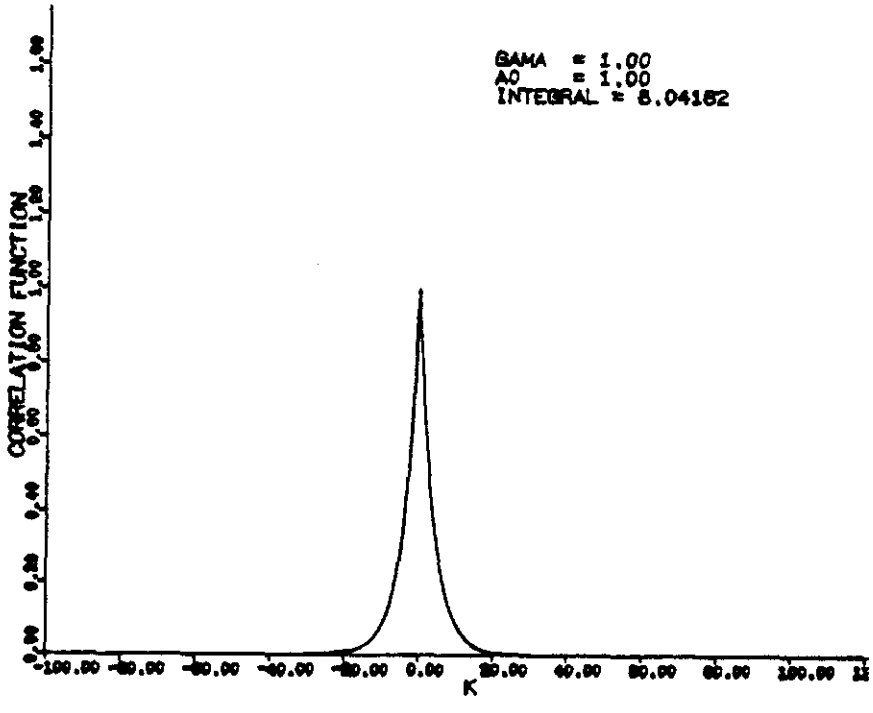

(i) Cross-correlation function

Figure 16 (cont'd.)

curves and the 4 curves in the preceding section give some idea of the shapes possible. In Figure 16(c,f,i), where $\gamma = 1$ we see the effect a_o has on the autocorrelation R(k), since for $\alpha=\gamma=1$, both R(k) and $R_{n_1 n_2}(k)$ are the same. In Figures 16(a,d,g), where $\gamma = 0$, the cross-correlation is constrained to be an odd function. In Figures 16(b,e,h), where $\gamma = 1/2$, the cross-correlation is nearly one-sided.

5.0 PERFORMANCE COMPARISON OF PCC WITH ANALOG DETECTORS FOR A WIDE RANGE OF CROSS-CORRELATION SHAPES

5.1 Positive Cross-correlation

The performance of the PCC is evaluated based on the developed general model for cross-correlation functions in equation (4-13) with R(k) equation (4-14) or the the shapes in Figure 16(a) through Figure 16(i), and for common input signals. The covariance matrix to calculate Q(k) in equation (2-4) is given by

$$P(k) = \begin{bmatrix} R(0) & ROE & R(k) & R_{n_1n_2}(-k) \\ ROE & R(0) & R_{n_1n_2}(k) & R(k) \\ R(k) & R_{n_1n_2}(k) & R(0) & ROE \\ R_{n_1n_2}(-k) & R(k) & ROE & R(0) \end{bmatrix} \quad (5\text{-}1)$$

where $ROE = R_{n_1n_2}(0)$

The detection parameter D_{pcc}, or output signal-to-noise ratio is plotted in Figure 17(a) through Figure 25(a) for three values of $\gamma(0, 0.5, 1)$, and three values of $a_0(0, 0.5, 1)$, and for positive α. Shown in the same figures are the performance of the unclipped correlator and sum and square detector. For odd cross-correlation functions ($\gamma = 0$), the performance of all detectors are nearly independent of α or the magnitude of $R_{n_1n_2}(k)$. For even cross-correlation functions ($\gamma = 1$),

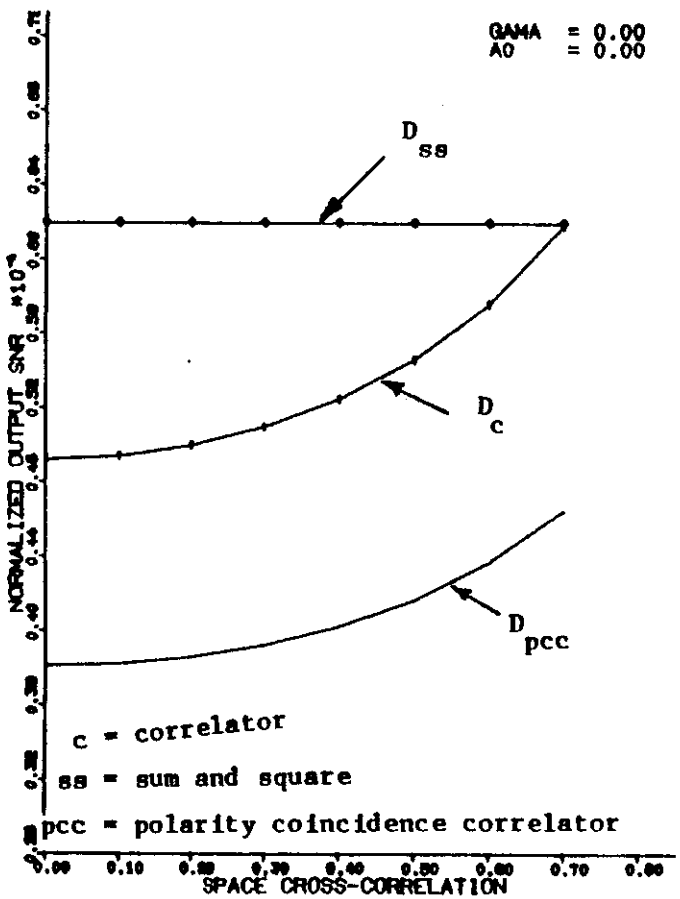

Figure 17 (a). Performance comparison for positive correlation

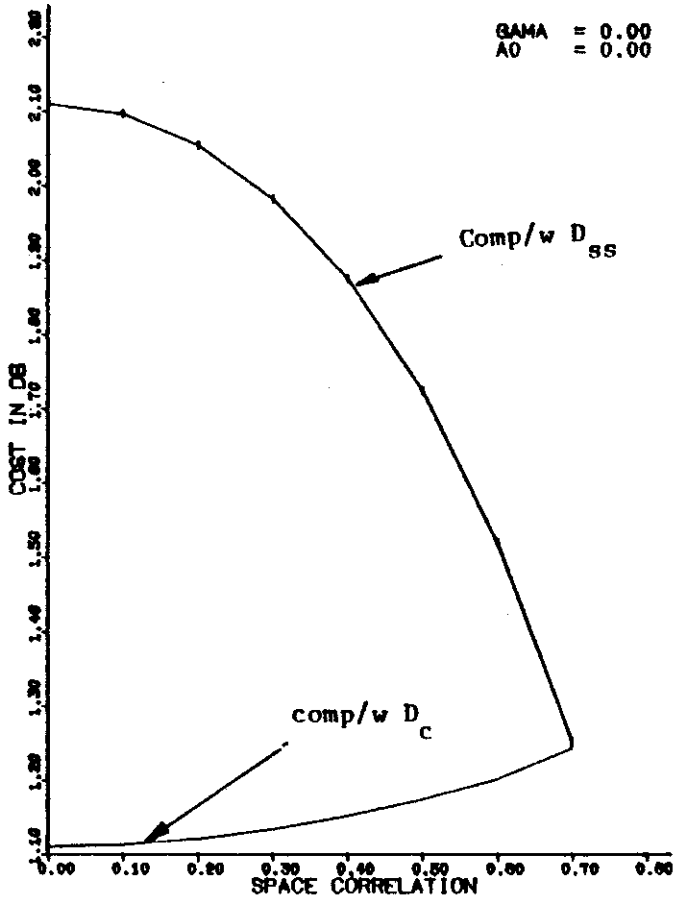

(b) Cost of clipping for positive correlation

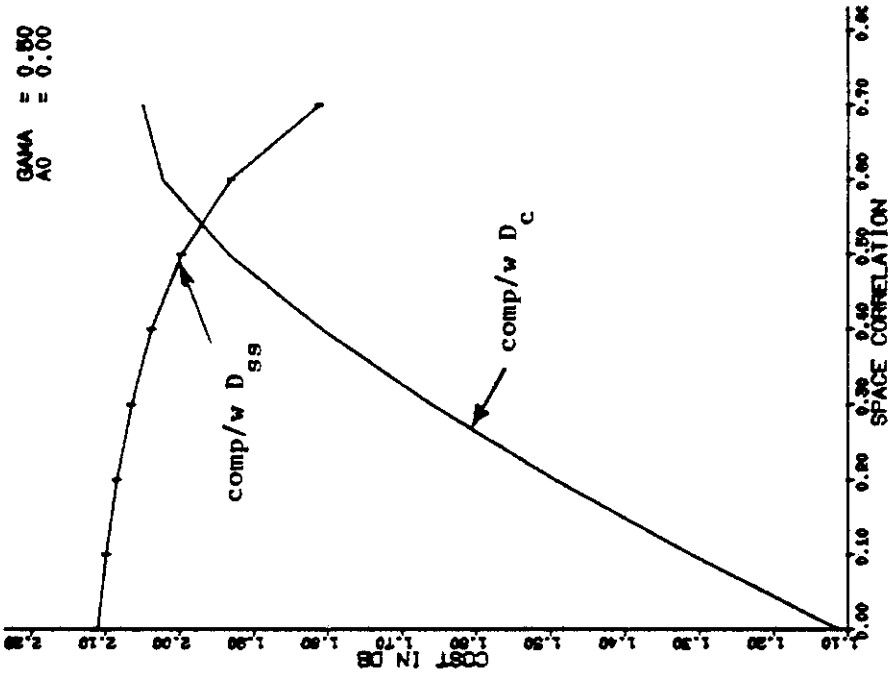

(b) Cost of clipping

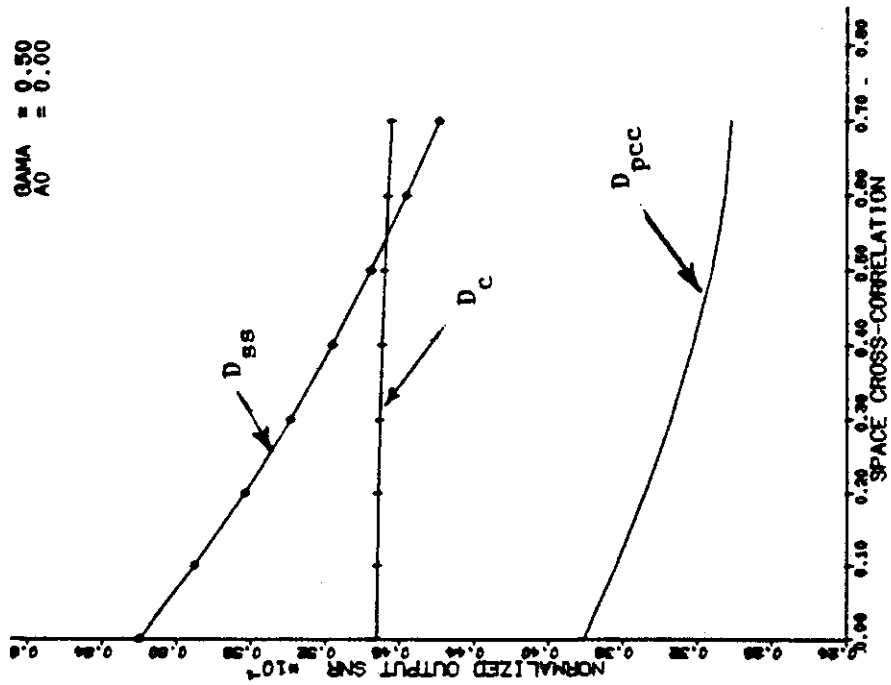

Figure 18 (a). Performance comparison

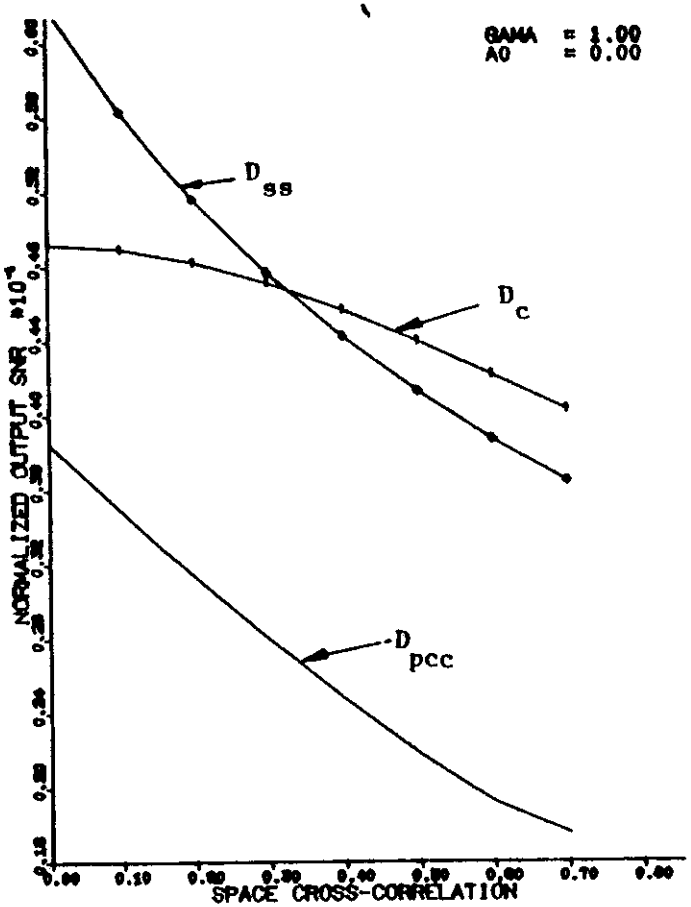

Figure 19 (a). Performance comparison

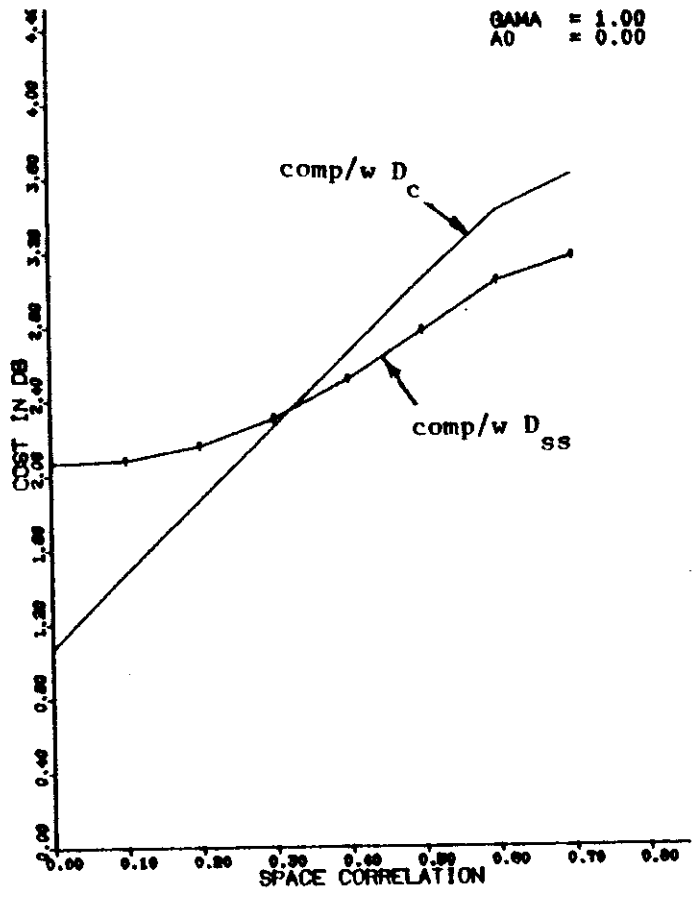

(b) Cost of clipping

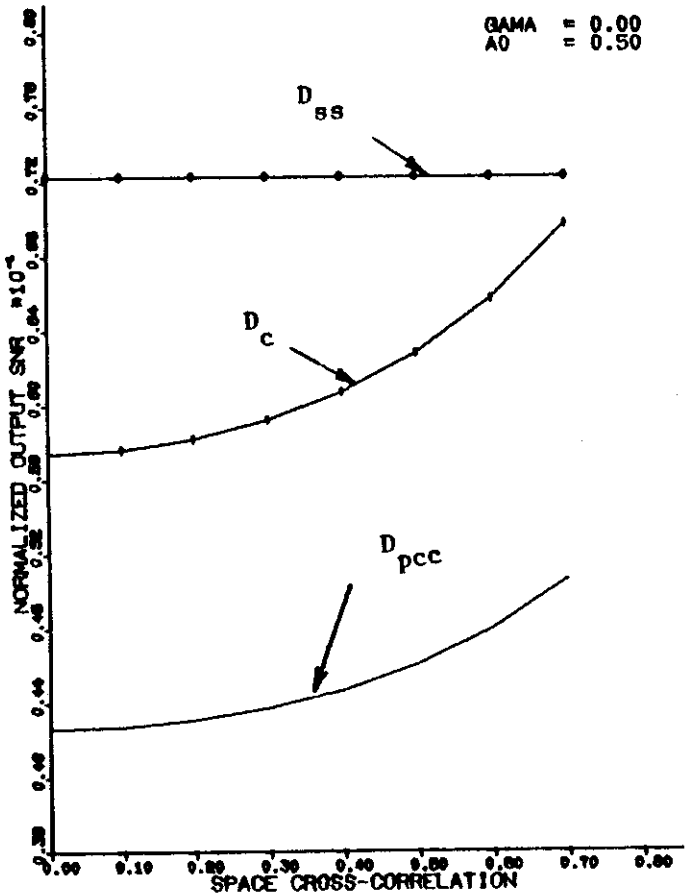

Figure 20 (a). Performance comparison

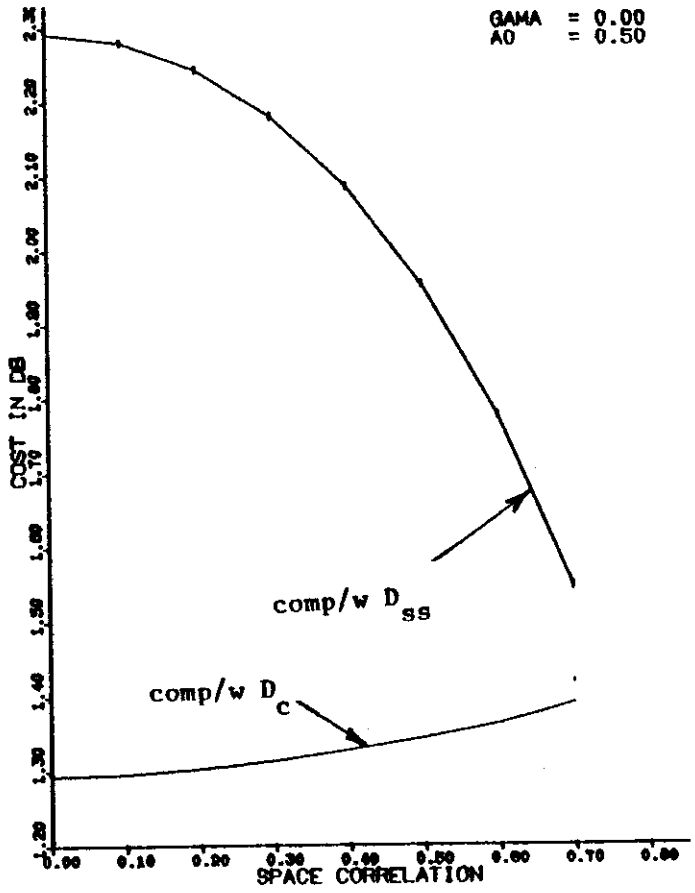

(b) Cost of clipping

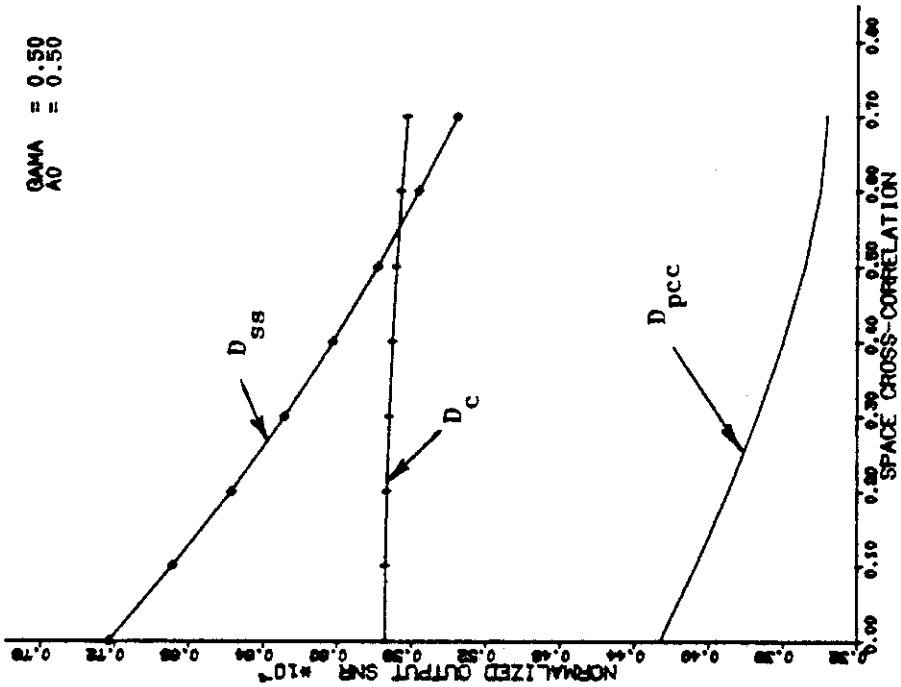

Figure 21 (a). Performance comparison

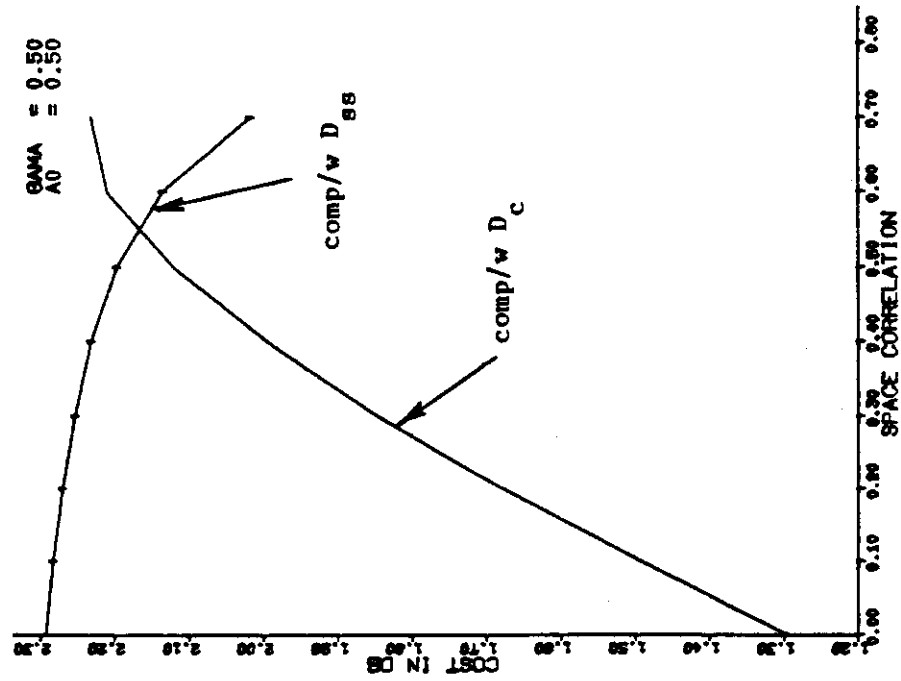

Figure 21 (b). Cost of clipping

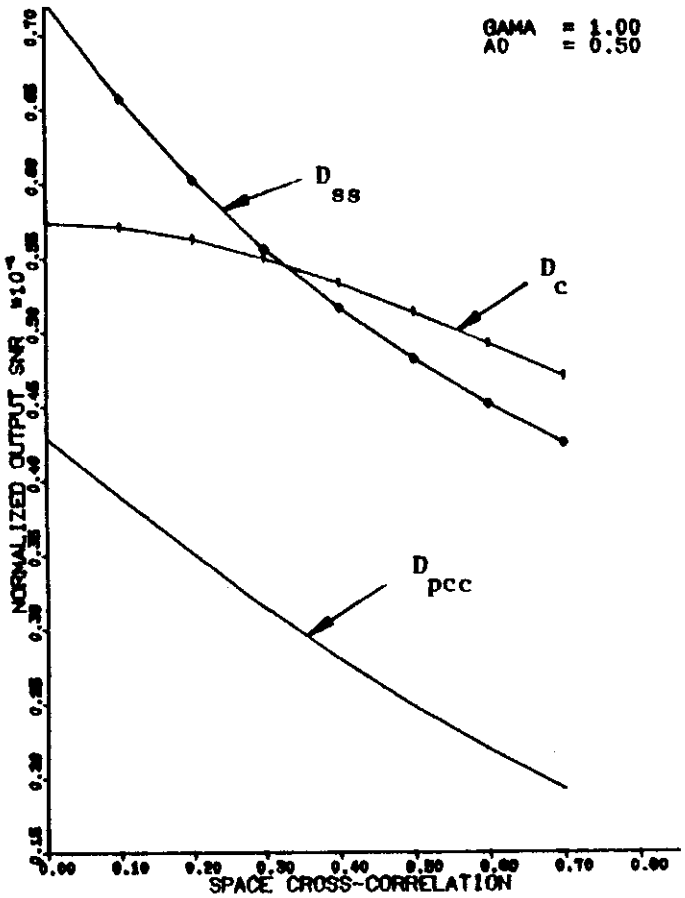

Figure 22 (a) Performance compariosn

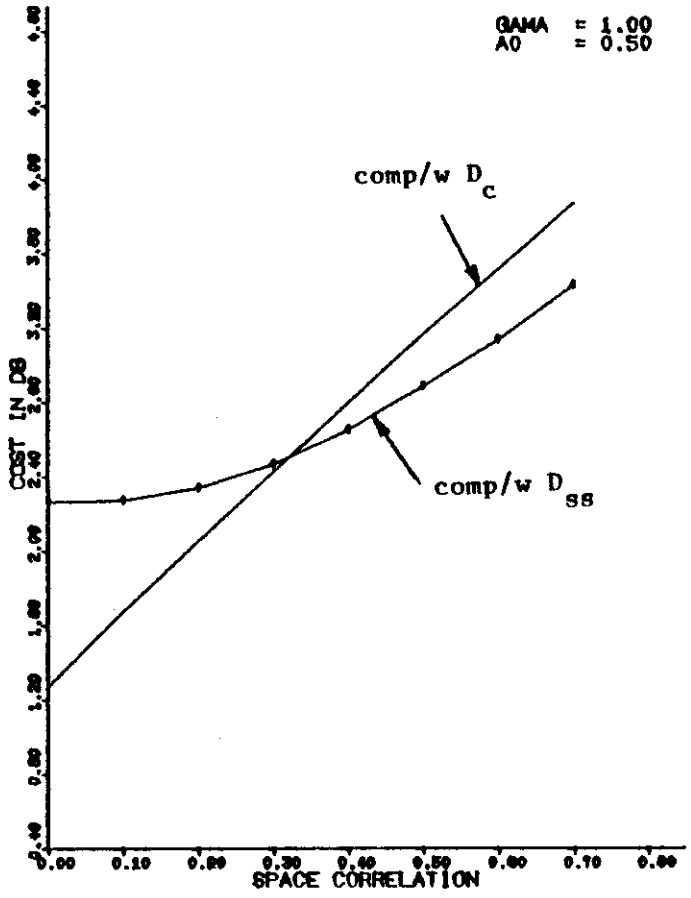

(b) Cost of clipping

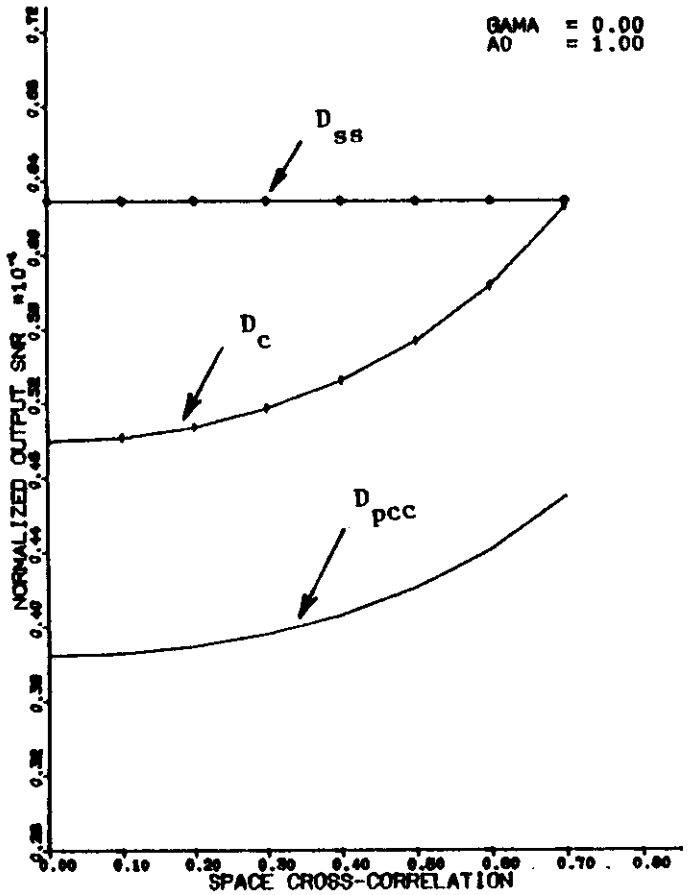

Figure 23 (a) Performance comparison

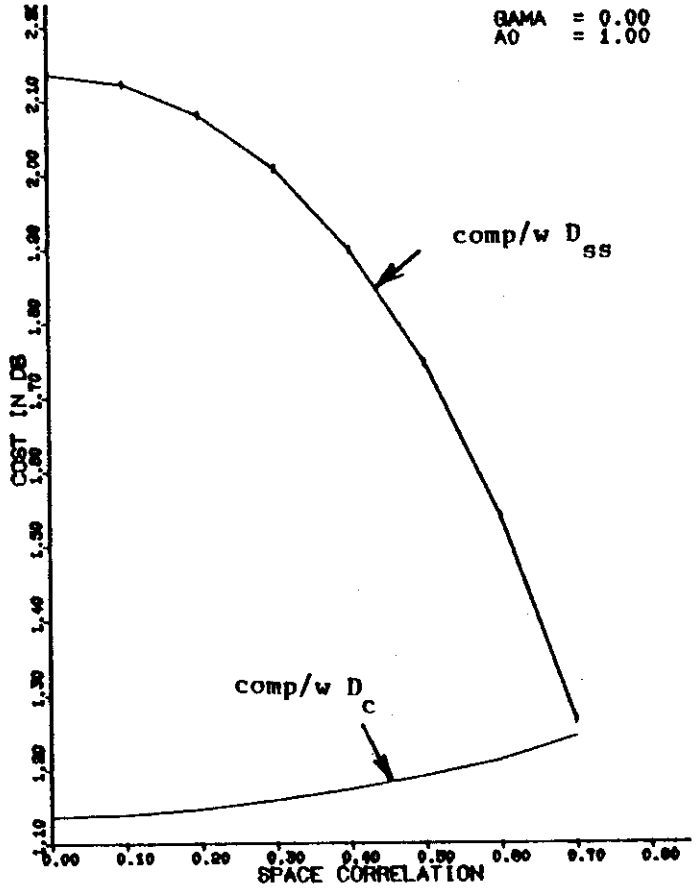

(b) Cost of clipping

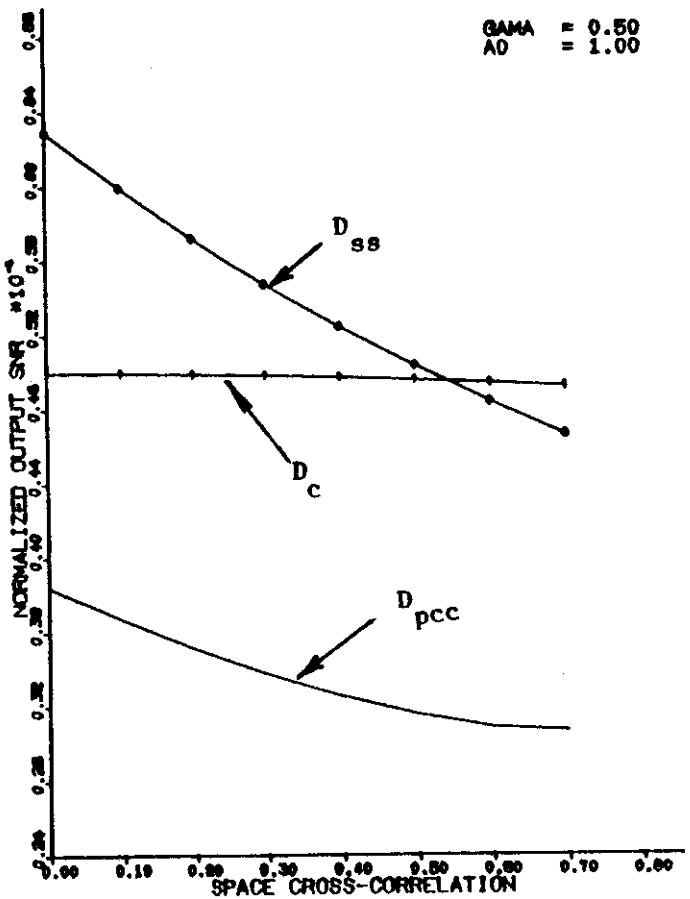

Figure 24 (a) Performance comparison

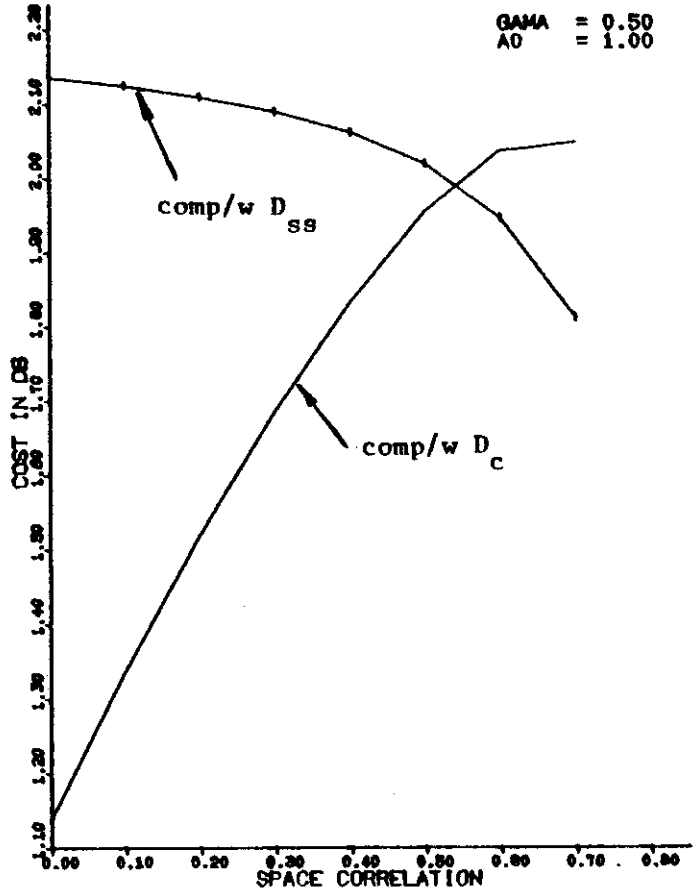

(b) Cost of clipping

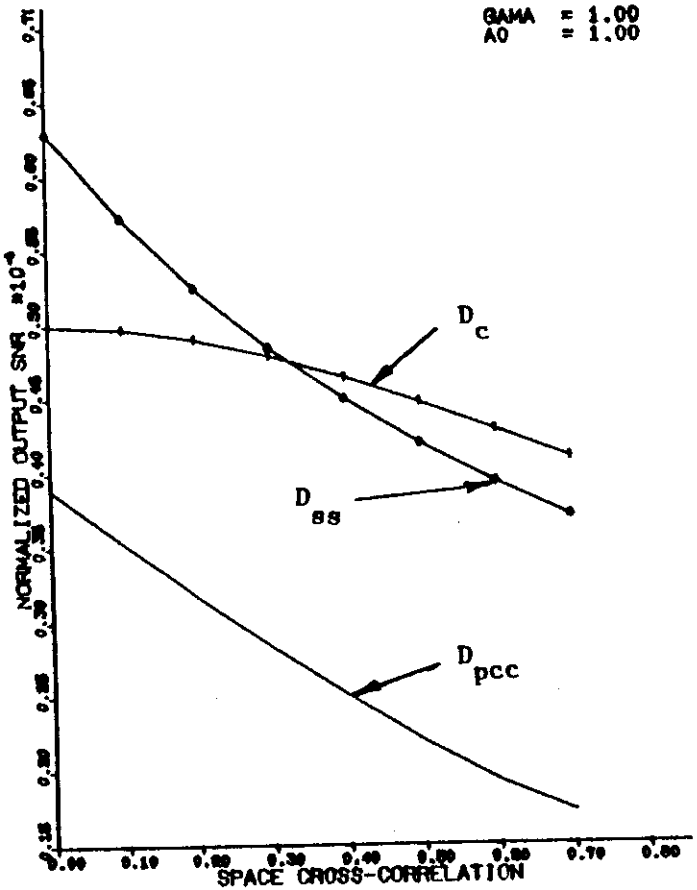

Figure 25 (a) Performance comparison

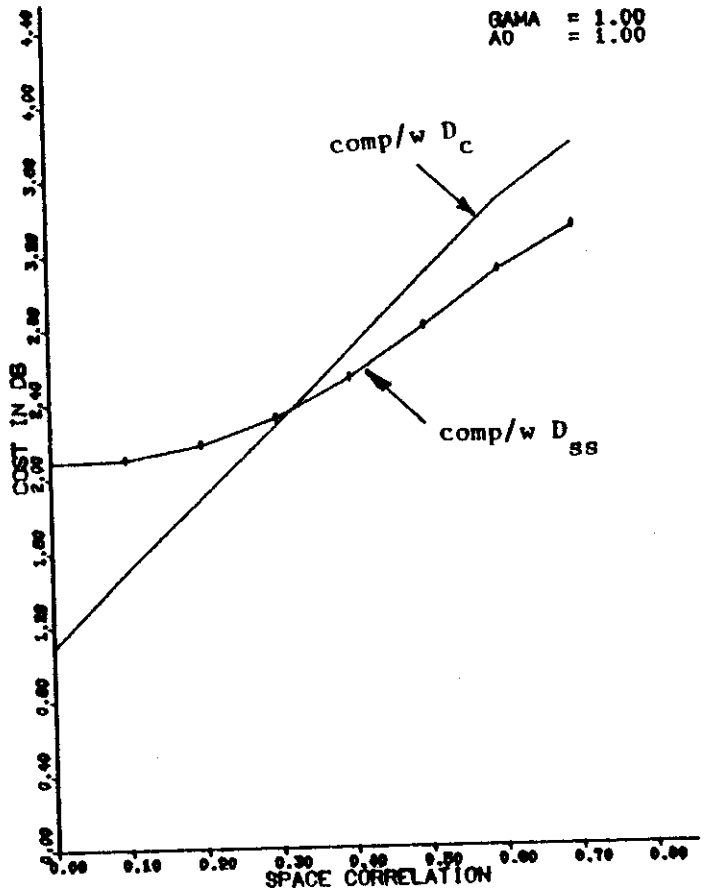

(b) Cost of clipping

the performance of the detectors decrease for an increase in α. The correlator outperforms the PCC and sum and square detectors for a sufficiently large α. The decrease in performance of the PCC is about -2db for $\alpha = 0.5$.

The cost of clipping compared to the correlator and sum and square detectors are plotted in Figure 17(b) through Figure 25(b), which remains almost constant compared to the correlator but drops off with compared to sum and square detector for γ=0. For $\gamma = 1$, on the other hand, the cost compared to the sum and square detector increases from 2db to 3db with moderately correlated inputs ($\alpha \leq 0.5$) and compared to the correlator detector increases from 1db to above 3db. The sum and square detector is locally optimun when the inputs are independent. For dependent inputs, however, the unclipped correlator can under certain conditions, outperform the sum and square detector.

5.2 *Negative Cross-correlation*

Since the performance of all three detectors is quite different, in most cases, for negative α, this case has been considered separately.

All three detection parameter curves are repeated in Figure 26(a) through Figure 34(a) for $\gamma = 0, 0.5, 1$ respectively and for negative cross-correlation. It can be observed that for $\gamma = 0$ the performance remains the same as for a positive α. The cost of clipping remains constant for $\gamma = 0.5$, but increases mostly for $\gamma = 1$ and for higher correlation. The cost comparison curves for negative correlation are shown in Figure 26(b) through Figure 34(b).

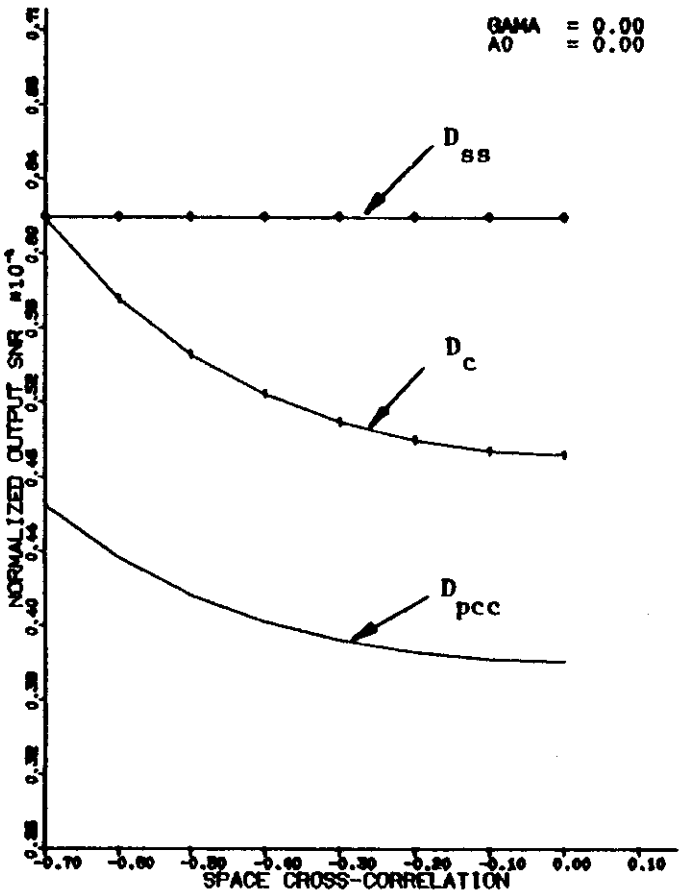

Figure 26 (a) Performance comparison for negative correlation

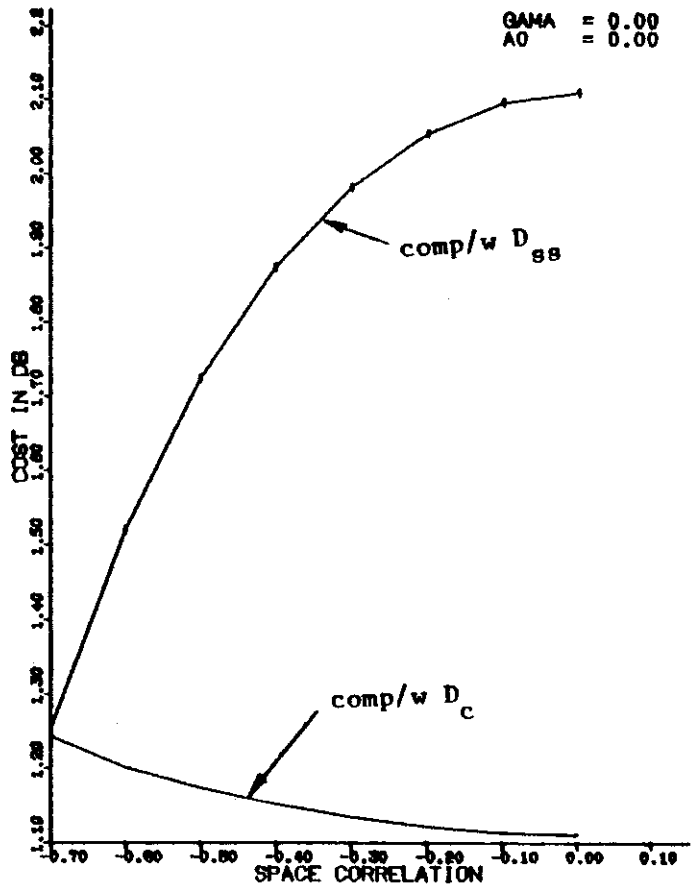

(b) Cost of clipping for negative correlation

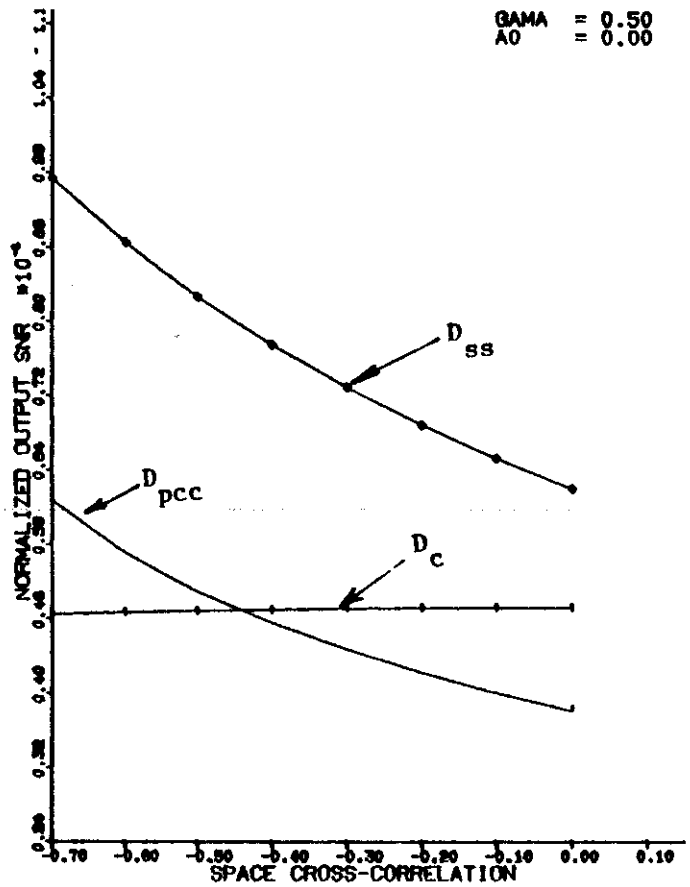

Figure 27 (a) Performance comparison

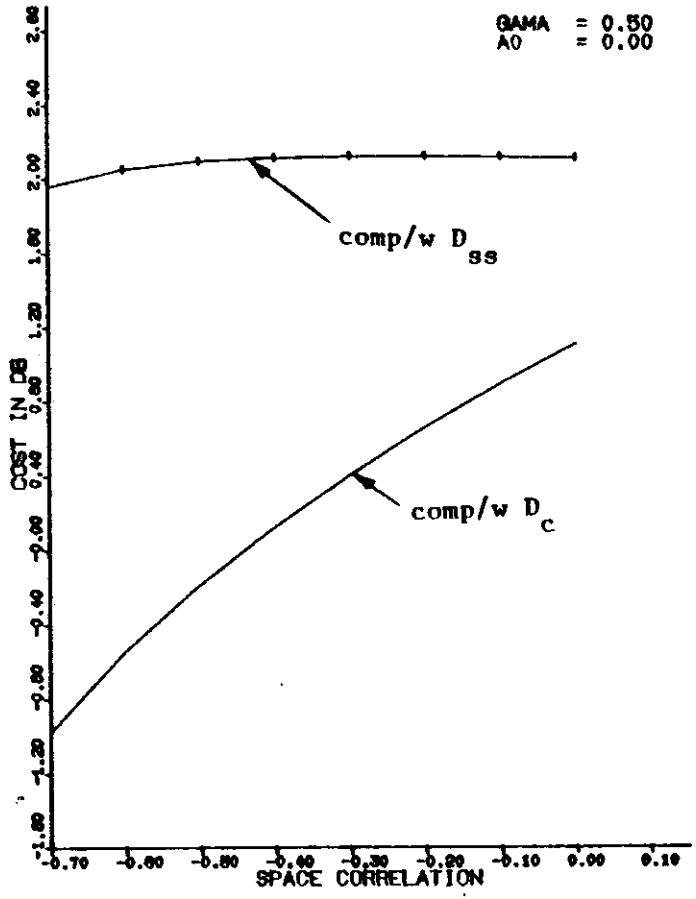

(b) Cost of clipping

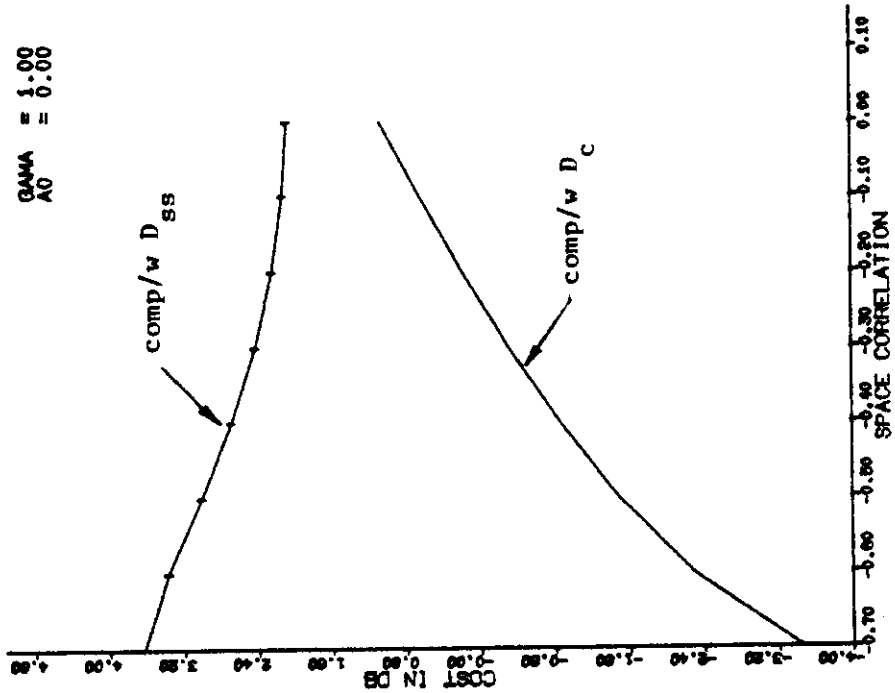

(b) Cost of clipping

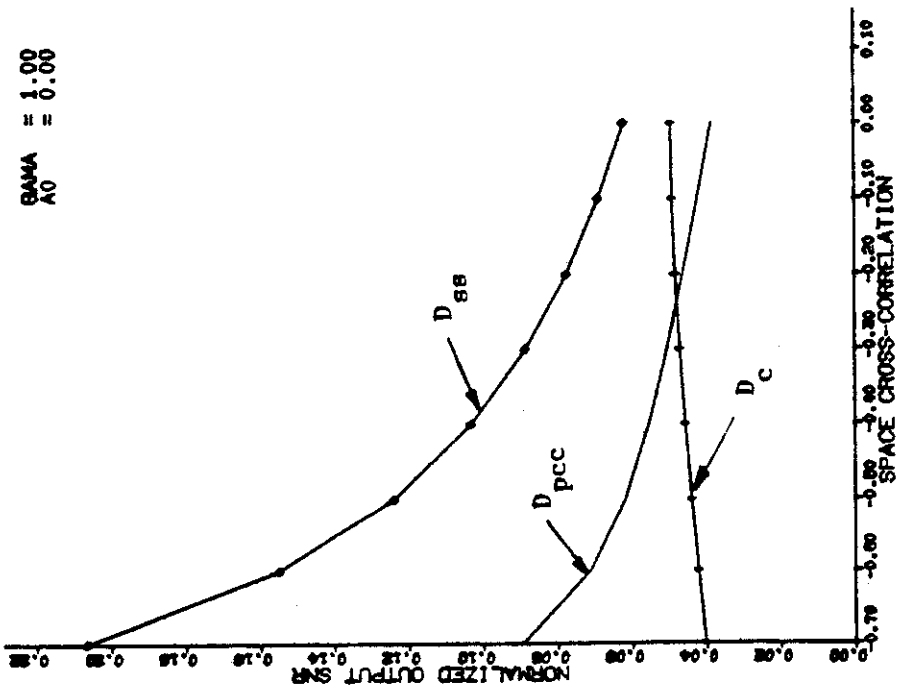

Figure 28 (a) Performance comparison

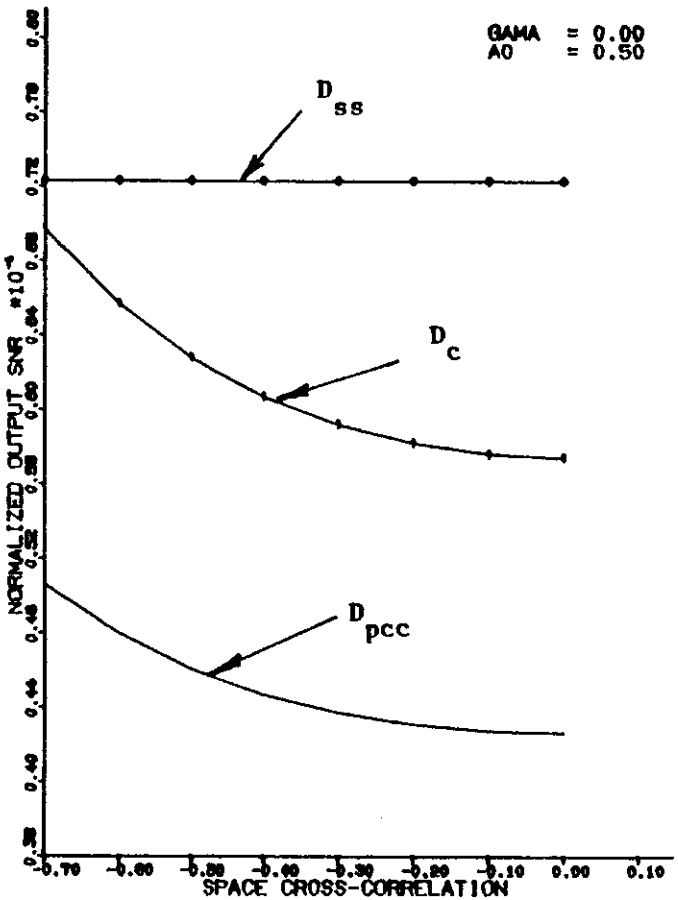

Figure 29 (a) Performance comparison

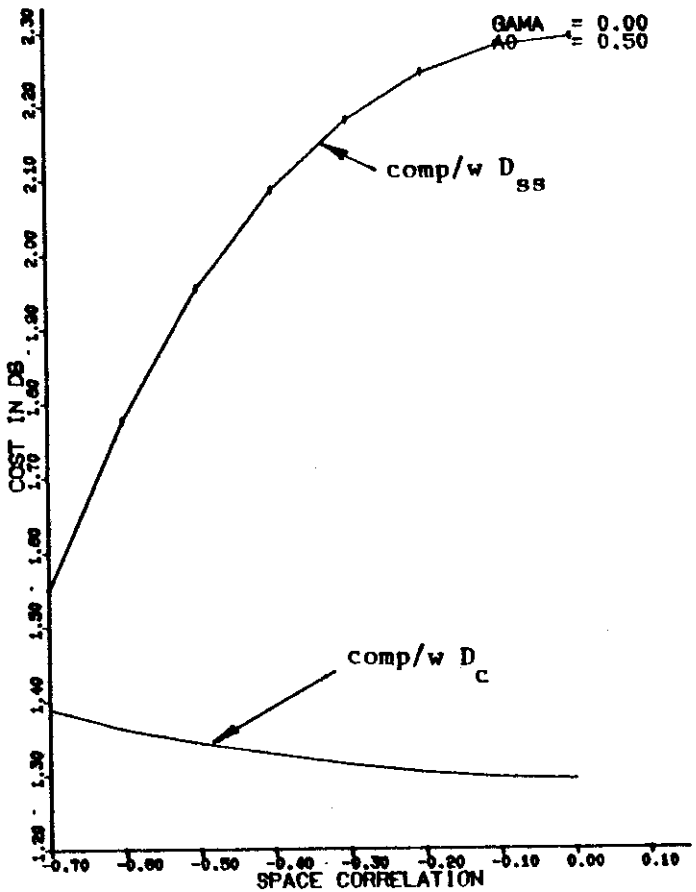

(b) Cost of clipping

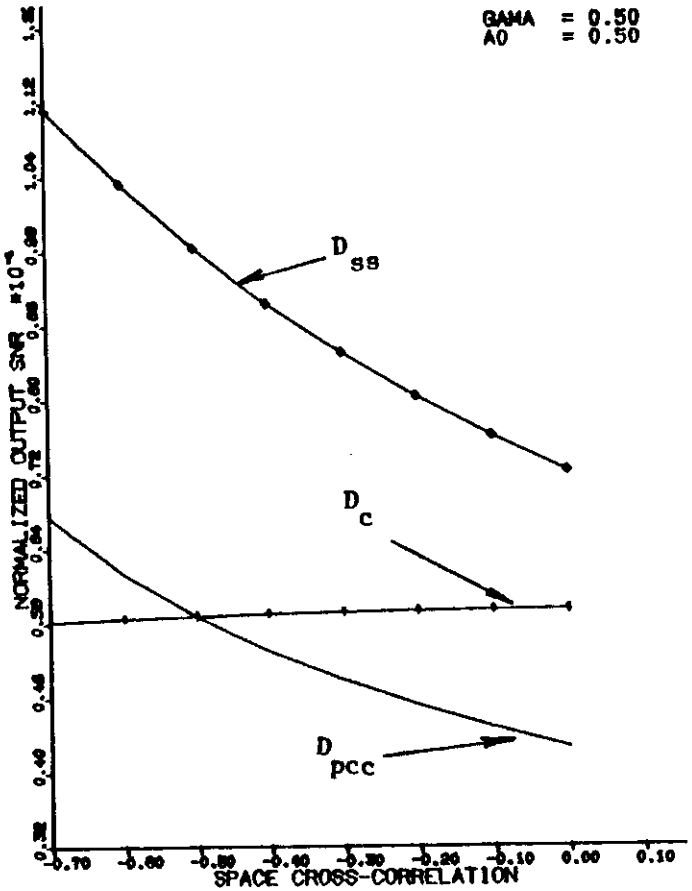

Figure 30 (a) Performance comparison

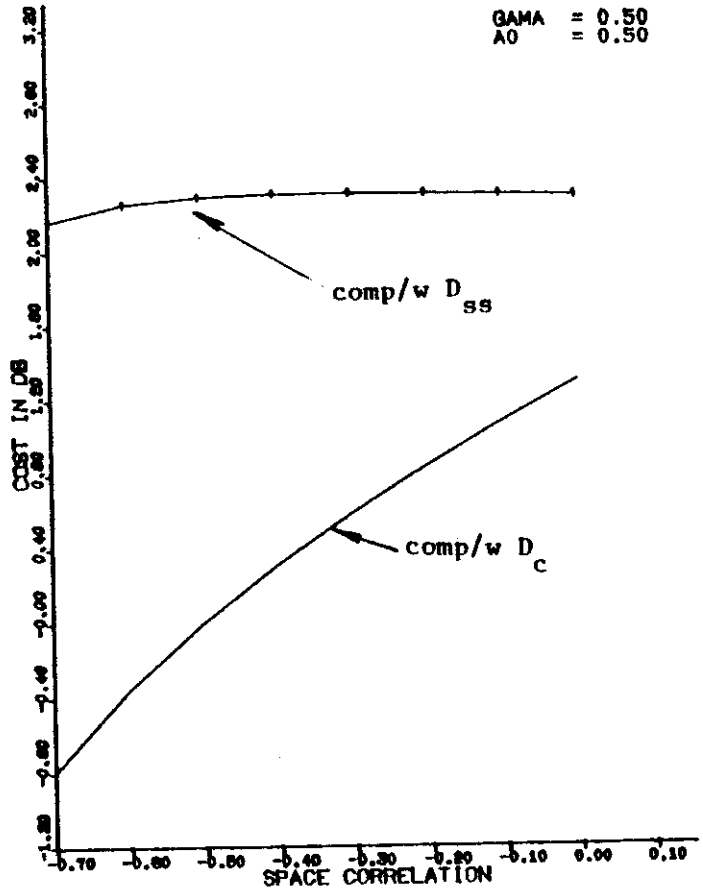

(b) Cost of clipping

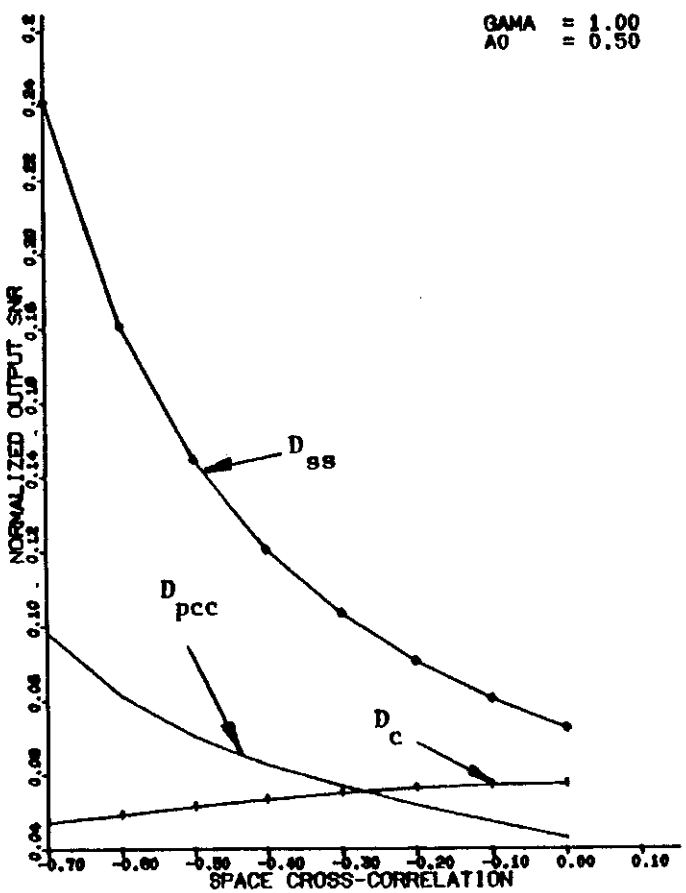

Figure 31 (a) Performance comparison

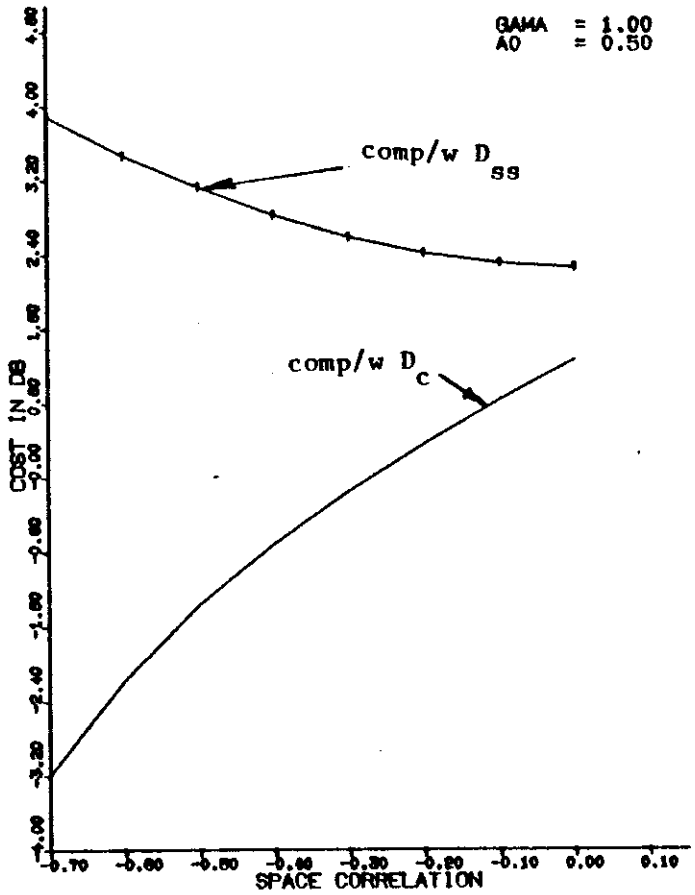

(b) Cost of clipping

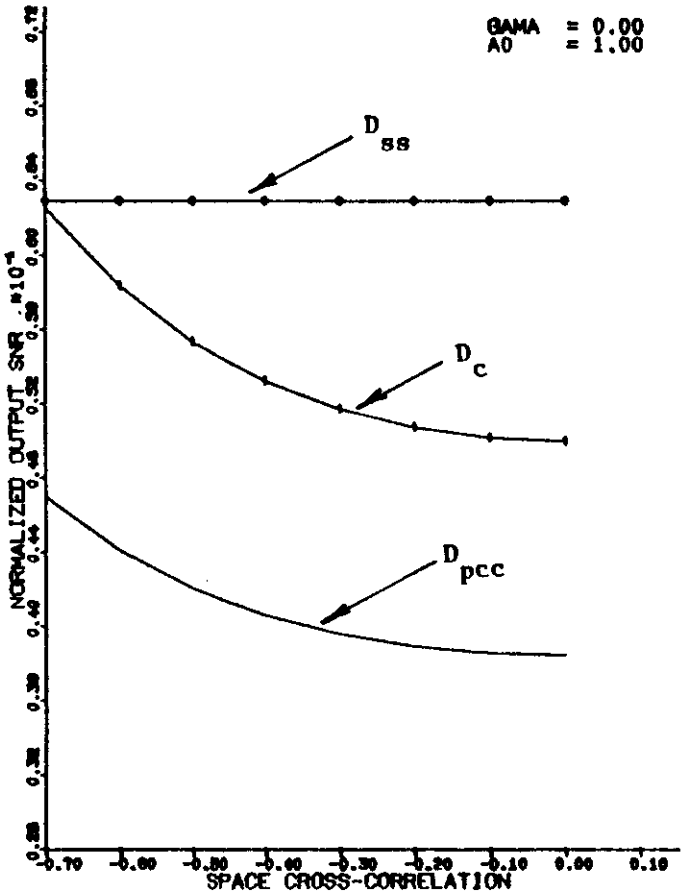

Figure 32 (a) Performance comparison

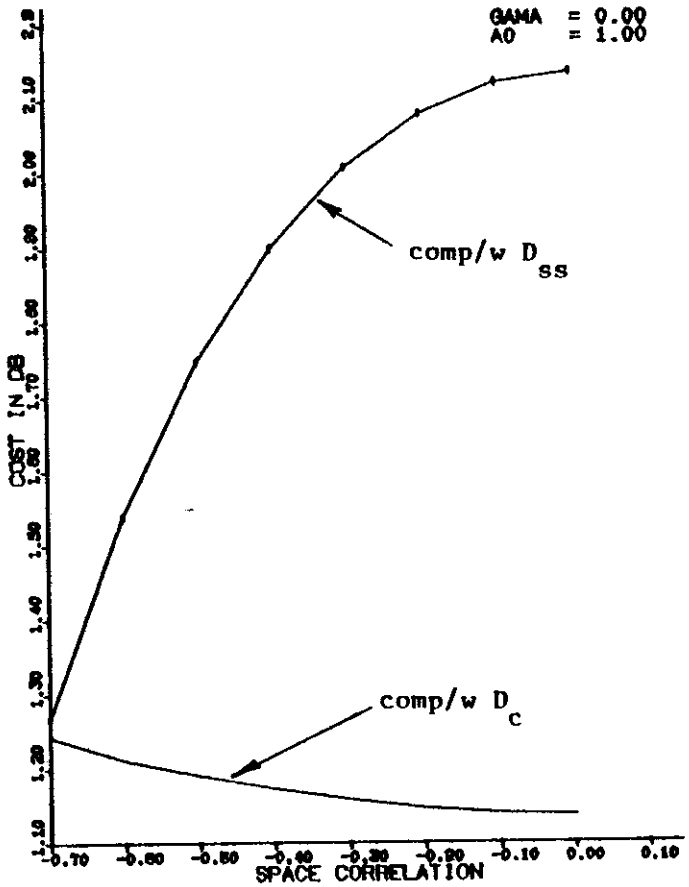

(b) Cost of clipping

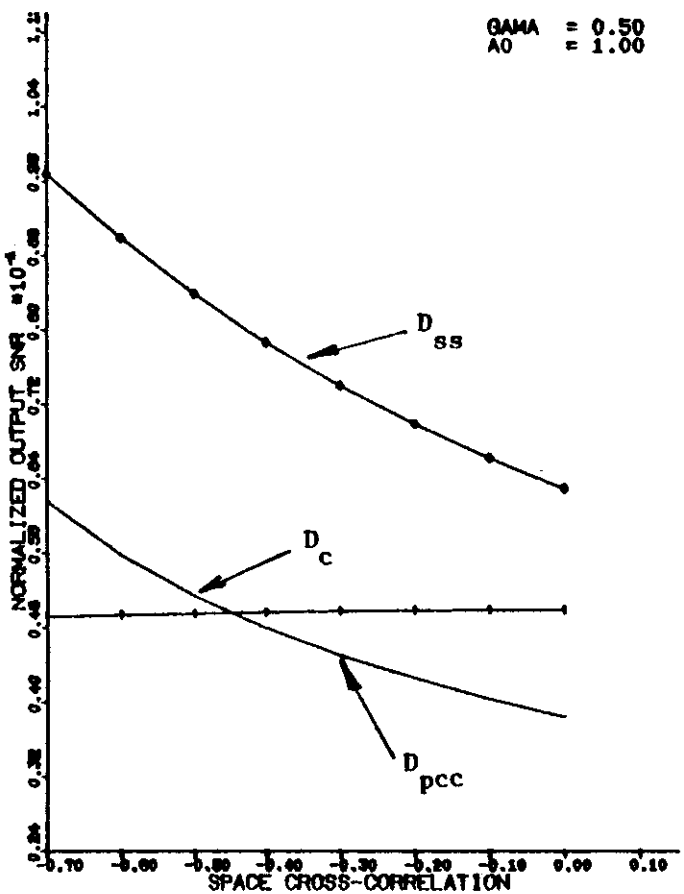

Figure 33 (a) Performance comparison

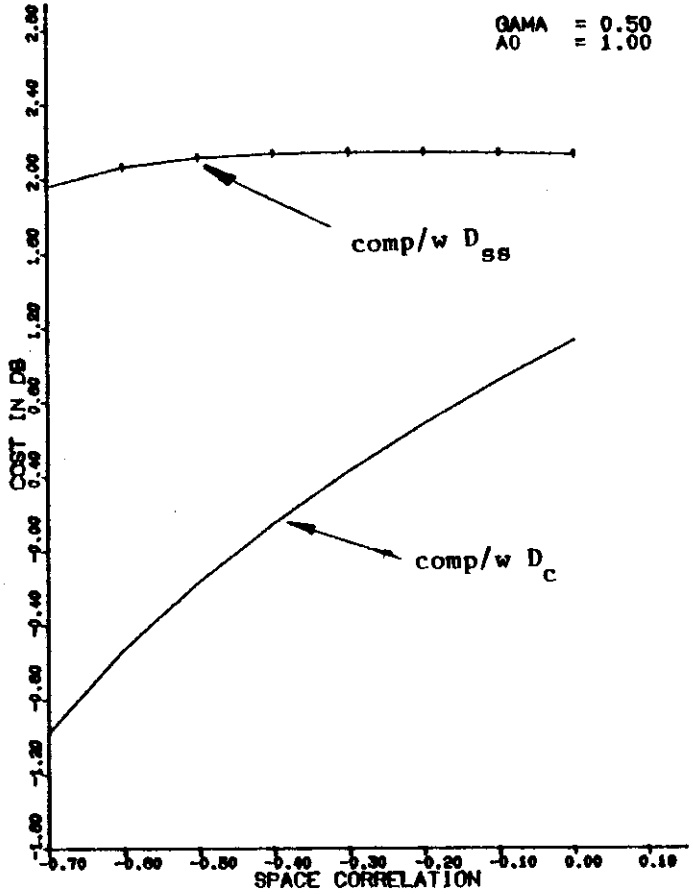

(b) Cost of clipping

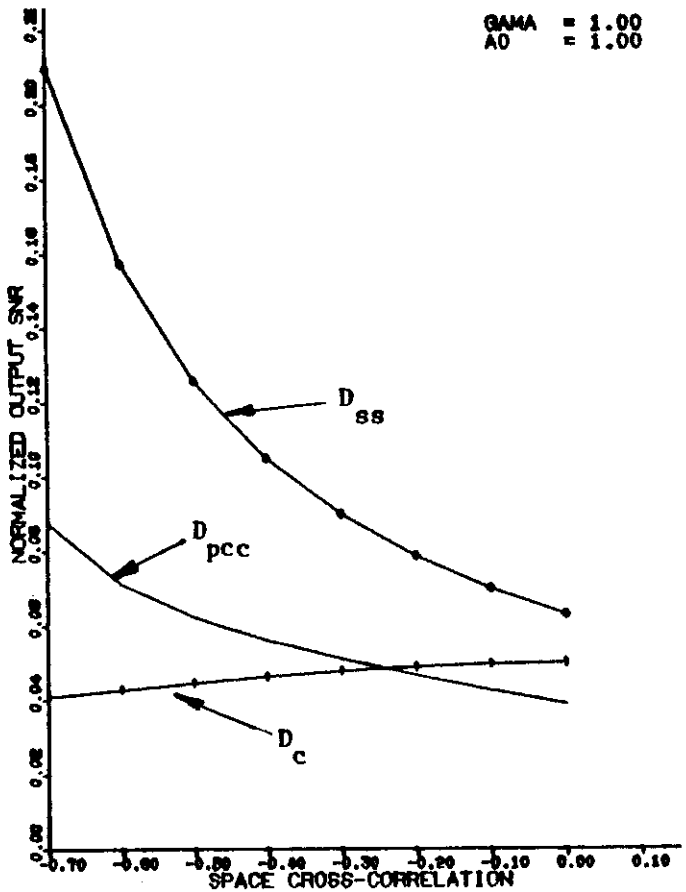

Figure 34 (a) Performance comparison

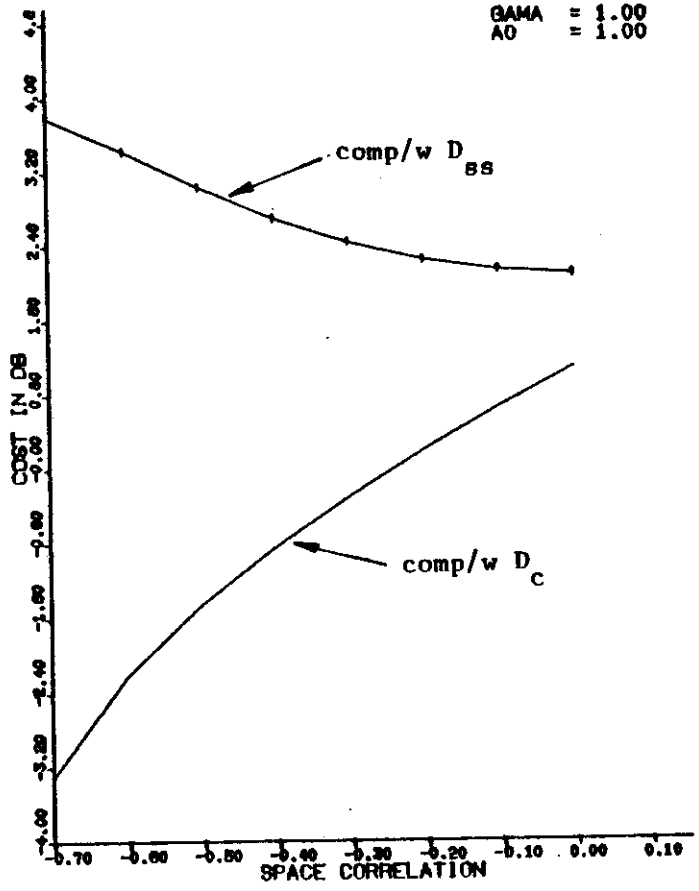

(b) Cost of clipping

For even cross-correlation functions ($\gamma = 1$), the performance of the PCC decreases for positive values of α(-2db for $\alpha = +0.5$) and increases a like amount for negative value of α(+2db for $\alpha = -0.5$). For cross-correlation function even and odd components ($\gamma = 0.5$) the performance lies somewhere in between the even and odd case.

We can see that the shape of the autocorrelation R(k), as determined by a_o has a modest affect on the performance of the PCC that is nearly independent of γ. The shape of the cross-correlation $R_{n_1 n_2}(k)$, as determined by γ on the other hand, has a significant effect.

6.0 PCC DETECTION OF SINUSOIDAL BURSTS WITH UNCERTAINTIES IN SIGNAL PARAMETERS

6.1 Sampling Speed

In Figure 35, the detection parameter of the PCC is evaluated for sampling speeds in the range of 1200 samples/sec to 24000 samples/sec. While this curve is for the $\gamma = 1$, $\alpha = +0.5$ case, it does not vary much with these parameters. The band width of the noise is of the order of 2,000 Hz but the nonlinearity used to obtain polarities spreads the spectrum further. For this reason we observe a substantial improvement in performance as the sampling rate is increased to about 8000 samples/sec. But after that, the improvement slows down and increasing the sampling rate from 12000 to 24000 results in a gain of only 0.4db. Therefore, sampling rates of 12000 samples/sec are assumed throughout.

6.2 Detection of Sinusoidal Bursts

Electromagnetic signals consisting of sinusoidal bursts have been considered for the detection of trapped miners. The signal is assumed to be 0.1 second long bursts of a 1000 Hz sinusoid repeated every second. For this non-gaussian signal the asymptotic analysis of PCC is carried out under various assumptions, as the input signal-to-noise ratio decreases to zero.

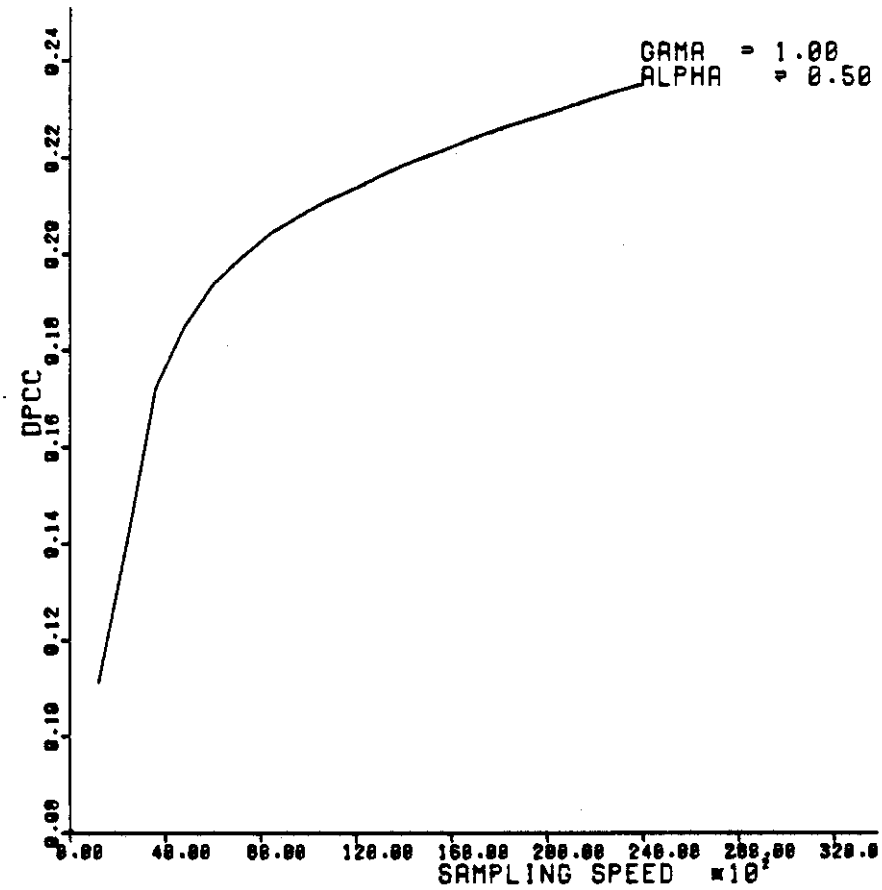

Figure 35. Performance of PCC versus sampling speed

6.2.1 Polarity Difference Statistics

Assuming that the signal is a sinusoidal burst of nearly known frequency, it is possible for the PCC detector to perform other statistics in addition to polarity coincidences. By adding a suitable delay in one channel the signal will be nearly 180° out of phase rather than in phase. For these signals, computing polarity differences is more appropriate. Computing polarity differences when the signals are out of phase and the noise inputs have a positive correlation is identical to computing polarity coincidence when the signals are in phase and the noise inputs have a negative correlation. Therefore, when the signals are out of phase polarity difference correlation can be evaluated using equation (2-4) by changing the sign of ρ_H. Using this technique, the polarity coincidence statistic is compared with polarity differences in Figure 36 (a,b,c) for γ = 0, 0.5, 1. The shift in either of channels is considered or in other words a shift of $\pm$180°. From Figure 36(a), (γ = 0) we can see that by adding a suitable delay an improvement can be achieved for both negative and positive cross-correlations. But for γ = 0.5 and γ = 1 in Figure 36 (b,c) we can see that possible improvement is for positive cross-correlation only with -180° shift. In general, we can say that for negative cross-correlation, polarity coincidences will outperform polarity differences whereas for positive cross-correlation, the opposite is true. To perform this analysis, it has to be kept in mind that ρ_H in equation (2-4) and ROE in matrix (5-1) have to be redefined.

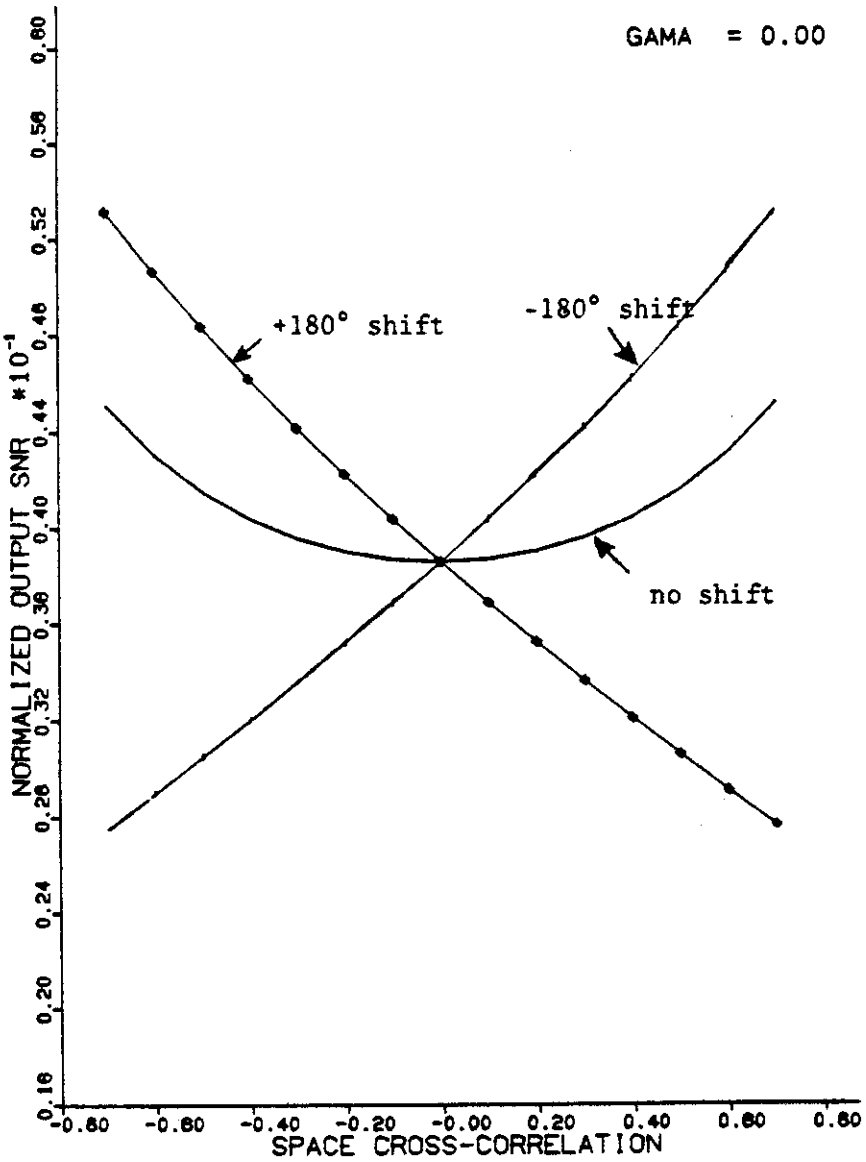

Figure 36 (a) Performance comparison of PCC with no shift, ±180° shift for a wide range of cross-correlation

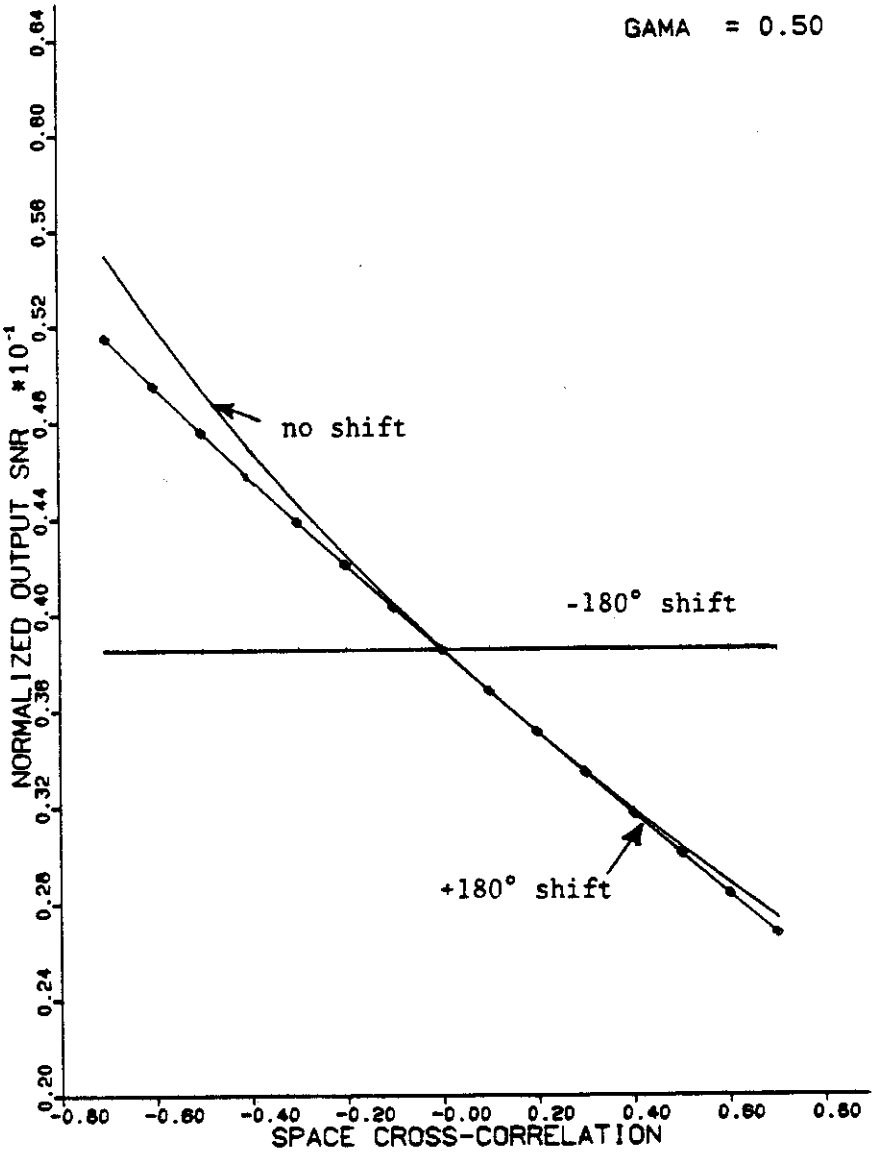
GAMA = 0.50
no shift
-180° shift
+180° shift
NORMALIZED OUTPUT SNR *10⁻¹
SPACE CROSS-CORRELATION
0.20
0.24
0.28
0.32
0.36
0.40
0.44
0.48
0.52
0.56
0.60
0.64
-0.80
-0.60
-0.40
-0.20
-0.00
0.20
0.40
0.60
0.80

Figure 36 (b)

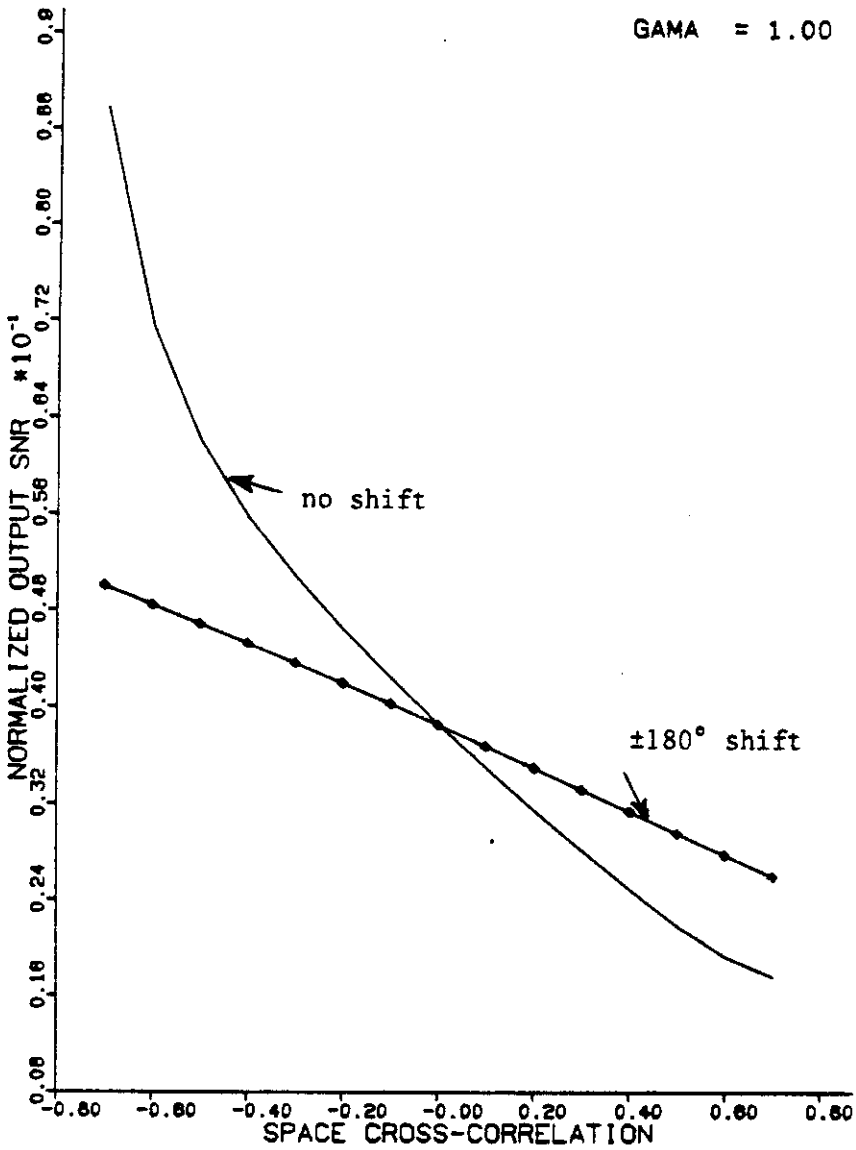
GAMA = 1.00
NORMALIZED OUTPUT SNR *10⁻¹
0.00
0.16
0.24
0.32
0.40
0.48
0.56
0.64
0.72
0.80
0.88
0.96
no shift
±180° shift
-0.80
-0.60
-0.40
-0.20
-0.00
0.20
0.40
0.60
0.80
SPACE CROSS-CORRELATION

Figure 36 (c)

It is of course possible to consider other phase shifts such as $m\pi$, where for m even polarity coincidences are performed and for m odd polarity differences are performed. For the case $\gamma = 1$, and $\alpha = +0.5$ the statistic D_{pcc} is plotted for various values of m in Figure 37. It seems that the improvement of 1.3db for m = 1 can be increased somewhat with a larger m. However this analysis does not take into consideration the possible error in the frequency.

6.2.2 Cost of Uncertainties in Signal Parameters

Let the difference or delay between the beginning of the 0.1 second pulse and the start of the processing be denoted by D. That is, D = 0 corresponds to perfect synchronization and D = 1 corresponds to missing the pulse completely. The numerator of equation (2-4) can be written as,

$$(1 - D)\ \sin^{-1}(\rho_K) + \sin^{-1}\rho_H - \sin^{-1}\rho_H$$

$$= (1 - D)\ [\sin^{-1}\rho_K - \sin^{-1}\rho_H] \quad , \tag{6-1}$$

where

$$\rho_K = \left\{ \frac{\overline{S_1(t)S_2(t)} + \rho_H}{\sigma_n^2} \Bigg/ \frac{\sqrt{\overline{S_1^2(t)} + \sigma_n^2}\ \sqrt{\overline{S_2^2(t)} + \sigma_n^2}}{\sigma_n^2} \right\} \tag{6-2}$$

and $S_1(t)$, $S_2(t)$ are the signals in the two channels. If the entire 1 second interval (or time between pulses) is divided into M overlapping 0.1 second processing times, then it follows that $D \leq \frac{5}{M}$. Thus if

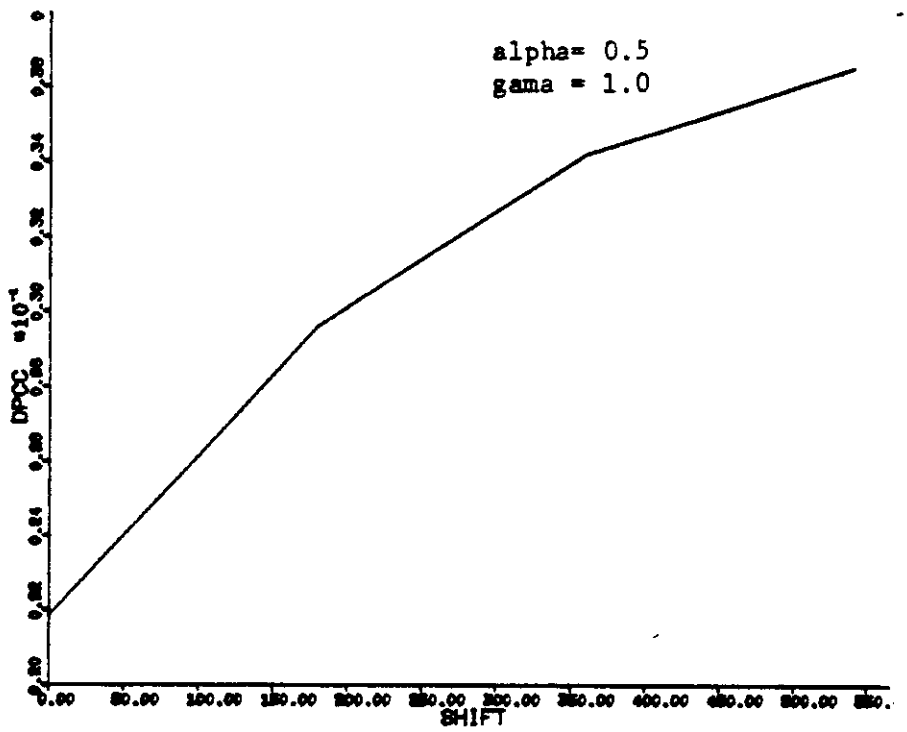

Figure 37. Performance of PCC versus various shifts

M = 40, in the worst case the degradation is only 0.58db.

Let

$$S_1(t) = A(1 + \Delta A)\ \mathrm{Sin}\ \{(w + \Delta w)t + \theta\}$$

$$S_2(t) = A(1 + \Delta A + \varepsilon A)\ \mathrm{Sin}\ \{(w + \Delta w)(t-\tau) + \theta + \varepsilon\theta\} \qquad (6\text{-}3)$$

where ΔA, Δw, and θ are unknown but the same for both channels and εA, $\varepsilon\theta$ are unknown differences in $S_1(t)$ and $S_2(t)$. It is assumed that $\tau = \frac{m\pi}{w}$ where m = 0,1,2, ... which means that we are going to consider polarity coincidences and differences only. In computation of equation (6-2), to a second order approximation, εA has almost no effect and we get,

$$\rho_K = \frac{\sigma_s^2/\sigma_n^2 \cdot \mathrm{Cos}\ (m\pi \frac{\Delta w}{w} - \varepsilon\theta) + \rho_H}{\sigma_s^2/\sigma_n^2 + 1},$$

where σ_s^2 is the average signal power in the two channels. It is seen that $\varepsilon\theta$ will not significantly degrade the performance unless it is large.

The results of Figure 37 are extended in Figure 38 for $\varepsilon\theta = 0$ and $\Delta f = 0, \pm 5\%, \pm 10\%$ of the assumed frequency. This figure shows the degradation caused by an error in the frequency. We observe that a real improvement is achieved for m = 1, but further shifts do not help unless the frequency is known with some precision.

We conclude that three statistics should be performed in addition to the polarity coincidence; polarity difference with a 180° delay in each channel should also be performed.

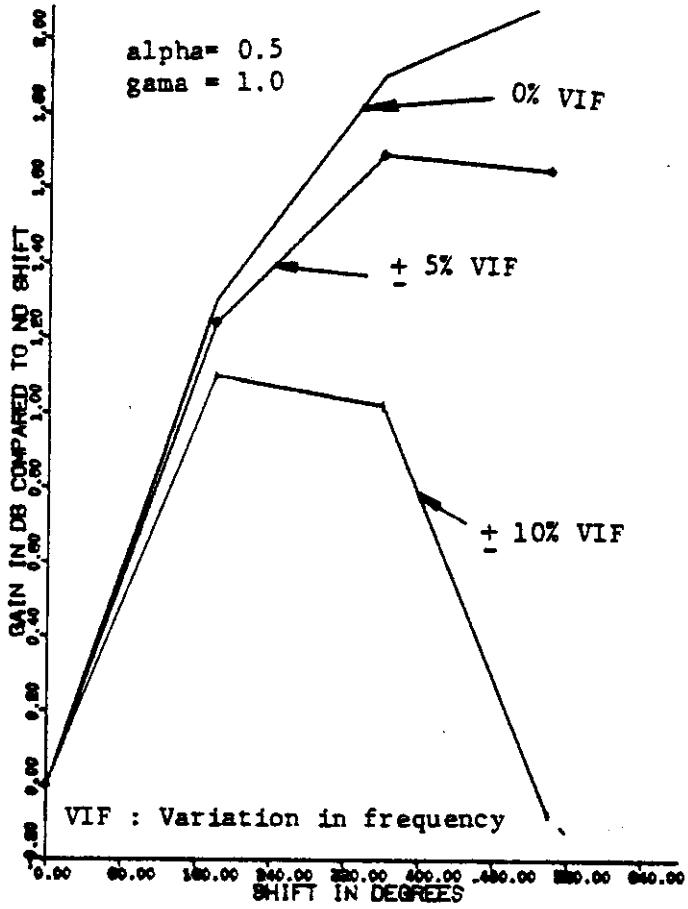

Figure 38. Improvement in performance versus various shifts when signal has 0%, ±5%, ±10% error

On combining Equations 6-1, 6-4, and 2-4 we obtain

$$D_{pcc} = \frac{\frac{2}{\pi}\sqrt{N}(1-D)\,[\sin^{-1}\rho_k - \sin^{-1}\rho_H]}{\sqrt{1 - (\frac{2}{\pi}\sin^{-1}\rho_k)^2 + 2\sum_{k=1}^{N}(1-\frac{1}{N})[Q_k(k) - (\frac{2}{\pi}\sin^{-1}\rho_k)^2]}} \qquad (6\text{-}5)$$

where $\rho_k = \dfrac{\frac{\sigma_s^2}{\sigma_n^2}\cos(m\pi\frac{\Delta\omega}{\omega} - \varepsilon\theta) + \rho_H}{1 + \frac{\sigma_s^2}{\sigma_n^2}}$

and where D(the loss in pulse sync) is bounded by $D \leq \frac{5}{M}$ where M is the number of processing intervals.

For very small input signal-to-noise ratios, the denominator can be evaluated under the Hypothesis of noise only, and the numerator can be approximated by the 1st two terms of a Taylor's expansion

$$\sin^{-1}\frac{a\frac{\sigma_s^2}{\sigma_n^2} + \rho_H}{1 + \frac{\sigma_s^2}{\sigma_n}} \approx \sin^{-1}[\rho_H + \frac{\sigma_s^2}{\sigma_n^2}(a - \rho_H)]$$

$$\approx \sin^{-1}\rho_H + \frac{a-\rho_H}{\sqrt{1-\rho_H^2}}\quad\frac{\sigma_s^2}{\sigma_n^2}$$

Incorporating these changes, and recognizing that N = 1,200 T(seconds) for our presumed sampling rate, we obtain

$$D_{pcc} \approx \frac{2}{\pi}\frac{\sqrt{1,200T}\,(1-D)}{\sqrt{1-\rho_H^2}}\,\frac{[\cos(m\pi\frac{\Delta\omega}{\omega} - \varepsilon\theta) - \rho_H]\,\frac{\sigma_s^2}{\sigma_n^2}}{\sqrt{1 - (\frac{2}{\pi}\sin^{-1}\rho_H)^2 + 2\sum_{k=1}^{N}(1-\frac{1}{N})[Q_H(k) - (\frac{2}{\pi}\sin^{-1}\rho_H)^2]}} \qquad (6\text{-}6)$$

Since $D \leq \frac{5}{M}$, the gain G (defined as $D_{pcc}/\sigma_s^2/\sigma_n^2$) is therefore bounded by

$$G > G_o\left[\frac{[\cos(m\pi\frac{\Delta\omega}{\omega} - \varepsilon\theta) - \rho_H](1 - \frac{5}{M})}{1 - \rho_H}\right]\sqrt{T}, \qquad (6\text{-}7)$$

where

$$G_o = \frac{\frac{2}{\pi}\,\frac{1-\rho_H}{1+\rho_H}\,34.64}{\sqrt{1-\left(\frac{2}{\pi}\sin^{-1}\rho_H\right)^2+2\sum_{k=1}^{N}\left(1-\frac{1}{N}\right)\left[Q_H(k)-\left(\frac{2}{\pi}\sin^{-1}\rho_H\right)^2\right]}} \qquad (6\text{-}8)$$

and the bracketed term represents the cost due to signal uncertainties.

The value of Go (between 10 and 20) is probably less than the gain of the human observer; perhaps by a factor of 2 or so. However, the human observer cannot accumulate information from one pulse to the next (i.e. no $\sqrt{T}$ term. Thus, for example, after 100 seconds (or 100 pulses), the gain of the PCC is improved by a factor of 10.

6.2.3 Use of Microprocessors in Parallel

We can effectively process the output of the PCC using microprocessor technology. For 40 overlapping intervals to be processed and assuming 0.1 seconds to read in the data and initial processing, and an additional 0.1 second to complete all three statistics,* we can process the data using only 8 microprocessors in parallel. The idea is shown in Figure 39(a) as the timing diagram of 8 microprocessors,[25-27] and the block diagram of an array processor in Figure 39(b). In the timing diagram the second microprocessor will start processing after 1/40 second and by the time the eighth microprocessor receives data, the first microprocessor has finished. Therefore, one processing cycle is complete after 0.2 seconds. Assuming 12000 samples/sec, only 300 words (each word corresponding to 8 quantized samples) are processed by an individual microprocessor which is quite reasonable for any available microprocessor in the market.

*The actual time depends on the microprocessor choice and the software package.

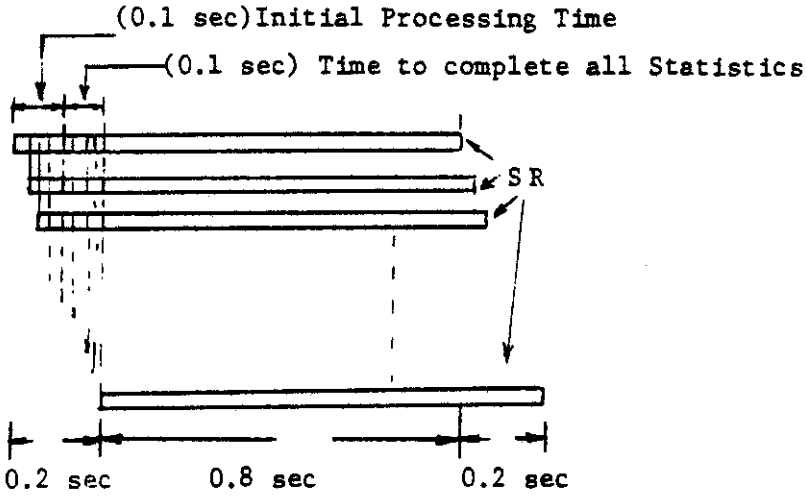

SR =Shift Register

Fig. 39(a) Timing Diagram

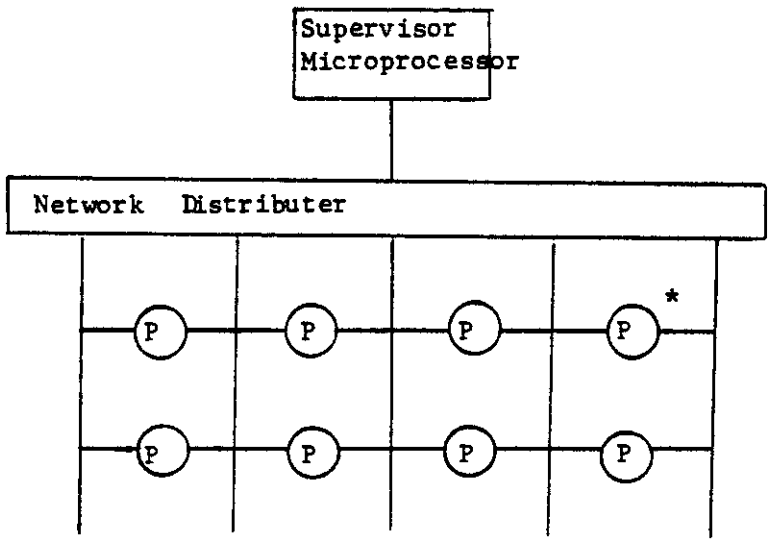

P= Processor

Fig. 39(b) Block Diagram of an Array Processor.

7.0 CONCLUSIONS AND SUGGESTIONS FOR FUTURE RESEARCH

7.1 Conclusions

A general expression was derived from the detection parameter of the polarity coincidence correlator, the inputs of which are assumed to consist of a common signal plus correlated, stationary gaussian noises. An expression was obtained for the expectation of the product of four hard limited (clipped) gaussian inputs with arbitrary cross-correlation, which is needed in order to evaluate the detection parameter of the PCC. A program to evaluate this expression has been implemented on the computer, evaluated and tested. This represents the most significant contribution of this study.

A general model for the kinds of cross-correlation functions that would result when passing two heavily correlated noise processes through identical band-pass filters were developed. The model was extended from band-pass to a combination of band-pass and low-pass processes. Based on this model, the performance of the PCC was evaluated and compared with the unclipped correlator and the sum and square detector. The sum and square detector is optimum for independent noise inputs and for negative magnitudes of cross-correlation. For positive and large magnitudes of cross-correlation, the unclipped correlator outperforms the sum and square detector, and so may be optimum in this range. We observed that, for positive cross-correlations, while the performance of all three detectors fall off substantially with an increase in the correlation coefficient, the cost of clipping relative to the optimum increases only

slightly, increasing from 2db to 3 db as the correlation increases from 0 to 0.5. For negative cross-correlation, while the unclipped correlator performed as before, the performance of the PCC and the sum and square detector increased as the magnitude of the correlation coefficient increased. As before, the cost of clipping compared to the optimum increases slightly. The increase in performance of the PCC is comparable for negatively correlated noise to the decrease for positively correlated noise.

The analysis is extended to two statistics, i.e., polarity coincidence and differences for 0.1 second duration sinusoidal bursts of nearly known frequency when the noise inputs are correlated. The decrease in performance relative to uncorrelated noise inputs is quite small. Indeed, for certain cross-correlation functions the performance increases. The increase in the cost of clipping with the correlation coefficient is also quite small. For the worst case, and perhaps the most likely case, where the cross-correlation function is proportional to the autocorrelation, i.e., $R_{n_1 n_2}(\tau) = \alpha R(\tau)$, the degradation can be kept low using the polarity difference statistic. For $\alpha = 0.5$, the degradation compared to the independent case is about 1db. The cost relative to the sum and square detector, for this case also increases by only 1db. The degradation caused by uncertainties of the signal parameters seem quite modest. A scheme to implement polarity coincidence and difference detectors, using microprocessor technology, is presented for the above problem.

7.2 Suggestions for Future Research

The analytical form of the expectation of the product of four clipped gaussian signals with correlated inputs, as calculated in Appendix E, diverges in certain regions. In this dissertation a scheme is presented to project those unstable points to a stable region. However, there is a need to develop a solution which converges in all regions. To possibly achieve that, the following four ways should be investigated.

a) A determination of the joint pdf of the outputs of four clippers whose inputs are jointly gaussian and correlated could be attempted. This joint pdf is expected to be the combination of delta functions, because every output can only take two values. Having this pdf in a closed analytical form can lead to an easier and possibly more accurate computation of the expectation, evaluated in Appendix E.

b) Using a transformation of cartesian coordinates into 4-dimensional spherical coordinates, the individual integrals in equation (E-5) of Appendix E might be formulated in a more stable form.

c) Another way to facilitate the computation of the above integrals originates from the fact that the correlation matrix between four gaussian inputs is symmetrical. Hence, one could find a suitable transformation to diagonalize this matrix, immediately transforming the 4-D integrals into product of four 1-D integrals.

d) Price[28] has generalized Van Vleck's approach to calculate the bivariate expected value of two random variables where these random variables are arbitrary functions of gaussian random variables.

While Gupta[29] has shown that multivariate normal expectation cannot be analytically expressed in closed form, a formulation based on Rice's approach may lead to a more stable numerical computation of this expectation.

Another subject for further research is related to implementation. The polarity coincidence correlator is simple in its hardware implementation. Since the PCC has been analyzed for a wide range of cross-correlation shapes and the results are, or can be made, very encouraging, its implementation can be the subject of further research.

Chapter 6 of this dissertation gives some idea about the arrangement of microprocessors. However, there is a need to develop this hardware structure and software carefully based on particular microprocessors. There are a few significant aspects of the implementation that we have not explored. We have not explored the manner in which either the supervisor microprocessor or the parallel processors accumulate the statistics from each signal pulse for display on a CRT. While we have determined that dividing each 1-second segment into 40 intervals seems reasonable, the number of parallel processors needed will undoubtedly be significantly less. This number will depend on the particular microprocessor and the efficiency of the software.

We are confident, however, that if the receiver suggested in this report were implemented and tested, it would prove to be a valuable detector.

APPENDIX A

OPTIMUM TWO-CHANNEL DETECTOR

Consider the problem of detecting a random, gaussian signal that is common to two channels containing stationary gaussian noise. If the product of the integration time (T) and the signal bandwidth (B) is large, both signals can be accurately represented by the Fourier Series where the coefficients are statistically independent [see reference 3 for example]. Thus we can write

$$s_j(t) = \sum_{i=1}^{BT} a_{ij}\sqrt{\frac{2}{T}} \cos i\omega_{ot} + b_{ij}\sqrt{\frac{2}{T}} \sin i\omega_{ot} , \qquad (A\text{-}1)$$

and

$$n_j(t) = \sum_{i=1}^{BT} c_{ij}\sqrt{\frac{2}{T}} \cos i\omega_{ot} + d_{ij}\sqrt{\frac{2}{T}} \sin i\omega_{ot} , \qquad (A\text{-}2)$$

where j = 1 or 2 and is the channel index. The assumptions that the signal is either common to both channels or 180° out of phase, that each noise input has the same power spectrum N(f), and that the coefficients are independent, enables us to write, for each frequency i, the following spatial correlation matrices for the signal only (P) and noise only (Q) cases.

$$P(i) = S(i) \begin{array}{c} \\ a_{i1} \\ b_{i1} \\ a_{i2} \\ b_{i2} \end{array} \begin{array}{c} \begin{array}{cccc} a_{i1} & b_{i1} & a_{i2} & b_{i2} \end{array} \\ \begin{bmatrix} 1 & 0 & \pm 1 & 0 \\ 0 & 1 & 0 & \pm 1 \\ \pm 1 & 0 & 1 & 0 \\ 0 & \pm 1 & 0 & 1 \end{bmatrix} \end{array}, \qquad \text{(A-3)}$$

$$Q(i) = N(i) \begin{array}{c} \\ c_{i1} \\ d_{i2} \\ c_{i2} \\ d_{i2} \end{array} \begin{array}{c} \begin{array}{cccc} c_{i1} & d_{i1} & c_{i2} & d_{i2} \end{array} \\ \begin{bmatrix} 1 & 0 & \rho(i) & 0 \\ 0 & 1 & 0 & \rho(i) \\ \rho(i) & 0 & 1 & 0 \\ 0 & \rho(i) & 0 & 1 \end{bmatrix} \end{array}, \qquad \text{(A-4)}$$

where S(i) is the value of the signal spectrum at frequency $i\omega_o$ and where

$$\rho_i = \frac{\overline{c_{i1} c_{i2}}}{\sqrt{\overline{c_{i1}^2 c_{i2}^2}}} = \frac{\int_0^T (1 - \frac{u}{T})\, R_{12}(u) \cos m\, \omega_o u\, du}{\int_0^T (1 - \frac{u}{T})\, R_n(u) \cos m\, \omega_o u\, du}, \qquad \text{(A-5)}$$

where $R_n(u)$ is the autocorrelation of the noise (or Fourier Transform of N(f)) and $R_{12}(\cdot)$ is the cross correlation between the two noise inputs. Under the assumption TB>>1, this is closely approximated by

$$\rho_i \cong \frac{N_{12}(i)}{N(i)} , \qquad \text{(A-6)}$$

where $N_{12}(f)$ is the Fourier Transform of $R_{12}(\tau)$.

If $\underline{z}_1$ is a vector representing the four Fourier Series coefficients of the detector inputs (a_i, b_i for each channel) at each frequency i, then

$$\ell n\ \Lambda = k + \sum_{i=1}^{BT} [-z_i^T T(i)^{-1}\ \underline{z}_1 + \underline{z}_i^T\ Q(i)^{-1}\ \underline{Z}_i] , \qquad \text{(A-7)}$$

where Λ is the likelihood ratio, $\frac{f(z/\text{signal and noise})}{f(z/\text{noise only})}$, and

$$T(i) = P(i) + Q(i) . \qquad \text{(A-8)}$$

The optimum detector [any statistic nonotonically related to the likelihood ratio] forms the statistic

$$D_{opt} = \sum_{i=1}^{BT} \underline{z}_i^T\ [Q(i)^{-1} - T(i)^{-1}]\ \underline{Z}_i \quad . \qquad \text{(A-9)}$$

After performing the algebra implied by equations A-9, A-8, A-3, and A-4, it can be shown that

$$D_{opt} = \sum_{i=1}^{BT} \frac{S_i}{(1+\rho_i)^2 N_i^2\ (1+2\ \frac{S_i}{N_i}\ \frac{1}{(1+\rho_i)})} \cdot [(a_{i1} \pm a_{i2})^2 + (b_{i1} \pm b_{i2})^2], \qquad \text{(A-10)}$$

where the + sign corresponds to signals exactly in phase and the - sign corresponds to signals 180° out of phase, and a_{i1}, b_{i1}, a_{i2}, b_{i2} are the variables of z_i.

We now wish to show that this statistic can be implemented by the following receiver:

$$X_1(t) = \Sigma \sqrt{\frac{2}{T}}\, a_{i1} \cos i\,\omega_o t + \sqrt{\frac{2}{T}}\, b_{i1} \sin i\,\omega_o t$$

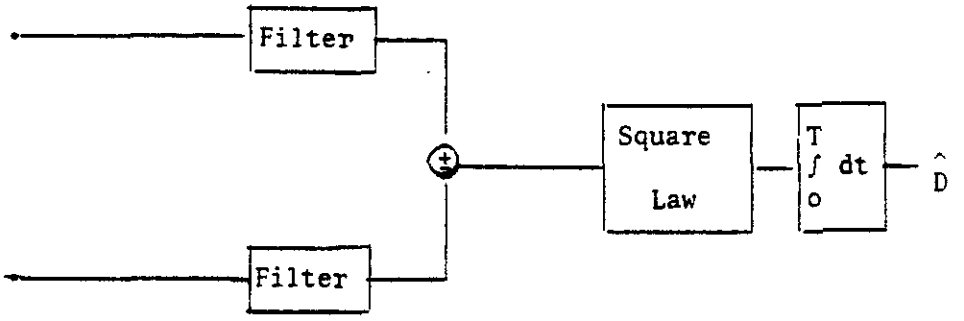

$$X_2(t) = \Sigma \sqrt{\frac{2}{T}}\, a_{i2} \cos i\,\omega_o t + \sqrt{\frac{2}{T}}\, b_{i2} \sin i\,\omega_o t \quad .$$

If $H(\omega)$ is the transfer function of the filter, the output of the summer (difference) can be written as

$$\sum_{i=1}^{TB} \sqrt{\frac{2}{T}}\, |H(i)|\, (a_{i1} \pm a_{i2}) \cos(i\omega_o t + \theta_i) + \sqrt{\frac{2}{T}}\, |H(i)|\, (b_{i1} \pm b_{12}) \cdot \sin i\,\omega_o t + \theta_1) \qquad \text{(A-11)}$$

where θ_i is the phase of $H(i\omega_o)$. The square law device and integrator calculates the energy in this signal or

$$\hat{D} = \Sigma\, |(H(i))|^2\, [(a_{i1} \pm a_{i2})^2 + (b_{i1} \pm b_{i2})^2] \quad . \qquad \text{(A-12)}$$

This is the same statistic as that of equation (A-10) provided

$$|H(i\omega_o)|^2 = \frac{S_i}{N_i{}^2 (1+\rho_i)^2}\, [1+2\, \frac{S_i}{N_i}\, \frac{1}{(1+\rho_i)}]^{-1}. \qquad \text{(A-13)}$$

Thus we have found the optimum detector if we can implement the filter indicated by equation (A-13).

APPENDIX B

DETECTION PARAMETER (OUTPUT SIGNAL-TO-NOISE RATIO) OF THE TWO CHANNEL DETECTOR THAT IS LOCALLY OPTIMUM FOR GAUSSIAN NARROW BAND INPUTS

For very small input signal-to-noise ratios $\frac{S_i}{N_i}$, the optimum filter (Equation A-13) can be replaced with

$$|H(i\omega_o)|^2 = \frac{S_1}{N_i^2(1+\rho_i)^2} \tag{B-1}$$

The resultant detector is called "locally optimum." For very narrow band signals, this amounts to just a narrow band filter that just passes the signal. If $n_i(t)$ are the noise in each channel just after the filter, the test statistic can be written as

$$S_{H_o} = \int_o^T [n_1(t) \pm n_2(t-\tau)]^2 \, dt, \tag{B-2}$$

where H_o represents the hypothesis of noise only and

$$S_{H_1} = \int_o^T [2\, s(t) \pm n_1(t) + n_2(t-\tau)]^2 \, dt, \tag{B-3}$$

where H_1 is the alternative of an additive common signal. The output signal-to-noise ratio (D_{opt}) is given by

$$D_{opt} = \frac{E_{H_1}(S) - E_{H_o}(S)}{\sqrt{Var_{H_o}(S)}} \tag{B-4}$$

After some lengthy but straight-forward calculations, it is determined that

$$E_{H_o}(S) = 2\sigma_n^2 T[1+\rho_{12}(\tau)] , \tag{B-5}$$

$$E_{H_1}(S) - E_{H_o}(S) = 4 < S^2(t)> T, \tag{B-6}$$

and

$$Var_{H_o}(S) = 4\sigma_n^2 T \int_o^T (1- \frac{k}{T}) [\rho_{11}(k) + \rho_{22}(k) + \rho_{12}(k-\tau) \pm \rho_{12}(k+\tau)]^2 dk, \tag{B-7}$$

where σ_n^2 is the variance of the noise, T is the integration time, $\rho_{12}(\tau)$ is the normalized cross correlation function between $n_1(t)$ and $n_2(t)$, and $\rho_{11}(\tau)$ is the autocorrelation function of $n_1(t)$ or $n_2(t)$. Substituting into equation (B-4) we get

$$D_{opt} = \frac{<S^2(t)>}{\sigma_n^2} \sqrt{\frac{2T}{\frac{1}{2}\int_o^T (1- \frac{k}{T}) \psi(k, \tau) dk}} , \tag{B-8}$$

where

$$\psi(k, \tau) = [\rho_{11}(k) + \rho_{22}(k) \pm \rho_{12}(k-\tau) \pm \rho_{12}(k+\tau)]^2 . \tag{B-9}$$

Let us now make the very unrealistic assumption that the noise inputs are uncorrelated or $\rho_{12}(\tau) = 0$ for all τ. Assuming further that $\rho_{11}(k) = \rho_{22}(k) = \rho(k)$, equation (B-7) becomes

$$Var_{H_0}(S) = 16\sigma_n^2 T \int_o^T (1- \frac{k}{T}) \rho^2(k)dk,$$

$$\cong 8T \int_{-\infty}^{\infty} \sigma_n^2 \rho^2(k)dk, \text{ for } BT >> 1$$

and in the frequency domain the above expression becomes

$$= 8\,T \int_{-\infty}^{\infty} \left\{\frac{N_o}{2}\,|H(jf)|\right\}^2 df,$$

$$\cong 8\,T\,\frac{N_o^2}{4}\,2\,B\ ,$$

where B is the filter bandwidth. If the signal is a sinewave with amplitude A, then equation (B-6) becomes

$$E_{H_1}(S) - E_{H_o}(S) = 4\,\frac{A^2}{2}\,T.$$

Substituting again into equation (B-4),

$$D_{opt} \cong \frac{A^2}{N_o}\sqrt{\frac{T}{B}}\ . \qquad \text{(B-10)}$$

Finally, if there are N bursts of 0.1 second duration signals, then $T = 0.1\,N$ and

$$D_{opt} \cong \frac{A^2}{N_o}\sqrt{\frac{N}{10B}}\ . \qquad \text{(B-11)}$$

APPENDIX C

DETECTION PARAMETER OF AN IDEAL ENVELOPE DETECTOR AND COMPARISON WITH THE TWO CHANNEL LOCALLY OPTIMUM DETECTOR

In this Appendix we evaluate the ideal envelope detector under the assumption of independent noise inputs and compare it with the two channel results of Appendix B. The output of an envelope detector is given by

$$S = \left[\int_o^T z(t) \cos \omega_c t \, dt\right]^2 + \left[\int_o^T z(t) \sin \omega_c t \, dt\right]^2 , \qquad \text{(C-1)}$$

where under the hypotheses H_o, $z(t) = N(t)$ and under the alternative H_1, $z(t) = s(t) + N(t)$. It is easily seen that

$$E(S) = \int_o^T \int_o^T E\{z(t_1) z(t_2)\} \cos \omega_c (t_1 - t_2) \, dt_1 dt_2 .$$

It follows that

$$E_{H_o}(S) = \int_o^T \int_o^T R_n(t_1 - t_2) \cos \omega_c (t_1 - t_2) \, dt_1 dt_2 \qquad \text{(C-2)}$$

and

$$E_{H_1}(S) - E_{H_o}(S) = \int_o^T \int_o^T s(t_1) s(t_2) \cos \omega_c (t_1 - t_2) \, dt_1 dt_2 . \qquad \text{(C-3)}$$

We let $s(t) = A \sin [(\omega_c + \Delta\omega) t + \theta]$, where $\Delta\omega$ is the uncertainty in the signal frequency. Equation (C-3) can be evaluated as

$$E_{H_1}(S) - E_{H_o}(S) = \frac{A^2}{4}\left\{\frac{\cos\left[(2\omega_c + \Delta\omega)\,T + \right] - \cos\theta}{2\omega_c + \Delta\omega} + \frac{\cos(\Delta\omega T+\theta) - \cos\theta}{\Delta\omega}\right\}^2$$

$$+ \frac{A^2}{4}\left\{\frac{\sin\left[2\omega_c + \Delta\omega)\,T+\theta\right] - \sin\theta}{(2\omega_c + \Delta\omega)} - \frac{\sin(\Delta\omega T+\theta) - \sin\theta}{\Delta\omega}\right\}^2 . \qquad \text{(C-4)}$$

The $(2\omega_c + \Delta\omega)$ terms are much smaller than the other terms. A good approximation involves ignoring these terms, and equation (C-4) can be manipulated into

$$E_{H_1}(S) - E_{H_o}(S) \cong \frac{A^2T^2}{4}\,\text{sinc}^2\,\pi\Delta\,ft \quad . \qquad \text{(C-5)}$$

It can be determined that for gaussian noise,

$$\text{Var}_{H_o}(S) = \frac{N_o^2}{2}\,T\int_o^T\left(1-\frac{u}{T}\right)\cos^2\omega_c u\,du$$

$$= \frac{N_o^2T^2}{4}\left[1 + \text{sinc}^2\,2\pi fcT\right] . \qquad \text{(C-6)}$$

The output signal-to-noise ratio D_{ENV} can be determined by dividing equation (C-5) by the square root of equation (C-6) or

$$D_{ENV} = \frac{A^2T}{2N_o}\,\frac{\text{sinc}^2\,\pi\Delta fT}{\sqrt{1+\text{sinc}^2\,2\pi fcT}} \qquad \text{(C-7)}$$

For T = .1 sec, fc = 1000 Hz, this becomes

$$D_{ENV} = \frac{A^2}{20N_o}\,\text{sinc}^2\left(\frac{\pi\Delta f}{10}\right) . \qquad \text{(C-8)}$$

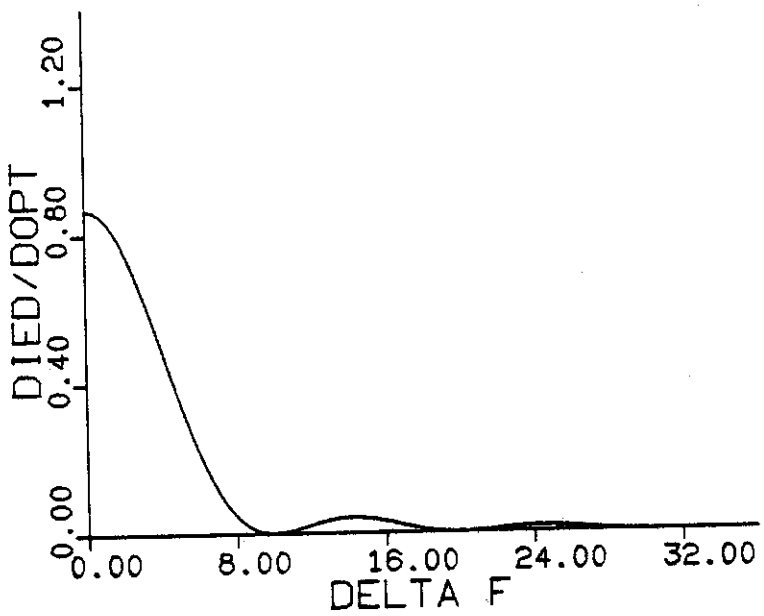

Figure C-1. Died/Dopt vs. Delta F

Finally for N pulses,

$$D_{ENV} = \frac{A^2}{2ON_o} \sqrt{N}\ \mathrm{sinc}^2\ (\frac{\pi\Delta f}{10}) \quad . \tag{C-9}$$

If we compare the two channel detector, equation (B-11) for a filter bandwidth (B) of 30 Hz with this one channel envelope detector, we get

$$\frac{D_{ENV}}{D_{opt}} = 0.866\ \mathrm{sinc}^2\ \frac{\pi\Delta f}{10} \quad . \tag{C-10}$$

This equation is plotted in Figure (C-1). For greater uncertainties it is considerably worse.

Of course this analysis is very preliminary because of the unrealistic assumption that the noise inputs are independent. If we compare two-channel detector with two outputs of I.E.D. then (C-10) becomes

$$\frac{D_{ENV}}{D_{opt}} = 1.7\ \mathrm{sinc}^2\ \frac{\pi\Delta f}{10} \tag{C-11}$$

In theory, we can extend coherent analysis beyond one pulse. But from Figure (C-1), for coherent detection, beyond one pulse of duration 0.1 sec, we should know the frequency to within 0.01%.

APPENDIX D

CALCULATION OF DETECTION PARAMETERS

I. Polarity Coincidence Correlator (PCC)

The detection parameter for the PCC is

$$D_{pcc} \triangleq \frac{E_K\{S\} - E_H\{S\}}{\sqrt{Var_K\{S\}}} , \qquad (D\text{-}1)$$

with hypothesis

$$H: \quad x(t) = n(t), \qquad \text{all } t \in (0,T)$$

$$K: \quad x(t) = n(t) + S(t)$$

n(t), S(t) are noise process and signal, and

$$S = \sum_{i=1}^{N} h\,[\bar{x}(t+i\tau)] , \qquad (D\text{-}2)$$

where

$$h[\bar{x}(t)] = \left|\frac{1}{2}\,(\mathrm{Sgn}\ x_1(t) + \mathrm{Sgn}\ x_2(t))\right|^2 , \qquad (D\text{-}3)$$

the $x_i(t)$ refer to two inputs and N is the number of obversations.

The variance of the test statistic is

$$Var\,[S] = E\,[S^2] - E^2[S]$$

$$\text{Var}\,[S] = E\Big\{\sum_{i=1}^{N}\sum_{j=1}^{N} h[\bar{x}(t+i\tau)]\; h[\bar{x}(t+j\tau)]\Big\} - \Big\{E\Big[\sum_{i=1}^{N} h[\bar{x}(t+i\tau)]\Big]\Big\}^2$$

$$= \sum_{i=1}^{N} [E\{h^2[\bar{x}(t+i\tau)]\} - E^2\{h[\bar{x}(t)]\}] + \sum_{\substack{i\ j\\ i\neq j}}^{N\ N} [E\{h[\bar{x}(t+i\tau)]$$

$$\cdot\; h[\bar{x}(t+j\tau)]\} - E^2\{h[\bar{x}(t)]\}$$

$$= N\ \text{Var}\,\{h[\bar{x}(t)]\} + 2\sum_{k=1}^{N} (N-k)\,\{E[h[\bar{x}(t)]\; h[\bar{x}(t+k\tau)]]$$

$$- E^2\,[h[\bar{x}(t)]]\} \qquad \text{(D-4)}$$

From Van Vleck[14] it is known that $E[\text{Sgn}\ x_1(t)\ \text{Sgn}\ x_2(t)] = (2/\pi)^2 \sin^{-1}\rho$, where ρ is the correlation coefficient. Using this result,

$$\text{Var}\,\{h[\bar{x}(t)]\} = \frac{1}{4} - 1/\pi^2\,(\sin^{-1}\rho)^2 \qquad \text{(D-5)}$$

and

$$E\,\{h[\bar{x}(t)]\; h[\bar{x}(t+k)]\} = \frac{1}{4} + 1/\pi\ \sin^{-1}\rho + \frac{1}{4}\,E\,[\text{Sgn}\ x_1(t)$$

$$\cdot\ \text{Sgn}\ x_2(t)\ \text{Sgn}\ x_1(t+k)\ \text{Sgn}\ x_2(t+k)] \qquad \text{(D-6)}$$

After substituting the results of (D-5) and (D-6) in (D-4) we obtain,

$$\text{Var}\,[S] = \frac{N}{4}\left[1 - (2/\pi \sin^{-1}\rho)^2 + \sum_{k=1}^{N}(1-\frac{k}{N})\{E[\text{Sgn}\,x_1(t)\,\text{Sgn}\,x_2(t)\right.$$

$$\left.\cdot\,\text{Sgn}\,x_1(t+k)\,\text{Sgn}\,x_2(t+k)] - (2/\pi \sin^{-1}\rho)^2\}\right] \qquad \text{(D-7)}$$

We now calculate the shift in the mean of the statistic or

$$E_K[S] - E_H[S]$$

$$E_K(S) = 2N \int_0^\infty \int_0^\infty (2\pi)^{-1}\,[\det P]^{-1/2} \cdot e^a \cdot dx_1 dx_2 \qquad \text{(D-8)}$$

where $a = -(1/2)\,(x_1,x_2)\,[P]^{-1}\begin{bmatrix} x_1 \\ x_2 \end{bmatrix}$

and correlation matrix

$$P_K = \begin{bmatrix} R_{x_1x_1}(0) & R_{x_1x_2}(0) \\ R_{x_1x_2}(0) & R_{x_2x_2}(0) \end{bmatrix} \qquad \text{(D-9)}$$

After changing the integral of (D-8) into polar coordinants and using the identity,

$$\int_0^{\pi/2} \frac{d\phi}{1-r\sin 2\phi} = (1-r^2)^{-1/2}\{\pi/2 + \sin^{-1}r\}\,, \qquad \text{(D-10)}$$

and after some simplifications, we get

$$E_K[S] = \frac{N}{\pi}\left[\pi/2 + \sin^{-1}\frac{R_{x_1x_2}(0)}{R_{x_1x_1}(0)}\right] \qquad \text{(D-11)}$$

Similarly,

$$E_H[S] = \frac{N}{\pi}\left[\pi/2 + \sin^{-1}\frac{R_{n_1 n_2}(0)}{R_n(0)}\right] \qquad \text{(D-12)}$$

Utilizing results of (D-6), (D-11), and (D-12) in (D-1) we get,

$$D_{pcc} = \frac{\sqrt{N}\,(2/\pi)\,[\sin^{-1}\rho_K - \sin^{-1}\rho_H]}{\left[1-\{(2/\pi)\sin^{-1}\rho_K\}^2 + 2\sum_{k=1}^{N}(1-\frac{k}{N})[Q(k) - \{(2/\pi)\sin^{-1}\rho_K\}^2]\right]^{1/2}} \qquad \text{(D-13)}$$

where,

$$\rho_K = \frac{R_{x_1 x_2}(0)}{R_{x_1 x_2}(0)}$$

$$\rho_H = \frac{R_{n_1 R_{n_2}}(0)}{R_n(0)}$$

and

$$Q(k) = E[\text{Sgn } x_1(t)\ \text{Sgn } x_2(t)\ \text{Sgn } x_1(t+k)\ \text{Sgn } x_2(t+k)] \qquad \text{(D-14)}$$

An evaluation of (D-14) is presented in Appendix E.

II. Detection Parameter for the Unclipped Correlator (D_c)

The test statistic for the correlator is

$$S = \sum_{i=1}^{N} x_1(t_i)x_2(t_i) \quad , \qquad \text{(D-15)}$$

where $x_i(t)$ refers to two zero mean gaussian inputs under the hypothesis. For the purpose of the evaluation of the detection parameter D_c, we will assume a general shape of the autocoreelation and cross-correlation. Thus in this case,

$$E_K(S) - E_H(S) = N\, R_s(0) \tag{D-16}$$

where $R_s(0)$ is the signal power

$$\mathrm{Var}_H(S) = E_H[S^2] - E_H^2[S]$$

$$= E_H\Big[\sum_{ij}^{NN} x_i(t_i)\, x_2(t_i)\, x_1(t_j)\, x_2(t_j)\Big] - E_H\Big[\sum_{j}^{N} x_1(t_i)\, x_2(t_i)\Big]^2 \tag{D-17}$$

The first part of the above expression for zero mean gaussian random variable can be expanded as follows:

$$E[x_1(t_1)\, x_2(t_2)\, x_3(t_3)\, x_4(t_4)] = R_{x_1x_2}(t_2-t_1)\, R_{x_3x_4}(t_4-t_3) + R_{x_1x_3}(t_3-t_1)\, R_{x_2x_4}(t_4-t_2) + R_{x_1x_4}(t_4-t_1) + R_{x_2x_3}(t_3-t_2) \tag{D-18}$$

Using the above expression in (D-16) and after some simplification, we can write

$$\mathrm{Var}_H(S) = N\Big[R^2(0) + R_{x_1x_2}(0) + 2\sum_{k=1}^{N}\left(1-\frac{k}{N}\right)\{R^2(k) + R_{x_1x_2}(k)\cdot R_{x_1x_2}(-k)\}\Big] \tag{D-19}$$

where R(k) and $R_{x_1x_2}(k)$ are the auto-correlation and cross-correlation of inputs $x_1(t)$ and $x_2(t)$ respectively. Using (D-16) and (D-19) the detection parameter for the correlator can be written as

$$D_c = \frac{\sqrt{N}\, R_s(0)}{\left[R^2(0) + R^2_{x_1x_2}(0) + 2 \sum_{k=1}^{N} (1 - \frac{k}{N})\ R^2(k) + R_{x_1x_2}(k)\ R_{x_1x_2}(-k)\right]^{1/2}} \qquad \text{(D-20)}$$

III. Detection Parameter for the Sum and Square Detector (D_{SS})

The test statistic of the sum and square detector is defined as

$$S = \sum_{i=1}^{N} [x_1(t_i) + x_2(t_i)]^2 \quad . \qquad \text{(D-21)}$$

The shift in mean becomes

$$E_K(S) - E_H(S) = 4NR_s(0) \quad . \qquad \text{(D-22)}$$

also

$$E_H(S)^2 = E_H \sum_{i}^{N} \sum_{j}^{N} [x_1(t_i) + x_2(t_i)]^2\ [x_i(t_j) + x_2(t_j)]^2 \qquad \text{(D-23)}$$

Expanding equation (D-23) and using the following equivalents

$$E[x_1(t_i)\ x_1(t_i)\ x_1(t_j)\ x_1(t_j)] = R^2(0) + 2R^2(t_i - t_j) \ ,$$

$$E[x_1(t_i)\ x_1(t_i)\ x_2(t_j)\ x_2(t_j)] = R^2(0) + 2R^2_{x_1x_2}(t_i - t_j) \ ,$$

$$E[x_1(t_i)\ x_1(t_i)\ x_1(t_j)\ x_2(t_j)] = R(0)R_{x_1x_2}(0) + 2R(t_i-t_j)\ R_{x_1x_2}(t_it_j)\ ,$$

$$E[x_1(t_i)\ x_1(t_j)\ x_2(t_i)\ x_2(t_j)] = R^2(t_i-t_j) + R^2_{x_1x_2}(0) + R_{x_1x_2}(t_i-t_j)$$

$$R_{x_1x_2}(t_j-t_i)\ ,$$

and $$E_H[S] = 2N[R_{x_1x_2}(0) + R(0)]\ ,$$

the variance becomes

$$\begin{aligned}
Var_H(S) &= E_H[S^2] - E^2_H[S] \\
&= 8N\ \{R^2(0)+R^2_{x_1x_2}(0) = 2R(0)R_{x_1x_2}(0) + \sum_{k=1}^{N}(1-\frac{k}{N})\ . \\
&\cdot[2R^2(k) + 0.5\ (R^2_{x_1x_2}(k) + R^2_{x_1x_2}(-k) + 2(R_{x_1x_2}(k) \\
&+ R_{x_kx_2}(-k)\ R(k) + R_{x_1x_2}(k)\ R_{x_1x_2}(-k)]\}
\end{aligned} \tag{D-24}$$

Therefore,

$$D_{SS} = \frac{4N\ R_s(0)}{\sqrt{Var_H(S)}} \tag{D-25}$$

where the variance is given in (D-24).

APPENDIX E

THE EXPECTATION OF THE PRODUCT OF FOUR CLIPPED GAUSSIAN RANDOM VARIABLES

We use the following notation

Variables	Random Variable (samples of Stochastic Process)
x_1 - - - - - - - - - - - - - - - - -	$x_1(t)$
x_2 - - - - - - - - - - - - - - - - -	$x_2(t)$
x_3 - - - - - - - - - - - - - - - - -	$x_1(t + k\tau)$
x_4 - - - - - - - - - - - - - - - - -	$x_2(t + k\tau)$

where the x_i are zero mean gaussian.

The general correlation matrix C is given as

$$C = \begin{bmatrix} R_{11}(0) & R_{12}(0) & R_{11}(k\tau) & R_{12}(-k\tau) \\ R_{12}(0) & R_{22}(0) & R_{12}(k\tau) & R_{22}(k\tau) \\ R_{11}(k\tau) & R_{12}(k\tau) & R_{11}(0) & R_{12}(0) \\ R_{12}(-k\tau) & R_{22}(k\tau) & R_{12}(0) & R_{22}(0) \end{bmatrix} \qquad \text{(E-1)}$$

where $R_{ii}(k\tau)$ and $R_{ij}(k\tau)$ are the autocorrelation and cross-correlation between x_i and x_j $\quad (i,j = 1,2)$.

The joint gaussian p.d.f of four variable can be written as

$$p(\underline{x}) = (2\pi)^{-2} [\det C]^{-1/2} \exp\{-(\tfrac{1}{2}) \sum_{i=1}^{4} \sum_{j=1}^{4} q_{ij} x_i x_j\} , \qquad \text{(E-2)}$$

where the coefficients q_{ij} are the elements of C^{-1}. We are to compute

$$R = E\left[\prod_{i=1}^{4} \text{Sgn } x_i\right] \tag{E-3}$$

where Sgn x(t) is 1 if $x(t) > 0$ and -1 if $x(t) < 0$.

$$R = \int_{-\infty}^{\infty}\int_{-\infty}^{\infty}\int_{-\infty}^{\infty}\int_{-\infty}^{\infty} \text{Sgn } x_1 \text{ Sgn } x_2 \text{ Sgn } x_3 \text{ Sgn } x_4 \; p(\underline{x}) \cdot d\underline{x} \tag{E-4}$$

which can be written as a sum of 16 integrals in equation (E-5) found on the following page.

Introducing a suitable change in variables, each of the 16 ingegrals can be written as

$$I \triangleq \int_{0}^{\infty}\int_{0}^{\infty}\int_{0}^{\infty}\int_{0}^{\infty} \exp\left\{-\left(\frac{1}{2}\right) \sum_{i=1}^{4}\sum_{j=1}^{4} w_{ij}\, x_i x_j\right\} d\underline{x} \tag{E-6}$$

where the coefficients w_{ij} are identical to q_{ij}, but with appropriate changes in signs which are due to the change of variables.

In this Appendix, the solution of one of the 16 integrals will be presented, where the remaining 15 can be solved with a similar result and the summation of the 16 results is the expectation of $\prod_{i=1}^{4} \text{Sgn } x_i$.

Let (E-6) be written as

$$I = \int_{0}^{\infty}\int_{0}^{\infty}\int_{0}^{\infty}\int_{0}^{\infty} e^{a}\; dx_1\, dx_2\, dx_3\, dx_4 \;, \tag{E-7}$$

where

$$R = \int_0^\infty\int_0^\infty\int_0^\infty\int_0^\infty p(\underline{x})d\underline{x} - \int_{-\infty}^0\int_0^\infty\int_0^\infty\int_0^\infty p(\underline{x})d\underline{x} - \int_0^\infty\int_{-\infty}^0\int_0^\infty\int_0^\infty p(\underline{x})d\underline{x} - \int_{-\infty}^0\int_{-\infty}^0\int_0^\infty\int_0^\infty p(\underline{x})d\underline{x}$$

$$- \int_0^\infty\int_0^\infty\int_{-\infty}^0\int_0^\infty p(\underline{x})d\underline{x} + \int_{-\infty}^0\int_0^\infty\int_{-\infty}^0\int_0^\infty p(\underline{x})d\underline{x} + \int_0^\infty\int_{-\infty}^0\int_{-\infty}^0\int_0^\infty p(\underline{x})d\underline{x} - \int_{-\infty}^0\int_{-\infty}^0\int_{-\infty}^0\int_0^\infty p(\underline{x})d\underline{x}$$

$$- \int_0^\infty\int_0^\infty\int_0^\infty\int_{-\infty}^0 p(\underline{x})d\underline{x} + \int_{-\infty}^0\int_0^\infty\int_0^\infty\int_{-\infty}^0 p(\underline{x})d\underline{x} + \int_0^\infty\int_{-\infty}^0\int_0^\infty\int_{-\infty}^0 p(\underline{x})d\underline{x} - \int_{-\infty}^0\int_{-\infty}^0\int_{-\infty}^0\int_{-\infty}^0 p(\underline{x})d\underline{x})$$

$$+ \int_0^\infty\int_0^\infty\int_{-\infty}^0\int_{-\infty}^0 p(\underline{x})d\underline{x} - \int_{-\infty}^0\int_0^\infty\int_{-\infty}^0\int_{-\infty}^0 p(\underline{x})d\underline{x} - \int_0^\infty\int_{-\infty}^0\int_{-\infty}^0\int_{-\infty}^0 p(\underline{x})d\underline{x} + \int_{-\infty}^0\int_{-\infty}^0\int_{-\infty}^0\int_{-\infty}^0 p(\underline{x})d\underline{x}$$

(E-5)

$$a = -(1/2) \sum_{i=1}^{4} W_{ii} x_i^2 + \sum_{\substack{i=1 \\ i \neq j}}^{4} \sum_{j=1}^{4} W_{ij}\, x_i x_j \qquad \text{(E-8)}$$

Integrating with respect to x_1 first,

$$I = A \int_0^{\infty} e^{-\frac{W_{11}}{2} x_1^2 (W_{12}x_2 + W_{13}x_3 + W_{14}x_4)} \cdot dx_1 \qquad \text{(E-9)}$$

where A represents all of the constant terms.

Using the identities,

$$e^x = \sum_{i=0}^{\infty} \frac{(x)^i}{i!} \quad \text{and}$$

$$\int_0^{\infty} x^i e^{-\frac{W}{2} x^2} \cdot dx = \frac{\Gamma(\frac{i+1}{2})}{2(\frac{W}{2})^{(i+1)/2}} \qquad \text{(E-10)}$$

(E-9) can be written as

$$I = \int_0^{\infty}\int_0^{\infty}\int_0^{\infty} \sum_{i=0}^{\infty} \frac{\Gamma(\frac{i+1}{2})}{2(\frac{W_{11}}{2})^{(i+1)/2}} \frac{(W_{12}x_2+W_{13}x_3+W_{14}x_4)^i}{i!} \cdot e^b \cdot dx_2 dx_3 dx_4$$

where

$$b = -(1/2)\,[W_{22}x_2^2+W_{33}x_3^2+W_{44}x_4^2] + W_{23}x_2x_3+W_{24}x_2x_4+W_{34}x_3x_4 \qquad \text{(E-11)}$$

Rearranging for x_2

$$I = B \int_0^\infty e^{-\frac{W_{22}}{2} \cdot x^2} \cdot e^{x_2(W_{23}x_3+W_{24}x_4)} (W_{12}x_2+W_{13}x_3+W_{14}x_4)^i \cdot dx_2 \qquad \text{(E-12)}$$

B represents the terms and constants which are not involved in the integral with respect to x_2. Using the binomial expansion,

$$I = B \int_0^\infty e^{-\frac{W_{22}}{2} \cdot x_2^2} \{ \sum_{j=0}^{\infty} \frac{x_2^j}{j!} (W_{23}x_3+W_{24}x_4)^j \} \cdot \sum_{k=0}^{i} (W_{12}x_2)^k \cdot (W_{13}x_3+W_{14}x_4)^{i-k} \binom{i}{k} \cdot dx_2 \qquad \text{(E-13)}$$

and integrating

$$I = B \sum_{j=0}^{\infty} \sum_{k=0}^{i} \binom{i}{k} \frac{W_{12}^k}{j!} (W_{23}x_3+W_{24}x_4)^j (W_{13}x_3+W_{14}x_4)^{i-k} \frac{\Gamma(\frac{j+k+1}{2})}{2(\frac{W_{22}}{2})^{(i+k+1)/2}} \qquad \text{(E-14)}$$

Again defining some E which represents the terms not involved in evaluation of the remaining integrals, we can write

$$I = E \int_0^\infty \int_0^\infty e^c \cdot (W_{23}x_3+W_{24}x_4)^j (W_{13}x_3+W_{i4}x_4)^{i-k} \cdot dx_3 dx_4 \qquad \text{(E-15)}$$

where $c = -(1/2) \{W_{33}x_3^2 + W_{44}x_4^2\} + W_{34}x_3x_4$

$$e^{W_{34}x_3x_4} = \sum_{r=0}^{\infty} \frac{(W_{34}x_3x_4)^r}{r!}$$

$$(W_{23}x_3+W_{24}x_4)^j = \sum_{s=o}^{j} (W_{23}x_3)^2 (W_{24}x_4)^{j-s} \begin{bmatrix} j \\ s \end{bmatrix} \qquad \text{(E-16)}$$

$$(W_{13}x_3+W_{14}x_4)^{i-k} = \sum_{m=o}^{i-k} (W_{13}x_3)^m (W_{14}x_4)^{i-k-m} \begin{bmatrix} i-k \\ m \end{bmatrix}$$

The term involved in the remaining integrations is

$$\int_o^{\infty}\int_o^{\infty} x_3^{r+s+m} \; x_4^{r+j-s+i-k-m} \; e^{-(1/2)(\{W_{33}x_3^2+W_{44}x_4^2\})} dx_3 dx_4 \qquad \text{(E-17)}$$

$$= \int_o^{\infty} x_3^{e+s+m} \; e^{-\frac{W_{33}}{2}x_3^2} dx_3 \int_o^{\infty} x_4^{r+j-s+i-k-m} \; e^{-\frac{W_{44}}{2}x_4^2} dx_4$$

$$= \frac{\Gamma(\frac{r+s+m+1}{2})}{2(\frac{W_{33}}{2})^{(r+s+m+1)/2}} \; \frac{\Gamma(\frac{r+j+i-k=m-s+1}{2})}{2(\frac{W_{44}}{2})^{(r+j+i-k-m-s+1)/2}} \qquad \text{(E-18)}$$

Putting (E-15) and (E-18) together we have the final results.

$$I = \sum_{i=o}^{\infty} \sum_{j=o}^{\infty} \sum_{r=o}^{\infty} \sum_{k=o}^{i} \sum_{s=o}^{j} \sum_{m=o}^{i-k} \binom{i}{k} \binom{j}{s} \binom{i-k}{m} \frac{\Gamma\left(\frac{i+1}{2}\right)}{i!\ 2\left(\frac{W_{11}}{2}\right)^{(i+1)/2}} \cdot \frac{\Gamma\left(\frac{j+k+1}{2}\right)}{j!\ \left(2\left(\frac{W_{22}}{2}\right)^{(j+k+1)/2}\right.} \cdot \frac{\Gamma\left(\frac{r+s+m+1}{2}\right)}{r!\ 2\left(\frac{W_{33}}{2}\right)^{(r+s+m+1)/2}}$$

$$\cdot \frac{\Gamma\left(\frac{i+j+r-k-s-m+1}{2}\right)}{2\left(\frac{W_{44}}{2}\right)^{(i+j+r-k-s-m+1)/2}} \cdot \{W_{12}{}^{k}\, W_{34}{}^{r}\, W_{23}{}^{s}\, W_{13}{}^{m}\, W_{24}{}^{j-s}\, W_{14}{}^{i-k-m}\} \qquad \text{(E-19)}$$

APPENDIX F

A Flow-Diagram for the FORTRAN program that computes the expectation of the product of four clipped, jointly gaussian functions is given. Another general Flow-Diagram follows, which uses this expectation. Subroutine to compute the Detection Parameter for the Polarity Coincidence Correlator and compares results with Analog Detectors.

Flow Diagram.

SUBROUTINE EXPECT(C,DET,IT,OUT)

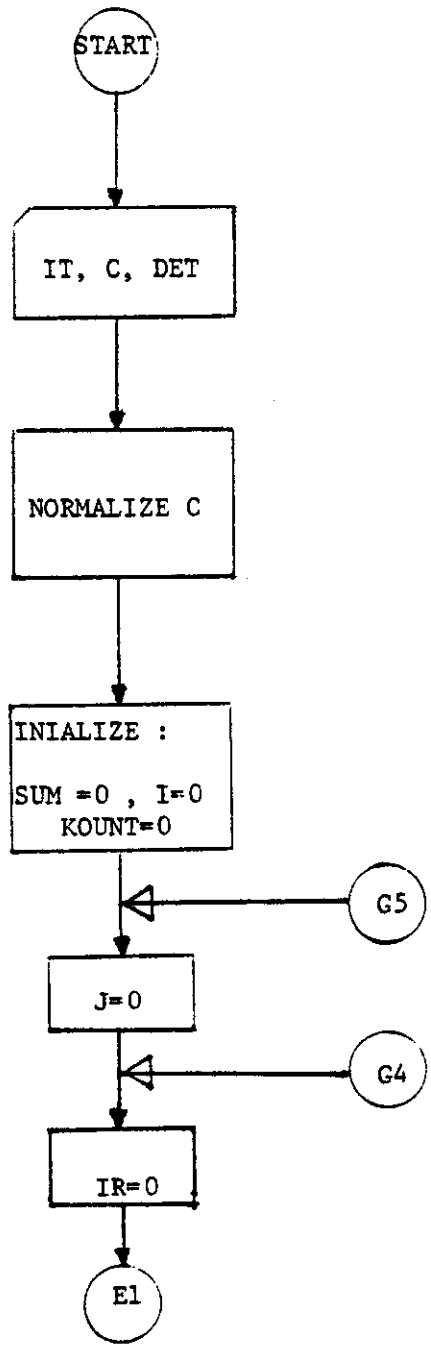

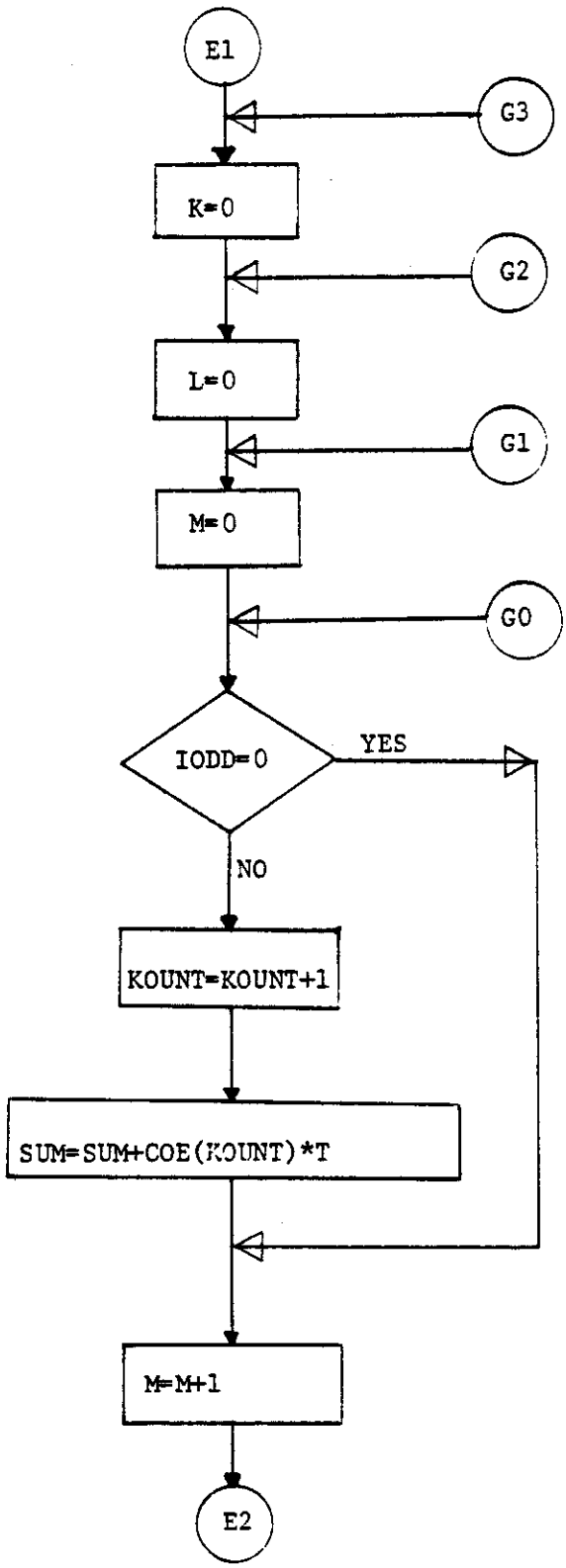
E1
G3
K=0
G2
L=0
G1
M=0
G0
IODD=0
YES
NO
KOUNT=KOUNT+1
SUM=SUM+COE(KOUNT)*T
M=M+1
E2

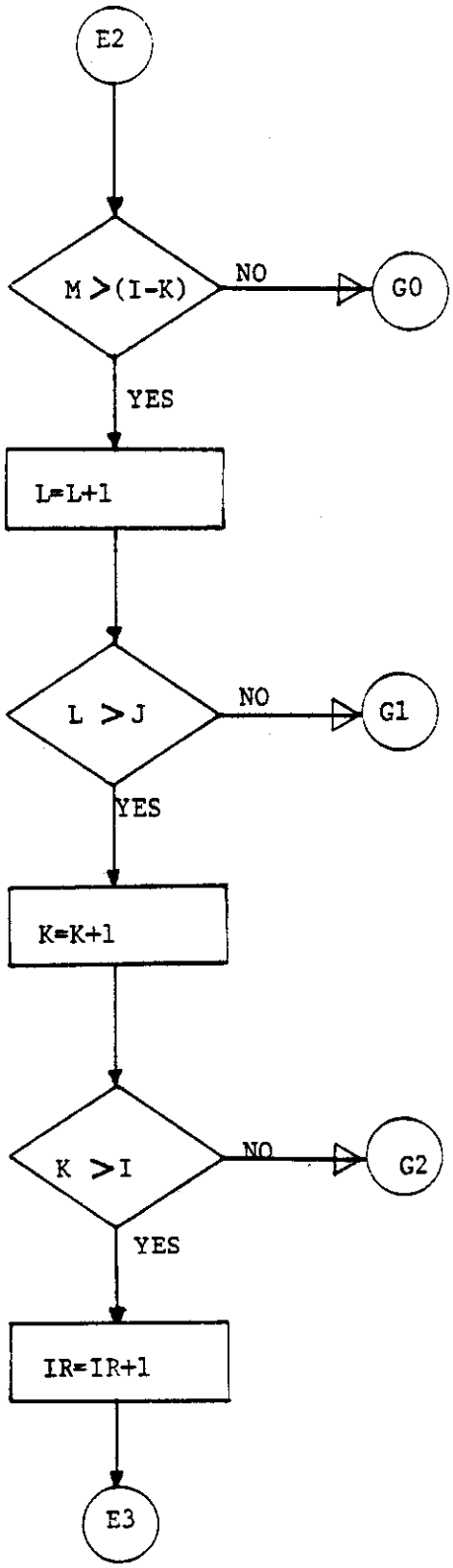
E2
M >(I-K)
NO
G0
YES
L=L+1
L > J
NO
G1
YES
K=K+1
K > I
NO
G2
YES
IR=IR+1
E3

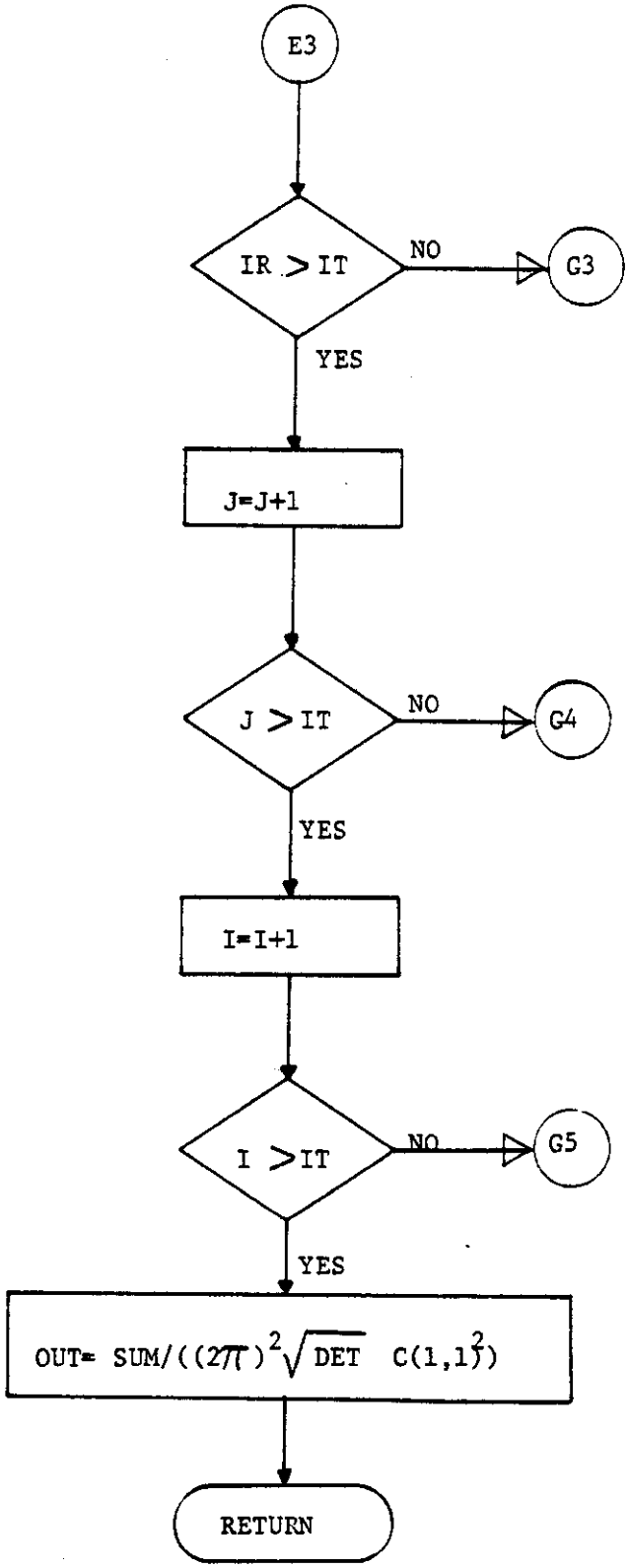
E3
IR > IT
NO
G3
YES
J=J+1
J > IT
NO
G4
YES
I=I+1
I > IT
NO
G5
YES
OUT= SUM/((2π)^2√DET C(1,1)^2)
RETURN

FORTRAN Implementation.

List of Principal Variables

Program Symbol	Definition
IT	Truncation of Infinite Summation.
C	Inverse of Correlation Matrix P.
DET	Determinant of Matrix P.
I,J,IR	Index of Infinite Summations.
K,L,M	Index of Finite Summations.
IODD	Checks Whether I or (K+J) or (M+L+IR) is Odd. If any of them is Even then that Calculation is Skiped.
SUM	Partial Result
T	Value of the Product of Elements of Upper Triangle of C Matrix, while Elements are raised to the Powers as mentioned in Appendix E.
OUT	Expectation of the Product of Four Clipped Gaussian Functions whose Correlation Matrix is P.

Flow Diagram.

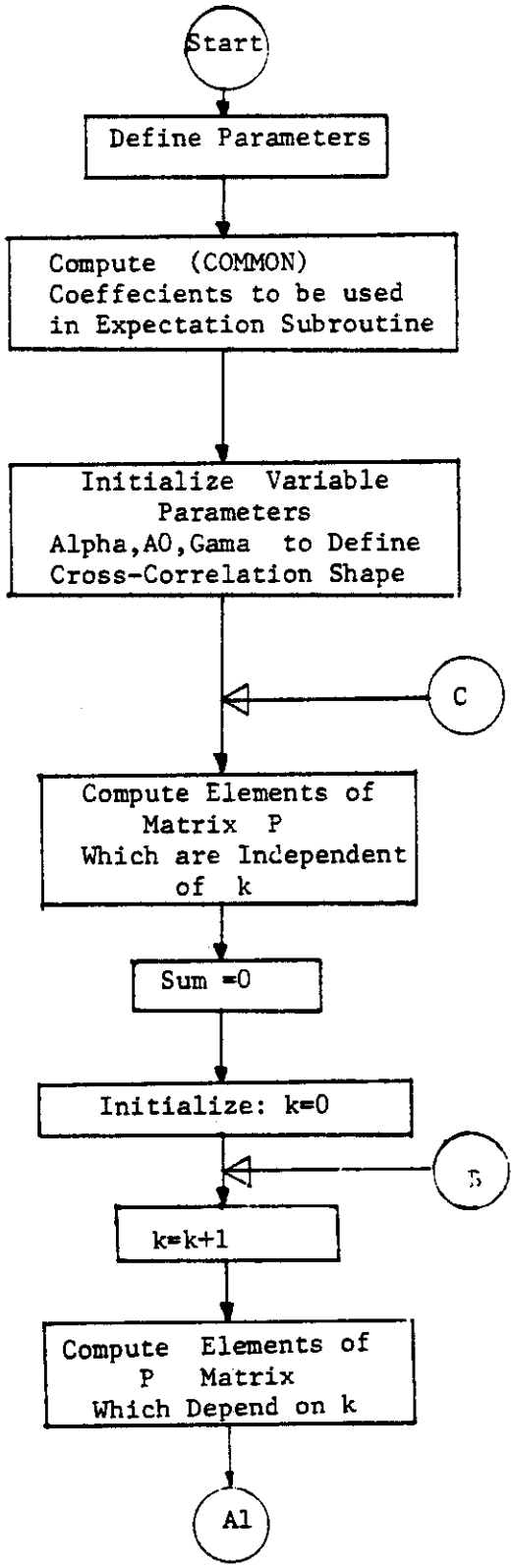

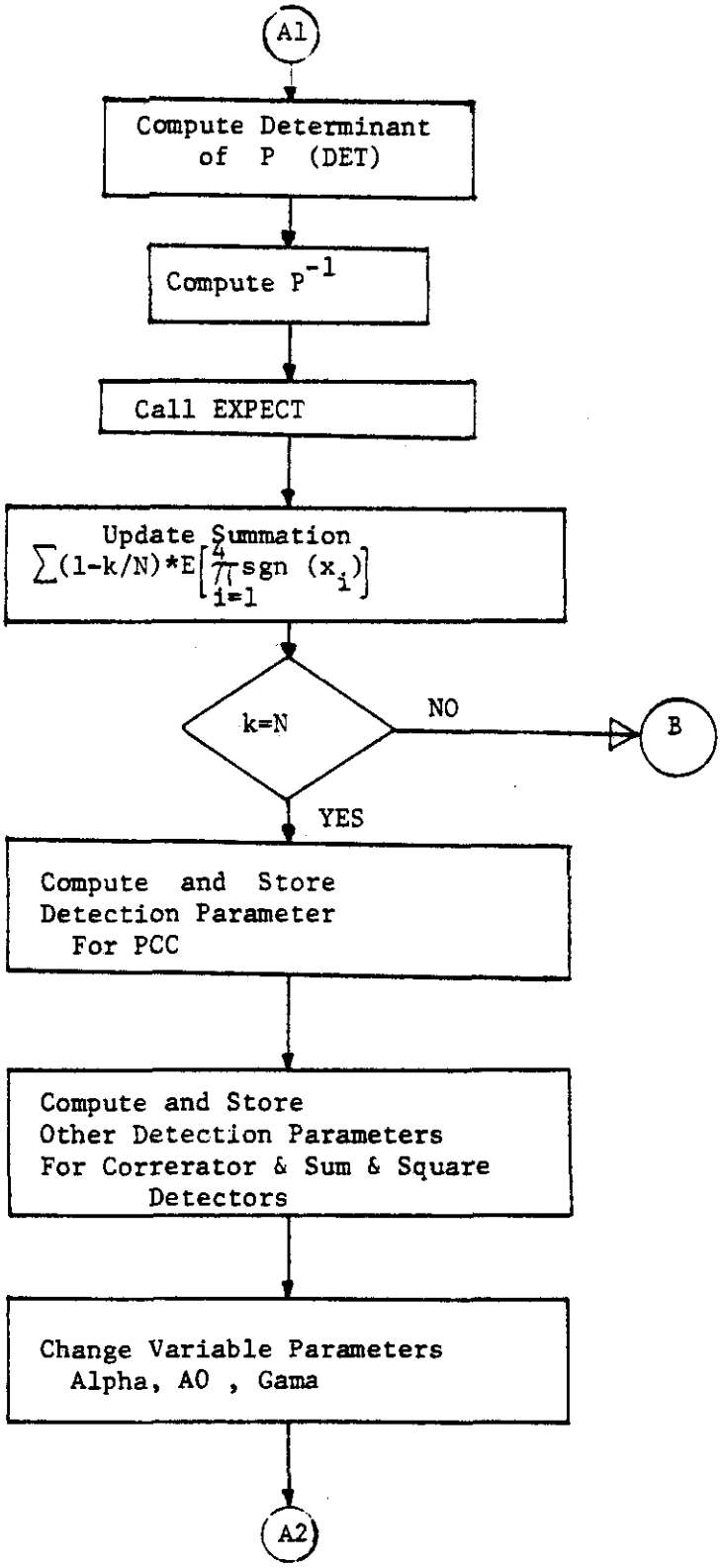
A1
Compute Determinant of P (DET)
Compute P^{-1}
Call EXPECT
Update Summation
$\sum(1-k/N)*E\left[\prod_{i=1}^{4} sgn\ (x_i)\right]$
k=N
NO
B
YES
Compute and Store Detection Parameter For PCC
Compute and Store Other Detection Parameters For Correrator & Sum & Square Detectors
Change Variable Parameters Alpha, A0 , Gama
A2

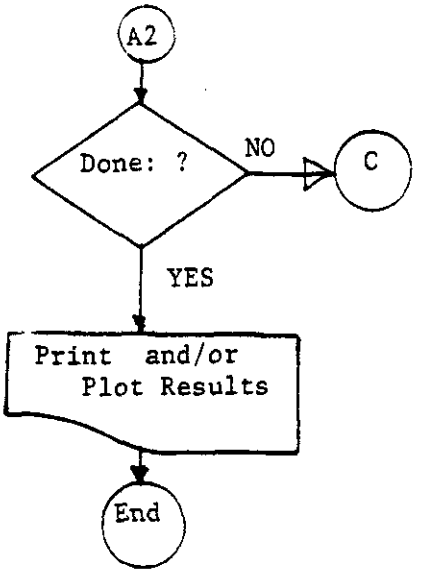
A2
Done: ?
NO
C
YES
Print and/or
Plot Results
End

BIBLIOGRAPHY

1. Wait, J. R., "Electromagnetic Induction Technique for Locating a Buried Source," IEEE Trans. Geosci. Electro., Vol. GE-9, No. 2 (April 1971), pp. 95-98.

2. Olsen, R. G. and Farstad, A. J., "Electromagnetic Direction Finding Experiments for Location of Trapped Miners," IEEE Trans. on Geosci. Electro., Vol. II, No. 4 (1973).

3. Ristenbatt, M. P., "Post-Disaster EM Communication Techniques," Post-Disaster Communication Contract Reviewing Meeting U.S. Bureau of Mines, Bruceton Research Center (January 8, 1980).

4. Lagace, R. L., and Doerfler, D. C., "Results of the Ability to Detect Trapped Miners by Electromagnetic Means," P.D.C. Reviewing Meeting, U.S. Bureau of Mines, Bruceton Research Center (January 8, 1980).

5. Moore, C., "Electromagnetic System for Deep Mines," P.D.C. Reviewing Meeting, U.S.Bureau of Mines, Bruceton Research Center (January 8, 1980).

6. Bryn, F., "Optimal Signal Processing of 3-Dimensional Arrays Operating on Gaussian Signals and Noise," JASA, Vol. 34, No. 3 (March, 1962).

7. Rudnick, P., "Small Signal Detection in the Dimus Array," JASA, Vol. 32 (1960), p. 867.

8. Schultheiss, P. M., and Tuteur, F. B., "Optimum and Suboptimum Detection of Directional Gaussian Signals in Isotropic Gaussian Noise Field, Part II: Degradation of Detectability Due to Clipping," IEEE Trans. on Milit. Electr., Vol. MIL-9 (July/October, 1965), pp. 208-211.

9. Wolff, S. S., Thomas, J. B., and Williams, J. R., "The Polarity Coincidence Correlator: A Nonparametric Detection Device," IRE Trans. on Info. Theory, Vol. IT-8 (January, 1962), pp. 1-19.

10. Kanefsky, M., and Thomas, J. B., "Polarity Coincidence Correlation Using Dependent Samples," Proc. 1964 Nat'l. Electr. Cong., Vol. 20, p. 714.

11. Kanesfsy, M., "Detection of Weak Signals with Polarity Coincidence Arrays," IEEE Trans. on Inf. Theory, Vol. IT-12, No. 2 (April, 1966).

12. Kanefsky, M., and Thomas, J. B. "On Polarity Detection Schemes with Non-Gaussian Inputs," Journal of the Franklin Institute, Vol. 280, No. 2 (April, 1965).

13. Faran, J. J., and Hills, R. Jr., "Correlators for Signal Reception," Acoustical Res. Lab., Cambridge, Mass.: Harvard University, Tech. Memo. 27 (1952).

14. Andrews, L. C., "Analysis of a Cross Correlator with a Clipper in One Channel," IEEE Trans. on Inf. Theo., Vol. IT-26, No. 62 (November, 1980).

15. Wolff, S. S., Thomas, J. B., and Williams, J. R., "The Polarity Coincidence Correlator: A Nonparametric Detection Device," IRE Trans. on Info. Theory, Vol. IT-8 (January, 1962), pp. 1-19.

16. Kanefsky, M., and Thomas, J. B., "Polarity Coincidence Correlation Using Dependent Samples," Proc. 1964 Nat'l. Electr. Conf., Vol. 20, p. 714.

17. Kanefsky, M., "Detection of Weak Signals with Polarity Coincidence Arrays," IEEE Trans. on Inf. Theory, Vol. IT-12, No. 2 (April, 1966).

18. Capon, J., "Application of Detection and Estimation Theory to Large Array Seismology," Proc. IEEE, Vol. 58, No. 5 (May, 1970), pp. 760-770.

19. Kanefsky, M., and Thomas, J. B., "On Polarity Detection Schemes with Non-Gaussian Inputs," Journ. of the Franklin Institute, Vol. 280, No. 2 (August, 1965).

20. Kendall, M. G., and Stuart, A., The Advanced Theory of Statistics-Inference and Relationship (New York: Hafner Publishing Co., Vol. 2, 1961), p. 162.

21. Van Vleck, J. H., and Middleton, D., "The Spectrum of Clipped Noise," Proc. IEEE, Vol. 54, No. 1 (January, 1966), pp. 2-19.

22. Andrews, L. C., "The Output pdf of a Polarity Coincidence Correlation Detector," IEEE Trans. on Aerospace and Electronic Systems, Vol. AES-10 (September, 1974), pp. 712-715.

23. Ekre, H., "Polarity Coincidence Correlation Detection of a Weak Noise Source," IEEE Trans. Inform. Theory, Vol. IT-9 (January, 1963), pp. 18-23.

24. Cheng, M. C., "The Clipping Loss in Correlation Detectors for Arbitrary Input Signal-to-Noise Ratios," IEEE Trans. on Inform. Theory, Vol. IT-14, No. 3 (May, 1968).

25. Weissberger, A. J., "Analysis of Multiple-Microprocessor System Architectures," Computer Design (June, 1977), pp. 34-42.

26. Thurber, J., "Parallel Processor Architecture--Part 1: General Purpose Systems," Computer Design (January, 1979), pp. 89-97.

27. Thurber, J., "Parallel Processor Architecture--Part 2: Special Purpose Systems," Computer Design (February, 1970), pp. 103-114.

28. Price, R., "A Useful Theorem for Non-Linear Devices Having Gaussian Inputs," IRE, PGIT, Vol. IT-4, 1958.

29. Gupta, S. S., "Probability Integrals of Multivariate Normal and Multivariate t," Ann. Math. Statist. (1963), Vol. 34, pp. 792-838.

REFERENCES NOT CITED

Abramowitz, M. and Stegun, I. Handbook of Mathematical Functions. New York: Dover, 1965.

Capon, J., Greenfield, R. J., and Lacoss, R. T. "Long Period Signal Processing Results for the Large Aperture Seismic Array." Geophics, Vol. 34, No. 2, June 1969.

Fano, R. M. "Signal-to-Noise Ratio in Correlation Detectors." Res. Lab. of Electronics, Cambridge, Mass.: M.I.T. Tech. Rept. No. 186, 1951.

Green, P. E. "The Output Signal-to-Noise Ratio of Correlation Detectors." IRE Trans. on Inf. Theo., Vol. IT-3 (March, 1957), pp. 10-18.

Middleton, D. An Introduction to Statistical Communication Theory. New York: McGraw Hill Book Co., 1960.

Miller, K. S. Multidimensional Gaussian Distributions. New York: John Wiley Co., 1964.

Rice, S. O. "Mathematical Analysis of Random Noise," Bell Sys. Tech. J., Vol. 23 (July, 1944), pp. 282-332.

Thomas, J. B., and William, T. R. "On the Detection of Signals in Nonstationary Noise by Product Arrays." JASA, Vol. 31 (April, 1959), pp. 453-462.

Usher, T. Jr., and Schultheises, P. M. "Space-Time Correlation in Isotropic Noise Fields." General Dynamics/Electric Boat Research, February, 1963, Progress Report #1.

Wait, J. R. "Criteria for Locating an Oscillating Magnetic Dipole Buried in the Earth." Proc. IEEE (Letters), Vol. 49, No. 6 (June, 1971), pp. 1033-1035.

Wait, J. R. "Locating an Oscillating Magnetic Dipole in the Earth." Electronic Letters, Vol. 8, No. 16 (August 10, 1972).

Wait, J. R., and Hill, D. A. "Transient Signals from a Buried Magnetic Dipole." Journal of Applied Physics, Vol. 42, No. 10 (September, 1971), pp. 3866-3869.